

**STEREOCHEMISTRY IN CATALYTIC OXIDATION
BY HEME ENZYMES**

Hui-Jun Yang

DOCTOR OF PHILOSOPHY

Department of Structural Molecular Science
School of Mathematical and Physical Science
The Graduate University for Advanced Studies

2000

CONTENTS

Part I GENERAL INTRODUCTION

Part II CONSTRUCTION OF HIGH ACTIVE ENZYMES BY USE OF
MYOGLOBIN AS A MODEL

Chapter 1.

The Role of Val68 (E11) on Oxidation Activity and Enantioselectivity
of Sperm Whale Myoglobin

Chapter 2.

Conversion of Sperm Whale Myoglobin into a Catalase-like Enzyme

Part III CATALYTIC OXIDATION BY DISTAL HISTIDINE RELOCATION
MYOGLOBIN MUTANTS

Chapter 1.

Asymmetric Oxidation Catalyzed by Sperm Whale Myoglobin Mutants

Chapter 2.

Characterization of I107H/H64L Myoglobin Mutant

Part IV SUMMARY AND CONCLUSION

ACKNOWLEDGMENT

LIST OF PUBLICATIONS

PART I

GENERAL INTRODUCTION

As is well known to all, hemoproteins are of great importance in physiological systems in that they play very versatile roles.¹ For instance, cytochromes are involved in electron transfer processes in the mitochondrial electron transport chain² and hemoglobin and myoglobin function as a carrier of molecular oxygen (O₂).³ Also very often briefed in literatures are hemoenzymes such as cytochrome P450s, peroxidases, catalases, nitric oxide synthases and cytochrome P450nor which are responsible for monooxygenations, electron abstract processes, the dismutation of hydrogen peroxide, nitric oxide synthesis, and the reduction of NO, respectively.^{4,7} In spite of these diverse functions, all hemoproteins have a common prosthetic group composed of an iron-protoporphyrin IX complex (heme) in the active site (Figure 1). The different functions therefore stem from the differences in the manner that the heme interacts with amino acid residues and small molecules (e.g. substrates) in the active site.

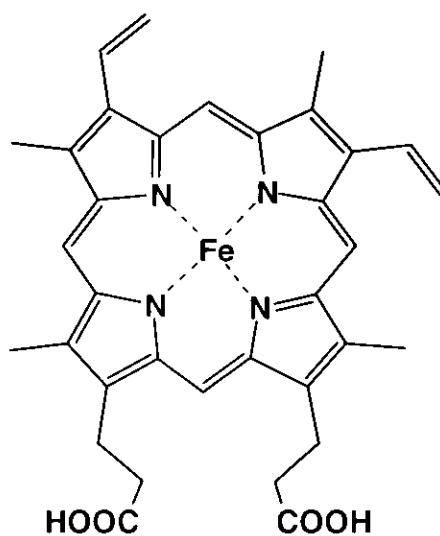
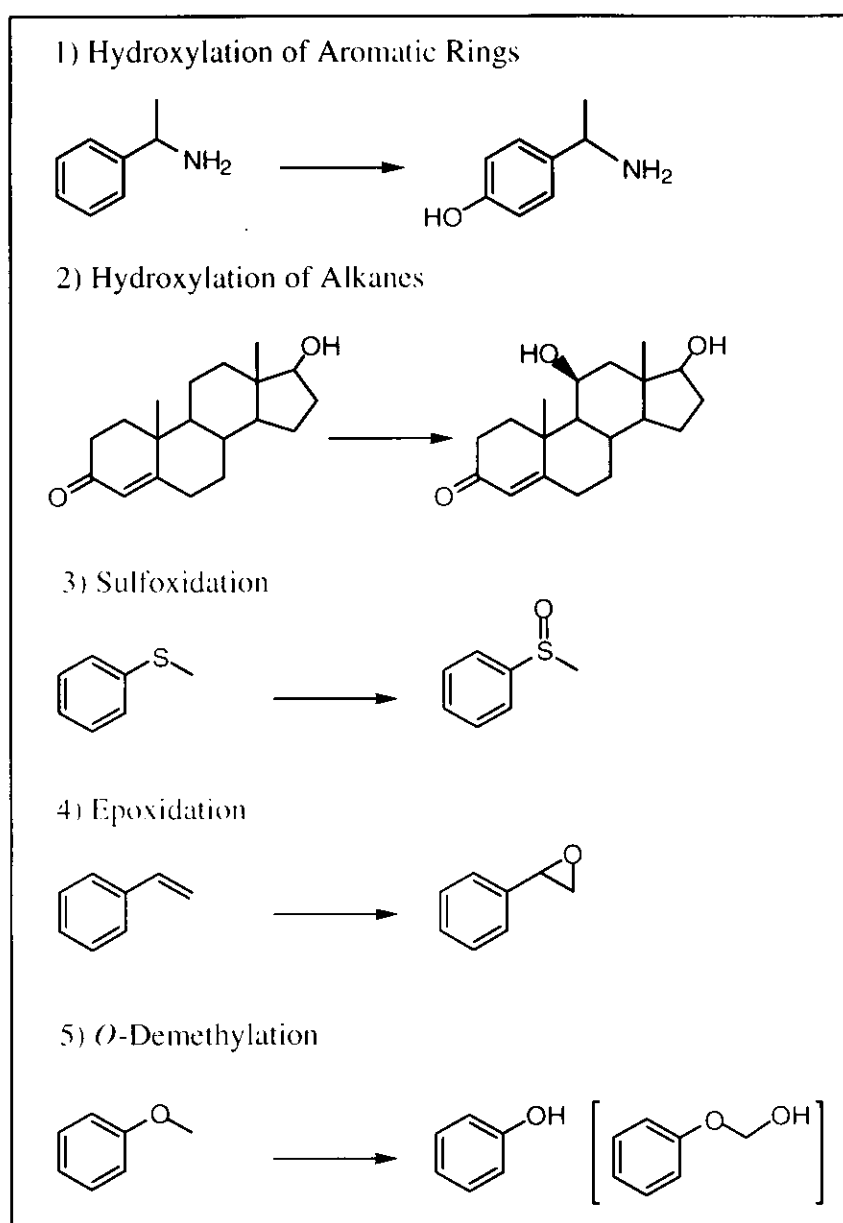


Figure 1. Protoporphyrin IX (*heme*)

In addition, proteins that contain the heme prosthetic group are responsible for many different types of catalytic reactions. A good example is cytochromes P450 which are known to catalyze hydroxylations, sulfoxidations, epoxidations, *N*-, *S*- and *O*-dealkylations, and other reactions (Table 1).⁸ The reactions catalyzed by heme enzymes have been challenged and intrigued by chemists for more than two decades.

Enantioselective oxidations such as sulfoxidation, epoxidation by hemoenzymes have been studied intensively to pursue practical applications for large-scale asymmetric organic syntheses as well as to understand the mechanistic details of oxygen activation. In planning the asymmetric synthesis, organic chemists would select a chemical procedure from the wide range of classic methods. However, biochemical methods or biotransformations, give us alternatives for organic synthesis. At present, biotransformations can provide two methods, whole-cell and isolated-enzyme system. For example,

Table 1. Typical reactions catalyzed by cytochrome P450s.



chloroperoxidase (a heme enzyme) isolated from *Cadariomyces fumago* (CPO)⁹ is one of the well studied enzymes for enantioselective oxidation of sulfides and olefins.¹⁰⁻¹⁶ Recently, a vanadium-containing non-heme bromoperoxidase from the alga *C. officinalis* (VBrPO)¹⁷ has been shown to perform sulfoxidation of aromatic bicyclic sulfides in high enantiomeric excess (% ee).¹⁸ In order to extend the biocatalytic methodology, we have constructed a series of sperm whale myoglobin (Mb) mutants and examined oxidation activity as well as elucidated catalytic mechanism by them, which are obtained through the rational protein engineering.

Myoglobin (Mb) functions as an oxygen storage and carrier protein in muscle. This protein has been one of the most intensively investigated hemoproteins as evident from the accumulated biochemical and spectroscopic data.^{3,19} It has protoporphyrin IX as a prosthetic group, and is the first protein structure determined to high resolution by X-ray crystallographic analyses. Thus, myoglobin has ever been serving as a model system for the study of structure-function relationships in heme proteins. Once methods of DNA sequencing become established,²⁰⁻²² the determination of the genetic code of sperm whale myoglobin paved the road to manipulate nucleic acids to make specific mutants.²³ Therefore, only a desired amino acid residue can be altered while the rest of the protein structure ideally remains intact. The pioneering work by Springer & Sligar²⁴ on the construction of a synthetic gene for sperm whale Mb and the resultant high-level expression of this gene as heme-containing protein in *Escherichia coli* have enabled us to genetically engineer sperm whale Mb *in vitro* mutagenesis techniques. The obvious advantage of having myoglobin expressed in such a bacterial system is that changes in the amino acid sequence can now be easily. So far, many investigations on the structure-function relationships of hemoproteins have already successfully performed; however, some questions concerning the introduction of desired function to hemoproteins, the origin of enantioselectivity, as well as the exact nature of the reactive intermediate remain to be clarified.

Part II in this thesis focuses on construction of highly enantioselective and active enzymes using myoglobin as a model. Apart from the physiological function, Mb can

support a variety of H₂O₂-dependent oxidation reactions such as one-electron oxidation by peroxidase,^{5,25,26} oxygenations by cytochrome P-450^{4,27-33} and dismutation of H₂O₂ by catalase,^{34,37} but less efficiently than these enzymes. Superposition of the active site structures of Mb and other hemoproteins enables us to utilize Mb as a heme enzyme model for the elucidation of structure-function relationships. Oxidation reactions catalyzed by heme enzymes are normally associated with a ferryl porphyrin cation radical (O=Fe^{IV} Por⁺) called compound I which is formed by the reaction of the resting ferric enzymes with peroxide (Figure 2).^{35,36} Chloroperoxidase from *Caldariomyces fumagus* affords compound

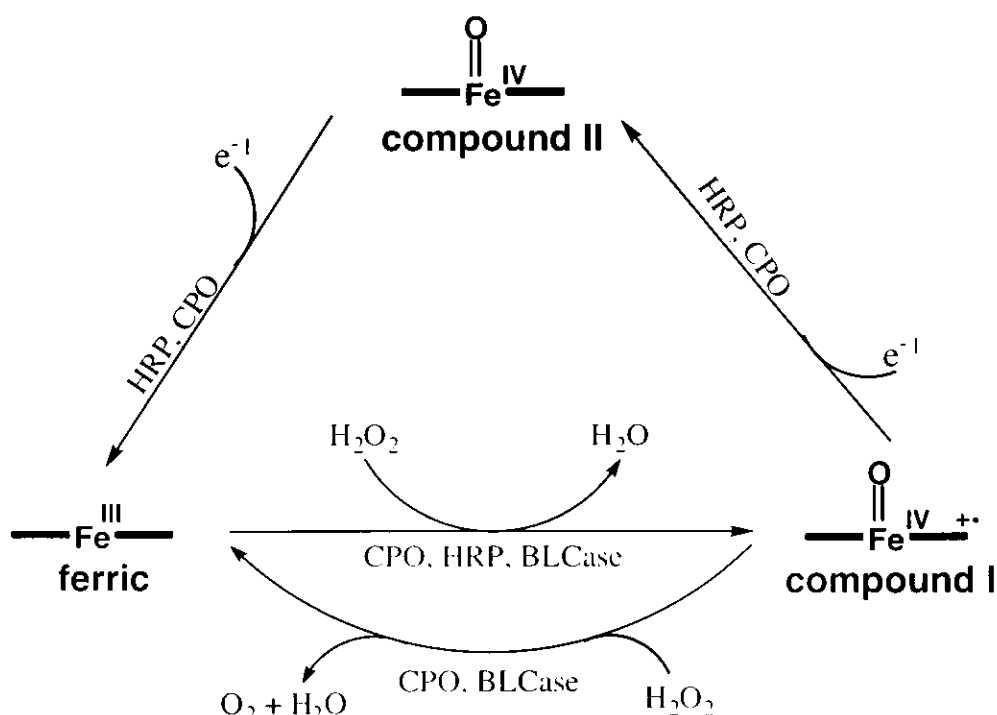
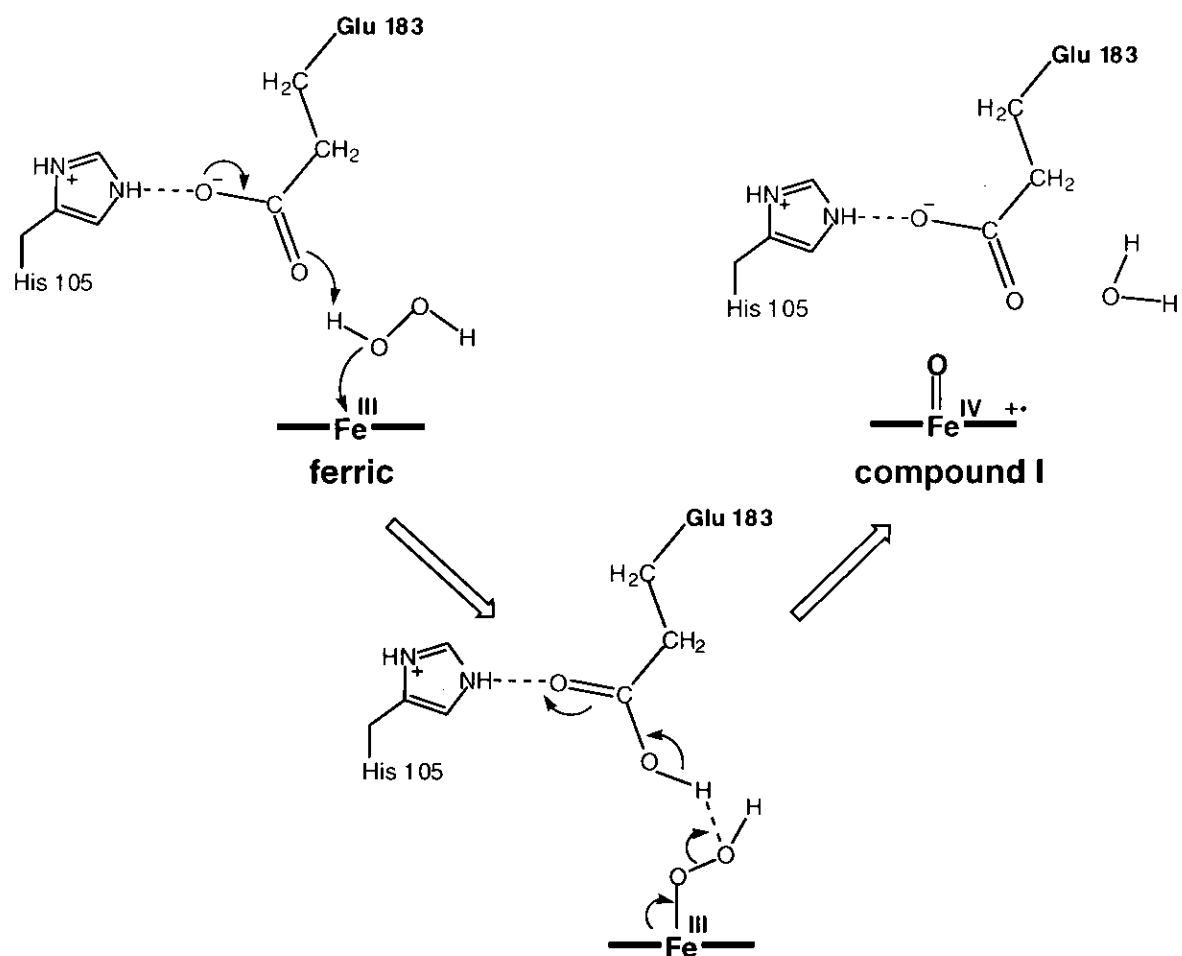


Figure 2. General Catalytic Cycles of Heme Enzymes. HRP: horseradish peroxidase, CPO: chloroperoxidase, BLCase: bovine liver catalase.

I at the rate of $2.4 \times 10^6 \text{ M}^{-1}\text{s}^{-1}$ in the presence of H₂O₂ (Scheme 1),^{37,38} which shows versatile oxidation ability including one-electron oxidation, H₂O₂ dismutation, and oxygenation in addition to its physiological chlorination. More recently, Matsui *et al.* have prepared the H64D mutant of sperm whale myoglobin to mimic the active site of chloroperoxidase.³⁹ The H64D Mb mutant provides the first evidence for the significant

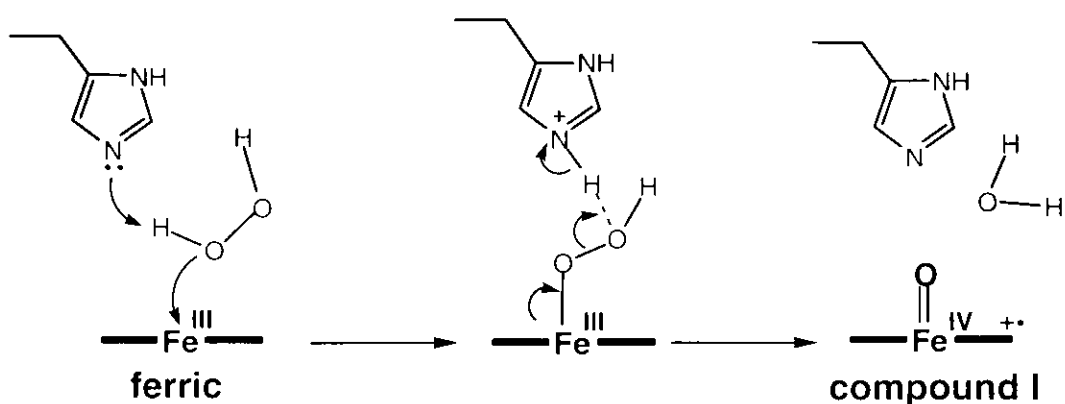


Scheme 1. Proposed mechanism of compound I formation for chloroperoxidase.

accumulation of the reactive intermediate, compound I, in the reaction with H_2O_2 . Also, the mutant shows 50-70-fold and 600-800-fold higher activity than the wild type in the peroxidations and peroxygenations, respectively, and has been the best enzyme in terms of catalytic activity among myoglobins. Despite of advantages of H64D Mb such as the high reactivity of ferric Mb with H_2O_2 and the improved stability of compound I, the origin of stereospecificity of the myoglobin mutant has not been well clarified yet. Chapter 1 discusses functions of Val-68 (E11) on stereochemistry and activity of sperm whale myoglobin. A series of Mb mutants (referred to as H64D/V68X mutants) have been prepared by replacing Val-68 with Gly, Ala, Ser, Leu, Ile, and Phe in H64D Mb. The mutants were designed to increase the life-time of catalytic intermediate as well as the accessibility of substrates to the heme iron. Thus the reactivity of catalytic intermediate, compound I, especially for the two-electron oxidations of the substrate thioanisole, has

been determined from single-turnover kinetics by means of a double-mixing rapid-scan technique. Moreover, the attempts to elucidate enantioselectivity of Mb were performed through investigations of UV spectroscopy, EPR and X-ray crystallography of phenylethylamine binding complexes for H64D/V68X Mbs.

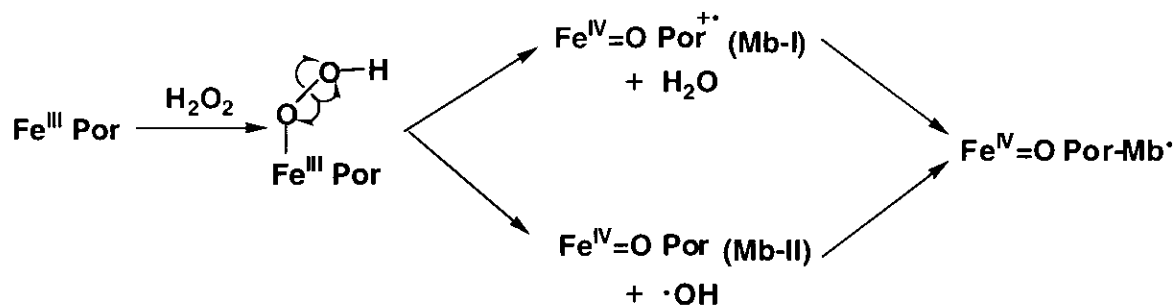
While the distal glutamic acid is suggested to be crucial for the rapid formation of compound I in CPO (Scheme 1 & Figure 3d),⁴⁰ classical peroxidases and catalases react with H_2O_2 to afford the reactive intermediate equivalent to so called compound I by utilizing distal histidine as a general acid-base catalyst (Scheme 2 & Figure 3b, c).⁴¹⁻⁴⁴ The function of the distal histidine in peroxidase and catalase (Scheme 2) is believed as follows: (1) the distal histidine first functions as a general base to abstract a proton from hydrogen peroxide to allow the binding of the hydroperoxy anion to the heme iron, (2) the protonated histidine then serves as a general acid to facilitate the heterolytic O-O bond cleavage through release of a water molecule. The resting ferric peroxidase and catalase react with



Scheme 2. Proposed mechanism of compound I formation for catalase and peroxidase

H_2O_2 at the rate of $\sim 10^7 \text{ M}^{-1} \text{ s}^{-1}$ to form compound I.⁴⁵⁻⁴⁷ The peroxidase compound I is reduced to the ferric state by two sequential one-electron oxidation via a ferryl species ($\text{Fe}^{\text{IV}}=\text{O}$ Por), known as compound II (Figure 2),⁵ whereas the catalase compound I oxidizes another H_2O_2 molecule by two-electron to yield dioxygen and water (Figure 2).³⁵ Myoglobin similarly possesses distal histidine in the heme pocket (Figure 3a), however it

reacts with H_2O_2 much slower ($\sim 10^2 \text{ M}^{-1} \text{ s}^{-1}$) than peroxidase and catalase to afford ferryl Mb (Mb II) paired with a transient protein radical (Scheme 3).



Scheme 3. Reactions of ferric Mb with hydrogen peroxide.

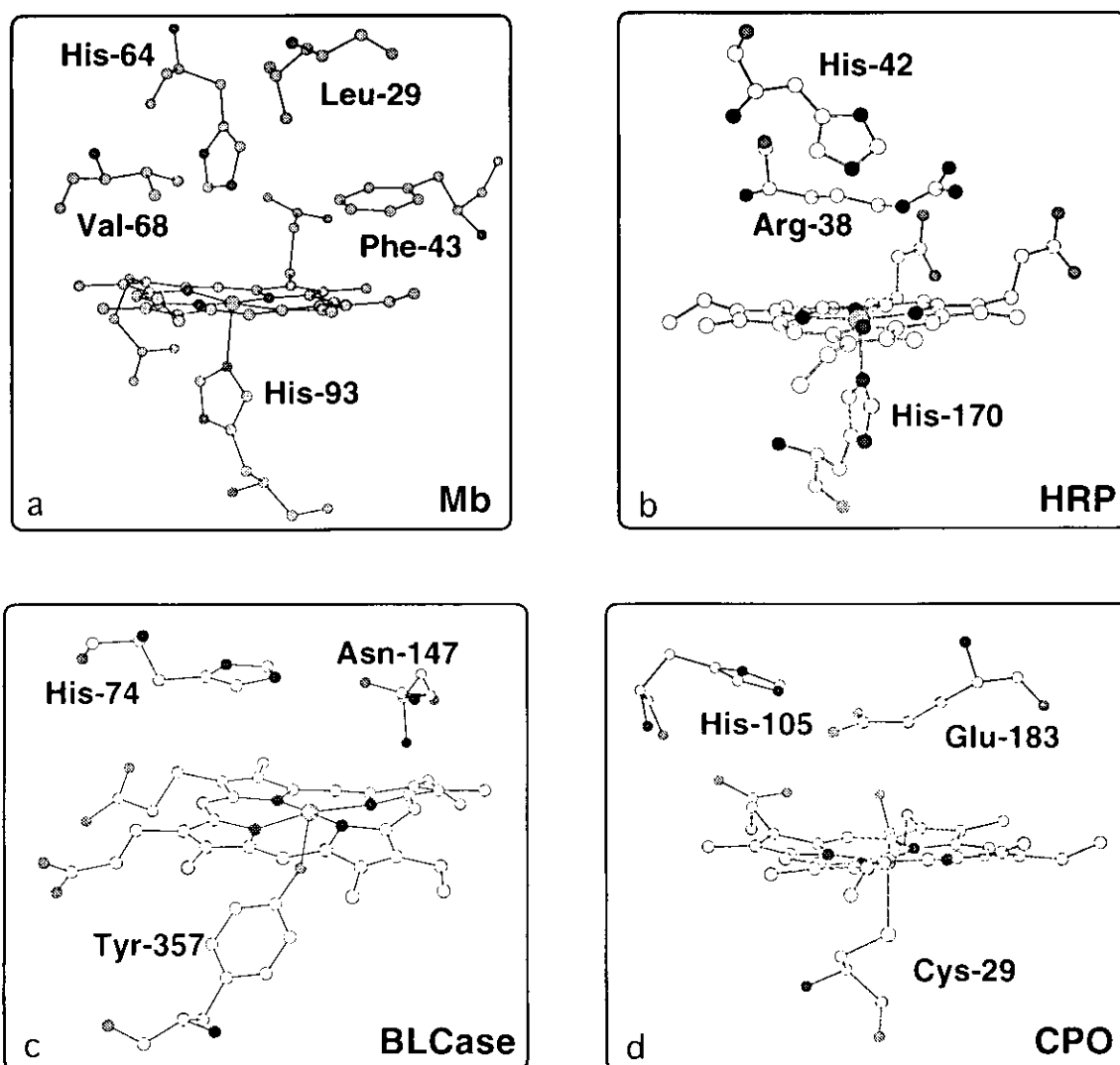


Figure 3. Active site of sperm whale myoglobin (Mb), horseradish peroxidase (HRP), bovine liver catalase (BLCase), chloroperoxidase (CPO) from *Caldariomyces fumago*. Heme, axial ligand, and some selected distal residues are presented in the figure.

On the basis of comparison of the crystal structure of Mb with that of peroxidase (CcP), which the distal histidine in Mb is more than 1 Å closer to the heme iron than that in peroxidase,⁴⁸ Ozaki et al. hypothesized that the distal histidine in Mb is too close to the heme iron to facilitate compound I formation and Mb's reactivity with H₂O₂ is consequently lower than that of the peroxidase. In order to examine this hypothesis, the distal histidine relocation mutants (F43H/H64L and L29H/H64L) and the distal histidine deletion mutants (His64 → Ala, Ser, Leu) were constructed in our research group previously.⁴⁹⁻⁵¹ X-ray crystal structures of F43H/H64L and L29H/H64L mutants solved at 1.8 Å (Figure 4)⁵² indicate that the distance between N_δ of the distal histidine and the ferric

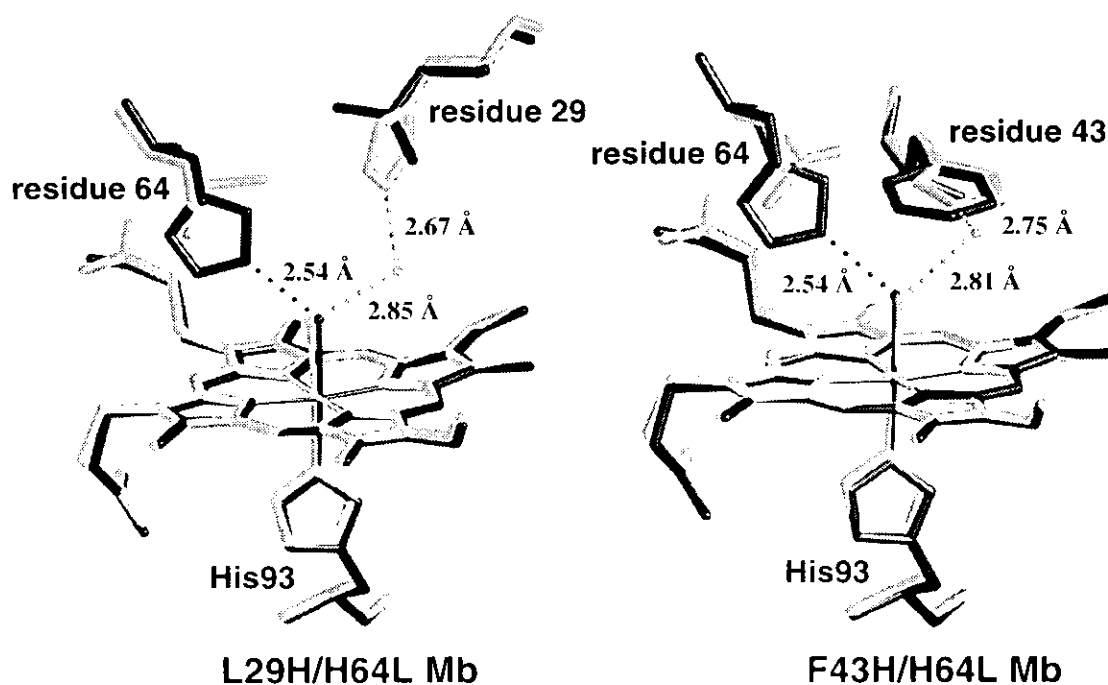


Figure 4. The X-ray crystal structures of F43H/H64L and L29H/H64L myoglobin mutants (resolution = 1.8 Å).

heme iron is 5.7 Å in F43H/H64L Mb, which is similar to those in peroxidases (5.5-6.0 Å). In contrast, the distal histidine in L29H/H64L Mb is located farther away from the heme iron (6.6 Å). As the results, the F43H/H64L mutant reacts with H₂O₂ much more efficiently than L29H/H64L and WT Mb. In addition, the distal histidine deletion mutants (H64A, H64S and H64L) of sperm whale Mb react with organic peracids including *m*-

chloroperbenzoic acid (*m*CPBA) to accumulate compound I,⁵¹ and Mb-I is capable of performing two-electron oxidation of H₂O₂ (catalase activity). Based on the previous results, F43H/H64A and F43H/H64N Mbs were prepared to mimic the active site of catalase (Chapter 2 in part II). We expected that His-43 in F43H/H64A or F43H/H64N Mb would cooperate with Ala-64 or Asn-64 in the activation of peroxide. Unfortunately, the substitution of Phe-43 in H64A and H64N Mbs with a histidine residue distorted in the rate of compound I formation with *m*CPBA although such a mutation increased the activity with H₂O₂ to somewhat extent. To elucidate the reason for the malfunction of His-43 in the F43H/H64A and F43H/H64N mutant, we crystallized F43H/H64A Mb and have attempted to solve the structure.

With desire to use Mb as a model system for the peroxygenation of a variety of substrates, i.e. sulfoxidation, epoxidation, and so on, the substrate selectivity by Mbs was investigated on a series of cyclic and acyclic sulfides as well as methyl styrene. Chapter 1 in part III illustrates enantioselective oxidation of sulfides and olefins catalyzed by F43H/H64L and L29H/H64L Mb mutants. Moreover, Chapter 2 of part III describes characterization of H07H/H64L Mb mutant that was constructed to mimic the active site of horseradish peroxidase.

REFERENCE

- (1) Lippard, S. J.; Berg, J. M. *Principles of Bioinorganic Chemistry*; University Science Book: California, Chapter 1, 1994.
- (2) Moore, G. R.; Pettigrew, G. W. *Cytochromes C*, Springer-Verlag, New York 1990.
- (3) Antonini, E.; Brunori, M. *Hemoglobin and Myoglobin in Their Reactions with Ligands*; North-Holland Publishing Co.: Amsterdam 1971.
- (4) Ortiz de Montellano, P. R. Ed. *Cytochrome P450*, second ed, Plenum Press, New York, 1995.
- (5) Everse, J.; Everse, K. E.; Grisham, M. B. Ed. *Peroxidase in Chemistry and Biology*, Vols. I and II, CRC Press, Boca Raton, 1991.
- (6) Griffith, O. W.; Stuehr, D. J. *Annu. Rev. Physiol.* **1995**, *57*, 707-736.
- (7) Park, S.-Y.; Shimizu, H.; Adachi, S.; Nakagawa, A.; Tanaka, I.; Nakahara, K.; Shoun, H.; Obayashi, E.; Nakamura, H.; Iizuka, T.; Shiro, Y. *Nat. Struct. Biol.* **1997**, *4*, 278.
- (8) Watanabe, Y.; Groves, J. T. *The Enzymes*, Boyer, P. D. and Sigman, D. S., Ed.; Academic Press: New York, Chapter 9, Vol. 20, 1992.
- (9) Morris, D. R.; Hager, L. P. *J. Biol. Chem.* **1966**, *241*, 1763-1768.
- (10) Colonna, S.; Gaggero, N.; Manfredi, A.; Casella, L.; Gullotti, M.; Carrea, G.; Pasta, P. *Biochemistry* **1990**, *29*, 10465-10468.
- (11) Colonna, S.; Gaggero, N.; Casella, L.; Carrea, G.; Pasta, P. *Tetrahedron: Asymmetry* **1992**, *3*, 95-106.
- (12) Colonna, S.; Gaggero, N.; Casella, L.; Carrea, G.; Pasta, P. *Tetrahedron: Asymmetry* **1993**, *4*, 1325-1330.
- (13) Allain, E. J.; Hager, L. P.; Deng, L.; Jacobsen, E. N. *J. Am. Chem. Soc.* **1993**, *115*, 4415-4416.
- (14) Dexter, A. F.; Lakner, F. J.; Campbell, R. A.; Hager, L. P. *J. Am. Chem. Soc.* **1995**, *117*, 6412-6413.
- (15) Allenmark, S. G.; Andersson, M. *Tetrahedron: Asymmetry* **1996**, *7*, 1089-1094.
- (16) Lakner, F. J.; Cain, K. P.; Hager, L. P. *J. Am. Chem. Soc.* **1997**, *119*, 443-444.
- (17) Butler, A.; Walker, J. V. *Chem. Rev.* **1993**, *93*, 1937-1944.
- (18) Andersson, M.; Willetts, A.; Allenmark, S. *J. Org. Chem.* **1997**, *62*, 8455-8458.
- (19) Springer, B. A.; Sligar, S. G.; Olson, J. S.; Phillips, G. N., Jr. *Chem. Rev.* **1994**, *94*, 699-714.

- (20) Sanger, F.; Tuppy, H. *Biochem. J.* **1951**, *49*, 463-490.
- (21) Sanger, F.; Thompson, E. O. P. *Biochem. J.* **1953**, *53*, 353-374.
- (22) Brown, H.; Sanger, F.; Kitai, R. *Biochem. J.* **1955**, *60*, 556-565.
- (23) Edmundson, A. B. *Nature* **1965**, *205*, 883-887.
- (24) Springer, B. A.; Sligar, S. G. *Proc. Natl. Acad. Sci. U.S.A.* **1987**, *84*, 8961-8905.
- (25) Everse, J.; Johnson, M. C.; Marini, M. A. *Methods in Enzymol* **1994**, *231*, 547-561.
- (26) Ortiz de Montellano, P. R.; Catalano, C. E. *J. Biol. Chem.* **1985**, *260*, 9265-9271.
- (27) Catalano, C. E.; Ortiz de Montellano, P. R. *Biochemistry* **1987**, *26*, 8373-8380.
- (28) Choe, Y. S.; Rao, S. I.; Ortiz de Montellano, P. R. *Arch. Biochem. Biophys.* **1994**, *314*, 126-131.
- (29) Rao, S. I.; Wilks, A.; Ortiz de Montellano, P. R. *J. Biol. Chem.* **1993**, *268*, 803-809.
- (30) Tschirret-Guth, R. A.; Ortiz de Montellano, P. R. *Arch. Biochem. Biophys.* **1996**, *335*, 93-101.
- (31) Adachi, S.; Nagano, S.; Ishimori, K.; Watanabe, Y.; Morishima, I.; Egawa, T.; Kitagawa, T.; Makino, R. *Biochemistry* **1993**, *32*, 241-252.
- (32) Matsui, T.; Nagano, S.; Ishimori, K.; Watanabe, Y.; Morishima, I. *Biochemistry* **1996**, *35*, 13118-13124.
- (33) Levinger, D. C.; Stevenson, J.-A.; Wong, L.-L. *J. Chem. Soc., Chem. Commun.* **1996**, 2305-2306.
- (34) Yonetani, T.; Schleyer, H. *J. Biol. Chem.* **1967**, *242*, 1974-1979.
- (35) Schonbaum, G. R.; Chance, B. *In The Enzymes*: 3rd ed.; Boyer, P. D. Ed.; Academic Press: New York, 1976. Vol. 13; pp 363-408.
- (36) Thomas, J. A.; Morris, D. R.; Hager, L. P. *J. Biol. Chem.* **1970**, *245*, 135-142.
- (37) Sundaramoorthy, M.; Turner, J.; Poulos, T. L. *Chemistry & Biology* **1998**, *5*, 461-473.
- (38) Araiso, T.; Rutter, R.; Palcic, M. M.; Hager, L. P.; Dunford, H. B. *Can. J. Biochem.* **1981**, *59*, 233-236.
- (39) Matsui, T.; Ozaki, S.; Watanabe, Y. *J. Am. Chem. Soc.* **1999**, *121*, 9952-9957.
- (40) Sundaramoorthy, M.; Turner, J.; Poulos, T. L. *Structure* **1995**, *3*, 1367-1377.
- (41) Erman, J. E.; Vitello, L. B.; Miller, M. A.; Shaw, A.; Brown, K. A.; Kraut, J. *Biochemistry* **1993**, *32*, 9798-9806.

- (42) Newmyer, S. L.; Ortiz de Montellano, P. R. *J. Biol. Chem.* **1995**, *270*, 19430-19438.
- (43) Rodriguez-Lopez, J. N.; Smith, A. T.; Thorneley, R. N. *J. Biol. Chem.* **1996**, *271*, 4023-4030.
- (44) Obinger, C.; Maj, M.; Nicholls, P.; Loewen, P. *Arch. Biochem. Biophys.* **1997**, *342*, 58-67.
- (45) Loo, S.; Erman, J. E. *Biochemistry* **1975**, *14*, 3467-3470.
- (46) Smith, A. T.; Sanders, S. A.; Thorneley, R. N.; Burke, J. F.; Bray, R. R. *Eur. J. Biochem.* **1992**, *207*, 507-519.
- (47) Chance, B.; Greenstein, D. S.; Roughton, F. J. *Arch. Biochem. Biophys.* **1952**, *37*, 301-321.
- (48) Poulos, T. L.; Freer, S. T.; Alden, R. A.; Edwards, S. L.; Skogland, U.; Takio, K.; Eriksson, B.; Xuong, N.; Yonetani, T.; Kraut, J. *J. Biol. Chem.* **1980**, *255*, 575-580.
- (49) Ozaki, S.; Matsui, T.; Watanabe, Y. *J. Am. Chem. Soc.* **1996**, *118*, 9784-9785.
- (50) Ozaki, S.; Matsui, T.; Watanabe, Y. *J. Am. Chem. Soc.* **1997**, *119*, 6666-6667.
- (51) Matsui, T.; Ozaki, S.; Watanabe, Y. *J. Biol. Chem.* **1997**, *272*, 32735-32738.
- (52) Matsui, T.; Ozaki, S.; Liong, E.; Phillips, G. N., Jr.; Watanabe, Y. *J. Biol. Chem.* **1999**, *274*, 2838-2844.

PART II

CONSTRUCTION OF HIGHLY ACTIVE ENZYMES BY USE OF MYOGLOBIN AS A MODEL

Chapter 1.

The Role of Val⁶⁸ (E11) on Oxidation Activity and Enantioselectivity of Sperm Whale Myoglobin

Chapter 2.

Conversion of Sperm Whale Myoglobin into a Catalase-like Enzyme

CHAPTER 1

The Role of Val68 (E11) on Oxidation Activity and Enantioselectivity of Sperm Whale Myoglobin

Abbreviations :

Mb, myoglobin;

CPO, chloroperoxidase from the marine *fungus Caldariomyces fumagus*;

compound I, a ferryl porphyrin cation radical;

compound II, a ferryl porphyrin;

Mb-I, myoglobin compound I;

*m*CPBA, *m*-chloroperbenzoic acid;

ABTS, 2,2'-azino-bis(3-ethylbenzothiazoline-6-sulfonic acid).

ABSTRACT: To probe the role of the distal valine 68 (E11) in sperm whale myoglobin (Mb) on the oxidation activity, site-directed mutagenesis was performed. A series of Mb mutants, H64D/V68X Mbs, have been prepared by replacing Val-68 with Gly, Ala, Ser, Leu, Ile, and Phe in H64D Mb. All of the mutant proteins are stable enough to be purified except for the H64D/V68G mutant. The oxidation of the substrate thioanisole by H64D/V68X Mb-I besides H64D/V68S was monitored by stopped-flow spectrometer and the sulfoxidation rate constants increase in the order of Phe \leq Val < Leu < Ala < Ile. The results suggest that the volume of hydrophobic residue at the 68 position influences the sulfoxidation activity. A similar pattern is observed for the catalytic sulfoxidation of thioanisole by H64D/V68X Mbs and H₂O₂. The dominant product in the catalytic sulfoxidation is the *R* isomer for the H64D/V68A and H64D/V68S mutants, with more than 84% enantiomeric excess (% ee). However, increasing the polarity of the distal pocket by substituting Ala-68 with Ser in H64D Mb decelerates the catalytic sulfoxidation rate by 2-fold. On the other hand, the H64D/V68I mutant affords dominantly the *S* isomer with the highest turnover rate up to 413 turnover/min. The substitution of Val-68 with Leu has little effect on enantioselectivity in the catalytic sulfoxidation but increases the reactivity with H₂O₂. Both the value of % ee and rate in the catalytic sulfoxidation decrease for H64D/V68F Mb in comparison with H64D/V68A Mb, implying a large benzyl side chain of phenylalanine at the 68 position inhibits the access of substrate to the heme pocket. Furthermore, the crystal structure of the mutant, H64D/V68A, has confirmed the previous report (*J. Am. Chem. Soc.* 121, 9952–9957, 1999, Matsui *et al.*) on catalytic mechanism and the spectroscopic studies on H64D/V68X Mb phenylethylamine complexes which are prepared to mimic the transition state of thioanisole sulfoxidation, have provided some information on enantioselectivity in the sulfoxidation.

ABBREVIATIONS

Mb, myoglobin;

CPO, chloroperoxidase from the marine *fungus Caldariomyces fumagus*;

compound I, a ferryl porphyrin cation radical;

compound II, a ferryl porphyrin;

Mb-I, myoglobin compound I;

*m*CPBA, *m*-chloroperbenzoic acid;

ABTS, 2,2'-azino-bis(3-ethylbenzothiazoline-6-sulfonic acid).

INTRODUCTION

Over the past decades, site-directed mutagenesis techniques have been used successfully to elucidate the functional roles of key amino acid residues in the active sites of human as well as several mammalian myoglobins. It is now clear that the overall polarity and the size of the distal pocket are key factors in controlling the rate and equilibrium constants for ligand binding.¹⁻⁵ For instance, the mutagenesis studies of His-64 (E7) suggest that for myoglobin the polarity of the residue at the 64 position rather than its size controls ligand entry into the heme pocket.⁶⁻¹⁰ In addition, the replacement of the distal valine, Val-68 (E11), is of interest (Figure 1) because it interacts with the bound ligand and the His-64 (E7) side chain as well as the non-coordinated water molecule in deoxymyoglobin. The mutation of Val-68 (E11) also causes remarkable changes in the ligand binding properties in myoglobin.¹¹⁻¹⁴ However, most of the work has focused on the ligand binding studies rather than the reactivity of the mutants with H₂O₂ and substrates.

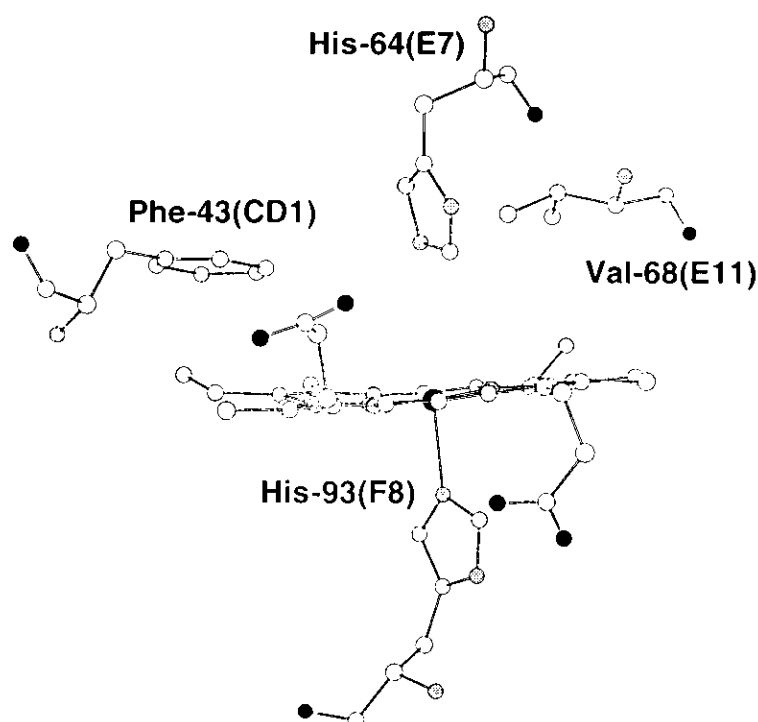


Figure 1. Heme environmental structure of sperm whale myoglobin. Heme and some selected residues including Val-68 (E11) are presented.

Recently, we proved that the distal histidine, His-64 (E7), of sperm whale myoglobin is the critical residue in destabilizing reactive intermediate, compound I (Mb-I), by utilizing the distal histidine deletion mutants (His 64 → Ala, Ser, and Leu) which afford an apparent Mb-I in the reaction with *m*-chloroperbenzoic acid (*m*CPBA).¹⁵ More importantly, the substitution of His-64 (E7) with Asp (H64D Mb) prepared to mimic the active site of chloroperoxidase from the marine fungus *Caldariomyces fumagus*, leads to dramatic increases in the peroxidation and peroxygenation.¹⁶ The aspartate in the distal side might increase the affinity of H₂O₂ to the pocket or/and fix H₂O₂ in a preferable position through the hydrogen bonding interaction.

The distal pocket in sperm whale myoglobin, according to the structure by X-ray diffraction,^{17,18} has no obvious pathway for a ligand to enter or leave due to the tightly packed globin structure. Case and Karplus,¹⁹ on the basis of theoretical dynamics calculations, suggested that a major pathway for ligand entry into the distal pocket of myoglobin lies between Val-68 and His-64. This idea was supported latterly by Kottlam and Case²⁰ in molecular dynamics calculations. Thus, we assume that the characteristics of the residue at the position 68 could affect access of substrates to the heme iron. In an attempt to examine the above assumption, we performed site-directed mutagenesis studies on the distal valine (Val-68, E11) in H64D myoglobin and synthesized a series of novel mutants, so called H64D/V68X Mbs, by the use of the synthetic gene and expression system of Springer and Sligar in 1987.²¹ The mutants provide a series of proteins containing polar and apolar residues of increasing size at the E11 position: Ala, Ser, Val, Leu, Ile, and Phe corresponding to the side chain volumes of 26, 33, 75, 101, 102, 137 Å³,²² respectively. The effects of these substitutions on oxidation activity and enantioselectivity of Mb were assessed as follows.

A key intermediate in the catalytic cycles of heme-containing peroxidase and peroxygenase is a ferryl porphyrin cation radical (O=Fe^{IV} Por⁺) called compound I which is formed by the reaction of the resting ferric enzymes with peroxide.^{23,24} As depicted in Figure 2, compound I can perform two types of oxidations: two sequential one-electron oxidation of substrate like 2,2'-azino-bis(3-ethylbenzothiazoline-6-sulfonic acid) (ABTS)

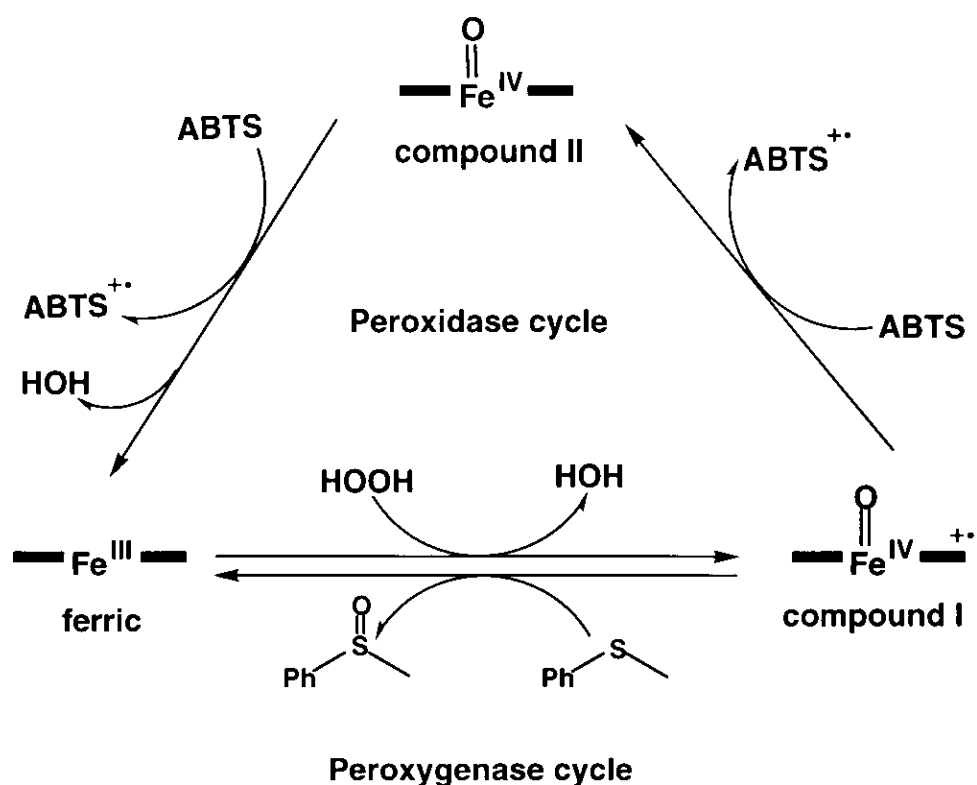


Figure 2. General Catalytic Cycles of Heme Enzymes.

and a ferryl oxygen transfer reaction such as thioanisole oxidation. In this study, we have performed one-electron (peroxidase) as well as two-electron (peroxygenase) oxidations catalyzed by the H64D/V68X mutants to examine effects of residue-68 on oxidation activity and enantioselectivity. To investigate the mechanistic details for the catalytic sulfoxidation, the rate constants of thioanisole oxidation by H64D/V68X Mb-I have been detected under single turnover conditions by the use of double mixing stopped-flow spectroscopy.

On the way to convert myoglobin into a peroxidase-like enzyme, we have successfully elucidated catalytic mechanism in details. However, how substrates gain access to the active sites of Mbs has not been understood completely. Unlike CPO,²⁵ Mb shows poor affinity to the substrate thioanisole, even within molecular dynamics simulation techniques. Thus, we chose 1-phenylethylamine to identify and characterize the heme active site including residue 64 and 68 because the coordination of 1-phenylethylamine to

ferric Mb may have a similar structure to the transition state in thioanisole sulfoxidation as depicted in Figure 3. Although 1-phenylethylamine binding to myoglobin is a dynamic process, the information on the binding should provide “snapshots” that can serve to elucidate the role of the distal residue-68 on enantioselectivity of myoglobin.

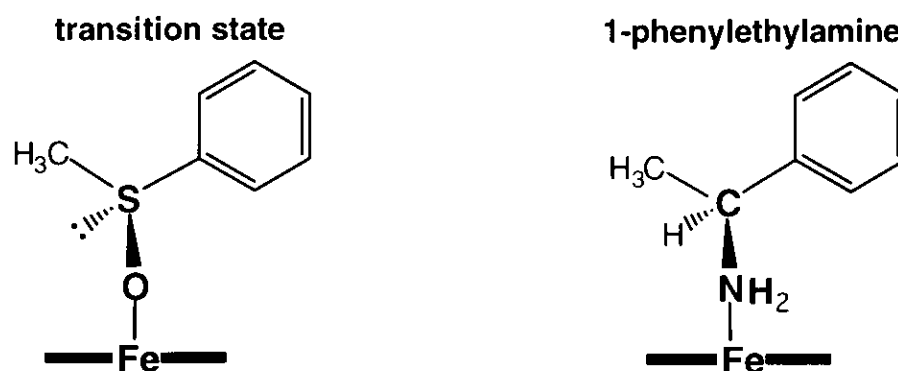


Figure 3. The proposed binding model for thioanisole and 1-phenylethylamine.

Spectroscopic methods have also been the principle tools employed here in elucidating the nature of binding between substrates and the heme iron. We have confirmed the spin state of the heme iron for the 1-phenylethylamine-Mb binding complex by UV-visible spectroscopy as well as EPR (electron paramagnetic resonance) spectroscopy at 14 K. Finally, we have attempted to solve the crystal structures of the mutants in the presence or absence of 1-phenylethylamine to understand the catalytic mechanism and the substrate binding mode.

EXPERIMENTAL PROCEDURES

Materials. All the chemicals were obtained from Wako and Nakalai Tesque, and used without further purification. The buffers used for the reactions were 50 mM sodium phosphate (pH 7.0) and 50 mM sodium acetate (pH 5.0), as well as 20 mM Tris-HCl (pH 9.0).

Preparation of the Myoglobin Mutants. The H64D/V68X (X represents A, S, V, I, L, F residues) sperm whale myoglobin mutants were constructed by the cassette

mutagenesis. The expression vector for wild type sperm whale Mb was a gift from Dr. J. S. Olson (Rice University, Houston, TX). The cassette including the desired His-64 and Val-68 substitutions and a new silent *HpaI* restriction site was inserted between the *BglII* and *HpaI* sites. Expression in *Escherichia coli* strain TB-1 and purification of the mutants were performed following the previous reports.⁷ To ensure that the proteins used in the experiments were all in the ferric form, the sample was oxidized by the addition of a small excess of potassium ferricyanide. Excess oxidant was subsequently removed by gel filtration on a column packed with Sephadex G-25 equilibrated with the reaction buffer. The final purified protein was stored at -80 °C until used.

Catalytic Sulfoxidation of Thioanisole. To a solution of either wild type Mb (5 μM) or Mb mutants (0.1 – 0.5 μM) in 0.5 mL of 50 mM sodium phosphate buffer (pH 7.0), the substrate of thioanisole (1 mM) was added and then H_2O_2 (1 mM) as the oxidant to start the sulfoxidation. After the incubation at 25 °C, the mixture was extracted with dichloromethane for HPLC analysis on a Daicel OD chiral-sensitive column installed on a Shimadzu SPD-10A spectrophotometer equipped with a Shimadzu LC-10AD pump system.²⁶ Standard curve prepared with commercial phenyl methyl sulfoxide was used for quantitative analysis. The absolute stereochemistry was determined based on a retention time. A linear relationship between time *versus* product formation was observed for at least 5 min for all except for H64D and H64D/V68L Mbs, but the incubations were stopped at 2 min in determination of turnover rates for all of the mutants. The sulfoxide formed in control incubations without enzyme was subtracted when necessary.

Catalytic Oxidation of ABTS. Activity for one-electron oxidation of ABTS was measured at 20 °C in 50 mM sodium phosphate buffer (pH 7.0) on a Shimadzu UV-2400 spectrophotometer. At least two experiments were performed for each experimental point. The formation rate of the ABTS cation radical was monitored at 730 nm ($\epsilon_{730} = 1.4 \times 10^4 \text{ M}^{-1} \text{ cm}^{-1}$)¹⁶ where the absorption of Mb was negligible. The reaction mixture contained 1 mM ABTS and variable amounts of H_2O_2 (0.2 – 1.0 mM). Final concentrations for H64D/V68X Mbs were in the range of 0.05 – 0.5 μM .

Reaction with *m*CPBA or Hydrogen Peroxide. All the spectral changes were monitored on a Hi-Tech SF-43 stopped-flow apparatus equipped with a MG6000 diode array spectrophotometer. An optical filter (360 nm) was used to avoid possible photoreduction of compound I by UV light. The reactions with *m*CPBA were carried out at pH 5.0 for observing a complete accumulation of compound I.¹⁵ Rate constant of thioanisole oxidation by Mb compound I was determined by means of a double-mixing rapid scan technique at 5.0 °C and pH 5.0. The first mixing of ferric Mb with a slight excess of *m*CPBA (1.3 – 2 mol equivalents) resulted in more than 70% accumulation of compound I, which was subsequently mixed with at least 10-fold excess of thioanisole. The bimolecular rate constants were calculated from observed rates at the least four different concentrations of the substrate thioanisole. The reaction for H64D/V68L Mb with H₂O₂ was performed at 20 °C and pH 7.0 because the compound I intermediate was best observed at pH 7.0 when H₂O₂ as an oxidant. The reduction of H64D/V68L Mb-I in the presence of thioanisole was performed at 5.0 °C (pH 5.0).

Spectroscopic Binding Studies. All UV-visible measurements were done at 20 °C on a Shimadzu UV-24000 spectrophotometer. Electronic absorption spectra for H64D/V68X Mbs were recorded in 20 mM Tris-HCl buffer (pH 9.0). Spin shift by 1-phenylethylamine on the mutant was induced as follows: 10 μ L of a 1 M solution of (*R*)- or (*S*)-1-phenylethylamine was added into a 3 mL solution of \sim 4.0 μ M mutants, each time. Then UV-visible spectral changes were monitored until Soret band did not shift.

EPR spectra were recorded on a Bruker E500 X-band CW-EPR spectrometer fitted with an Oxford liquid helium flow-cryostat ESR-910 at a 100 kHz field modulation and 14 K. Highly concentrated ferric H64D/V68A, H64D/V68V and H64D/V68I Mbs were dialyzed overnight against 20 mM Tris-HCl buffer (pH 9.0) for the background EPR spectrum. To obtain the amine binding complex sample, the mutants were dialyzed overnight against the same buffer containing 5 – 20 mM of (*R*)- or (*S*)-1-phenylethylamine, respectively. Color of the Mb-amine-complex solution changed from brown to red during the dialysis.

X-ray Crystallography. Crystals were grown in the P6 space group using

hanging drop method. 10 μ L of 65 mg/mL HPLC cation ion column-purified protein was mixed with a solution of 3.2 M ammonium sulfate, 20 mM Tris-HCl, and 1 mM EDTA (pH 9.0) to give a final concentration of 2.4 – 2.6 M ammonium sulfate. The hanging drops were set up at room temperature and incubated at 4.0 °C. The crystal was mounted and the diffraction data were collected at room temperature.

RESULTS

Spectroscopic Features of H64D/V68X Mbs. The Soret absorption band is known to be sensitive to the coordination structure of hemoproteins.²⁷⁻³⁰ Ferric H64D/V68X Mbs except for H64D/V68I exhibit similar absorption spectra to that of the wild type including the Soret maximum, centered around 408 nm (Table 1), which are typical of hexa-coordinated ferric high-spin heme.^{17,18} The sixth ligand in the wild type is a water molecule stabilized by His-64 through a hydrogen-bonding.³¹ However, ferric H64D/V68I Mb exhibits a blue-shifted Soret maximum at 396 nm (Table 1) which suggests that the mutant loses the water ligation and shows a typical penta-coordinated protein.³²

Table 1. Coordination Geometry of Wild Type Mb and Its Mutants

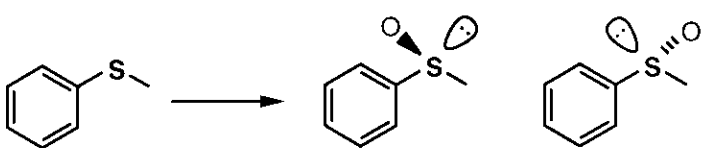
Soret peak	Coordination structure	Proteins
~408nm	6c-HS*	wild type
		H64D/V68A
		H64D/V68S
		H64D/V68V
		H64D/V68L
396nm	5c-HS*	H64D/V68I

*c-HS indicates coordination heme structure.

Catalytic Sulfoxidation of Thioanisole. The catalytic sulfoxidation (peroxy-generation) of thioanisole was examined at 25 °C and pH 7.0. The results are shown in Table 2. Myoglobin catalyzes the sulfoxidation of thioanisole with the incorporation of an

oxygen atom from the peroxide into the sulfoxide via a ferryl oxygen transfer mechanism.^{33,34} The H64D/V68X mutants retain the sulfoxidation activity, but they show different enantiospecificity and turnover rate from the distal histidine relocation or deletion myoglobin mutants.³⁵

Table 2. Catalytic Sulfoxidation of Thioanisole by Mbs and H₂O₂.



	WT	H64D/ V68A	H64D/ V68S	H64D/ V68V	H64D/ V68L	H64D/ V68I	H64D/ V68F
ee% ^a	25	84	88	6.0*	3.2	25(<i>S</i>)	46
rate ^b	0.25	121	64	145*	261	413	48

^a The absolute stereochemistry of the dominant isomer is *R* except where indicated.

^b The unit for rate is turnover per minute. *Data refer to ref 16.

The H64D/V68A and H64D/V68S mutants show almost the same enantioselectivity, in that both give *R* isomer as a major product with an enantiomeric excess of 84% and 88%, respectively. In contrast, H64D Mb yields almost racemic product (only 6% ee *R*-isomer sulfoxide). The turnover rate in the sulfoxidation decelerates 2-fold for the H64D/V68S than H64D/V68A mutant. It appears that hydroxyl group on Ser-68 has an effect on the reactivity but not on the enantioselectivity of Mbs. When the residue at position 68 is substituted by phenylalanine in H64D/V68F Mb, both turnover rate and enantioselectivity in the sulfoxidation decrease 2 – 3 times compared with H64D/V68A Mb. Instead, % ee value in the reaction by H64D/V68F Mb increases 8-fold against H64D/V68V Mb (i.e. H64D). Interestingly, H64D/V68I Mb shows different enantioselectivity and reactivity from other H64D/V68X Mbs in the reaction. The dominant isomer is (*S*)-sulfoxide (Table 2) with the value of 25% ee in the sulfoxidation. In addition, H64D/V68I Mb shows 3-fold higher reactivity than H64D Mb, which has been the best enzyme in terms of the sulfoxidation rate. However, H64D/V68L Mb in which

Leu-68 has the similar volume to Ile (the volume of Leu and Ile is 101 and 102 Å³, respectively), does not exhibit different enantioselectivity compared to that of H64D Mb and it performs the sulfoxidation reaction by 2-fold faster than the H64D mutant.

Oxidation of Thioanisole by H64D/V68X Mb Compound I. In the case of peroxidase such as native HRP, compound I, a ferryl porphyrin radical cation has been well characterized as a catalytic species equivalent to the proposed active intermediate of P450. Recently, a ferryl porphyrin radical cation species (O=Fe^{IV} Por^{•+}) of myoglobin, equivalent to compound I of peroxidase, has been confirmed as the catalytic species of a two-electron oxidation process by the His-64 deletion Mb mutants.^{15,16} In this study, we have found that H64D/V68X Mbs show much different reactivity in the catalytic sulfoxidation of thioanisole (Table 2). In order to elucidate the catalytic mechanism by H64D/V68X Mbs and examine the roles of residue at the position 68 on catalytic species reactivities in the oxidation of thioanisole, we have performed double mixing stopped-flow experiments at 5.0 °C and pH 5.0. An oxidant, *m*-chloroperbenzoic acid (*m*CPBA), was used to generate compound I in the first mixing, and sulfide was added to compound I in the second mixing. UV-visible spectra began to be collected just after the second mixing to monitor the spectral changes.

Figure 4 (A) shows absorption spectral changes in the reaction of ferric H64D/V68L Mb with *m*CPBA. The decrease in the absorbance of the Soret and the increase in the absorbance around 650 nm are indicative of the compound I formation from the ferric state. The H64D/V68X mutants except for H64D/V68S afford more than 70% accumulation of Mb-I based on the Soret intensity in the reaction with 1.3 – 2 equivalents of *m*CPBA. In the case of H64D/V68S Mb, no compound I but compound II accumulation is observed under the same reaction condition (spectra not shown).

Upon the mixing with thioanisole, H64D/V68L Mb-I species reduces directly back to the ferric form with complete recovery of the Soret intensity (Figure 4 (B)). Essentially the similar spectral changes were observed for other H64D/V68X Mbs besides H64D/V68S

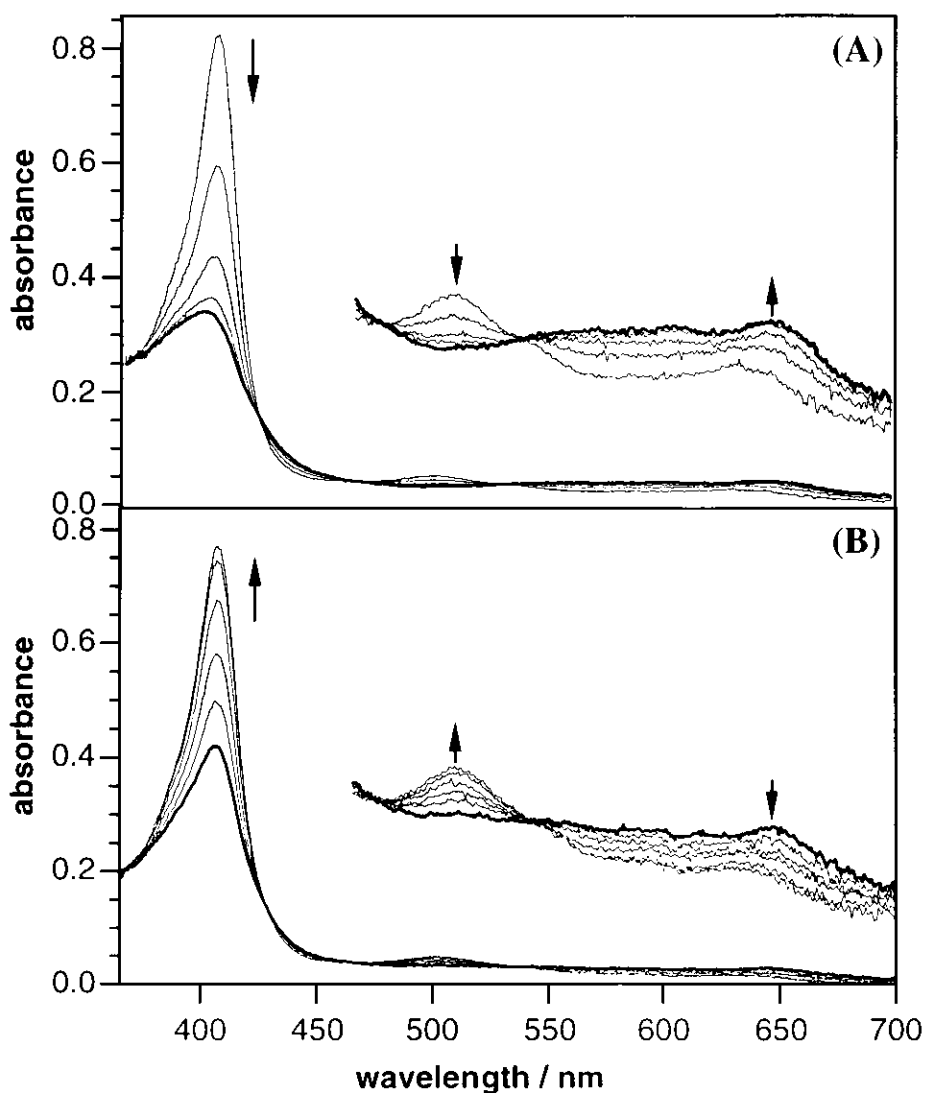


Figure 4. Rapid-scan absorption spectra of formation (A) and reduction (B) of H64D/V68L Mb-I (thick line) in 50 mM sodium acetate buffer at 5.0 °C and pH 5.0. Directions of the spectral change were indicated in the figure by arrows.

(A) the reaction with *m*CPBA: final concentrations, 4.5 μ M Mb, 100 μ M *m*CPBA.

(B) final concentrations: 4.3 μ M Mb, 7.5 μ M *m*CPBA, 50 μ M thioanisole. The spectra were recorded for 24-360 ms after mixing with a 1.2 s interval.

in the reactions. Since compound II ($O=Fe^{IV}$ Por), bearing one oxidation equivalent with respect to the ferric state, is not observed, the sulfoxidation catalyzed by H64D/V68X Mbs appears clearly to proceed with a direct two-electron oxidation of thioanisole. The time course of Mb-I reductions using the absorbance increase at 406 nm obeyed pseudo-first-order kinetics and fit well to single exponential expressions. The rate constants are

summarized in Table 3. The reactivity for H64D/V68X Mb-I increases in the order of Phe \leq Val < Leu < Ala < Ile.

Catalytic Oxidation of ABTS. In order to estimate the reactivity with H₂O₂ for ferric H64D/68X Mbs, we performed the one-electron oxidation (peroxidation) of ABTS supported by H₂O₂ at 20 °C and pH 7.0. The results are shown in Figure 5.

Among H64D/V68X double mutants, only the H64D/V68L mutant shows approximately 2-fold higher reactivity than the H64D mutant in the ABTS oxidation, and

Table 3. Rate Constants of Thioanisole Oxidation by H64D/V68X Mb-I in 50 mM Sodium Acetate Buffer (pH 5.0) at 5.0 °C.

	H64D/ V68A	H64D/ V68S	H64D/ V68V	H64D/ V68L	H64D/ V68I	H64D/ V68F
k	445	ND	220*	386	642	219

The unit for k is mM⁻¹s⁻¹. *Datum is taken from ref 16.

ND: compound I was not observed in the reaction with *m*CPBA.

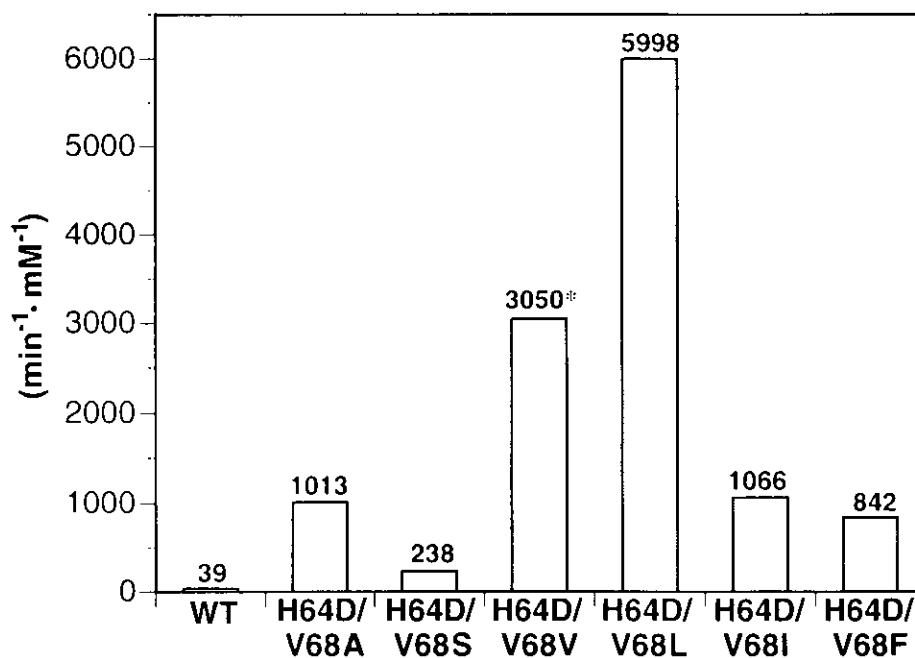


Figure 5. Rate constants for catalytic oxidation of ABTS and H₂O₂ by wild type Mb and the H64D/V68X mutants at 20 °C in 50 mM sodium phosphate buffer (pH 7.0).

* Datum refers to ref 16.

the reactivity of others decreases in comparison with H64D Mb. On the one hand, the rate constant in the oxidation of ABTS by the H64D/V68A mutant is over 4-fold greater than that by H64D/V68S Mb. Interestingly, when the residue-68 is replaced by a larger one like Ile or Phe, H64D/V68I and H64D/V68F Mbs show the reactivity similar to H64D/V68A Mb in the oxidation. On the other, H64D and H64D/V68L Mbs show extraordinarily high reactivity in the ABTS oxidation, 70- and 150-fold greater than the wild type respectively.

Reactions of Ferric Myoglobin with Hydrogen Peroxide. Ferric wild type Mb reacts with H_2O_2 to yield a ferryl heme ($O=Fe^{IV}$ Por), equivalent to compound II of peroxidase. As reported previously,^{15,36,37} the instability of Mb-I could be resulted from its rapid reduction by the distal histidine which is located very close to the heme center in wild type Mb. More recently, H64D Mb prepared by our research group, showed the formation of compound I in the reaction with H_2O_2 .¹⁶ In this study among H64D/V68X double mutants, only H64D/V68L Mb yields a detectable amount of compound I with H_2O_2 .

In the reaction with H_2O_2 , ferric H64D/V68L Mb affords 90% compound I accumulation (based on Soret intensity). To our knowledge, this is the first example in Mb mutants which produces almost pure compound I by H_2O_2 (Figure 6). As shown in Figure 6, the spectral changes clearly indicate the accumulation of an intermediate species prior to the compound II formation, which has characteristics of compound I formation: Soret absorption decreasing to almost the half and a broad visible band having a peak around 650 nm appeared. Upon the addition of thioanisole into the reaction of ferric H64D/V68L Mb and H_2O_2 , the compound I-like species goes directly back to the ferric state. The observation can be rationalized by the rapid reduction of compound I to the ferric state by thioanisole.

To determine the rate of compound I formation with H_2O_2 for H64D and H64D/V68L Mbs, we next performed single mixing stopped-flow experiments at 20 °C and pH 7.0. In Figure 7 is shown experimental trace of absorbance at 415 nm *versus* time in the reaction of 1 mM H_2O_2 with H64D and H64D/V68L Mbs, respectively. The amount of compound I formation for H64D/V68L Mb is greater than that for H64D Mb. Since the

accumulation of compound I for both mutants with 1 mM H_2O_2 is evident, the observed rate of compound I formation are determined to be 55.2 s^{-1} (standard error 1.4) and 106 s^{-1} (standard error 2.2) for H64D and H64D/V68L Mbs, respectively. Herein, the reactivity with H_2O_2 by H64D/V68L Mb is about 2-fold higher than that by H64D Mb. The results might suggest that Lue-68 cooperates with Asp-64 in the distal pocket of Mb to fix H_2O_2 more efficiently, probably through a hydrogen-bonding, although the detailed mechanism of H_2O_2 activation by both H64D/V68L and H64D Mbs remains to be clarified.

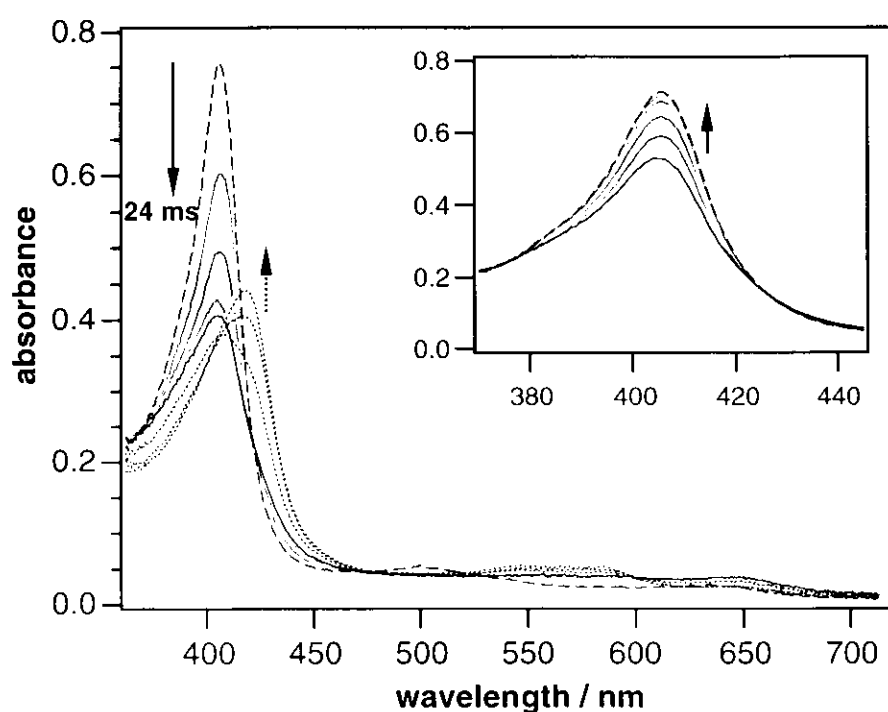


Figure 6. Absorption spectral changes of H64D/V68L Mb upon mixing with 1 mM H_2O_2 at 20 °C in 50mM sodium phosphate buffer, pH 7.0. The spectra were recorded before mixing (broken line) and at 6, 12, 20, 24 ms (solid line), 0.2, 0.4, 0.6 sec (dotted line) after mixing. (Inset) The reduction of H64D/V68L Mb-I (thick solid line) in the presence of 100 μM thioanisole. The spectra recorded before mixing and 10, 30, 60, 90, 160 ms (thin solid and dotted line) after mixing.

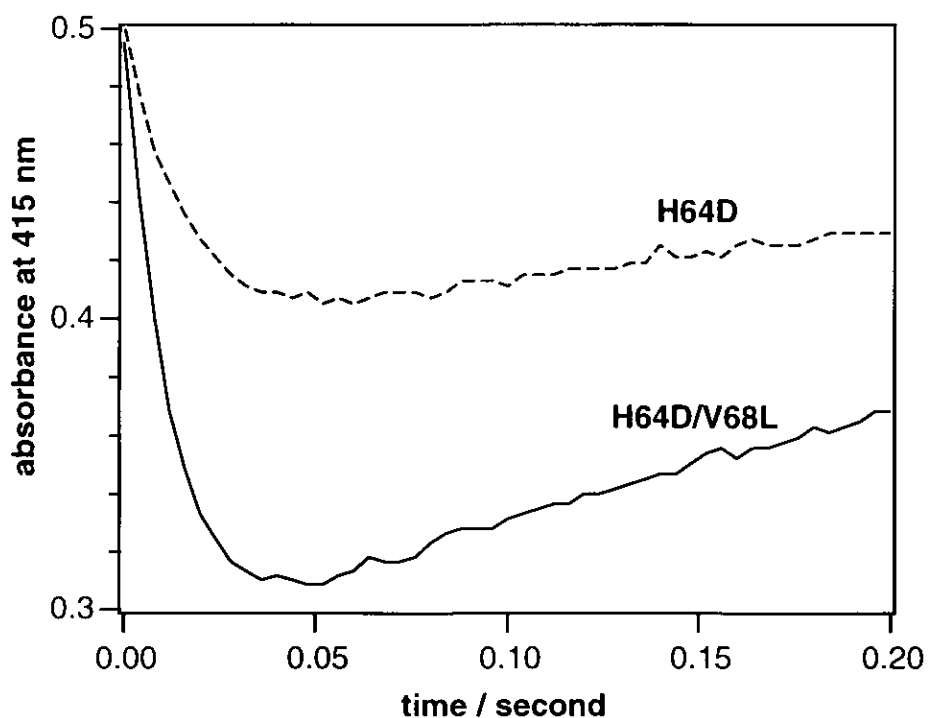


Figure 7. Experimental trace of absorbance at 415 nm vs. time resulting from the reaction of 1 mM H_2O_2 and 5 μ M Mbs at 20 °C and pH 7.0.

Spectroscopic Study on the Substrate Binding. In order to obtain the information on the transition state of thioanisole oxidation by H64D/V68X Mb-I, we performed the spectral titration of the enzyme with (*S*)- and (*R*)-1-phenylethylamine (called amine as follows). The amine binding complex is expected to be a transition state analogue of the sulfoxidation.

H64D/V68A Mb has Soret maximum at 408 nm of UV spectrum (Figure 8), indicating the heme state of hexa-coordinated high spin.¹⁷ In the presence of 10 mM of *S*-amine, the Soret band shifts to 413 nm with the decrease in the absorbance. In the visible region, the 632 nm absorption band of the ferric state disappears by the addition of the *S*-amine. The absorption spectrum of H64D/V68A Mb-amine-complex, having a β -band at 532 nm and an α -band shoulder around 560 nm, is typical low-spin ferric hemoprotein.³⁸ More importantly, H64D/V68A Mb exhibits different enantio-preferences in binding with *R*- and *S*-isomer of amine based on Soret band change in the amine titration (Figure 9). Basically, other H64D/V68X mutants can also distinguish *R*- and *S*-isomer of amine in UV-visible spectral changes (see the discussion below).

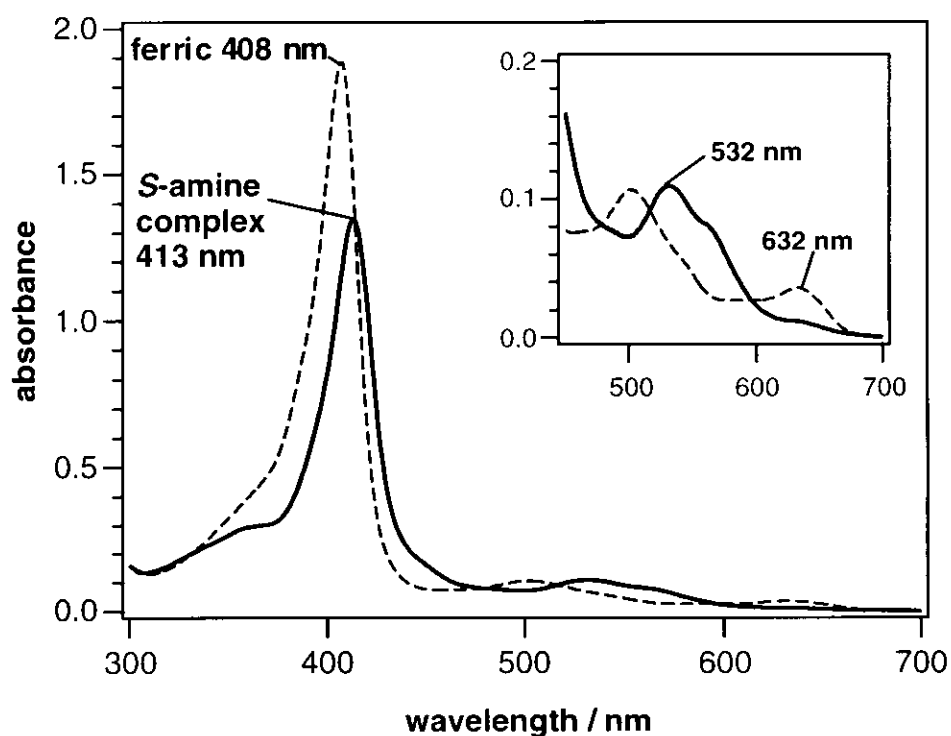


Figure 8. Absorption spectral change for H64D/V68A Mb in the presence of (*S*)-1-phenylethylamine in 20 mM Tris-HCl buffer (pH 9.0). The concentration of Mb is 10 μ M, and (*S*)-1-phenylethylamine is 10 mM. Inset: Expand of Q-band.

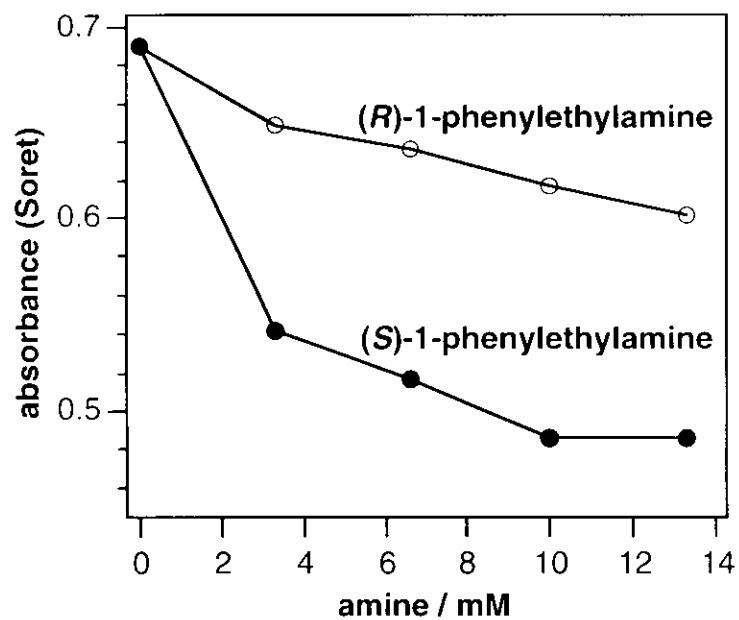


Figure 9. Different preference of H64D/V68A Mb on (*S*) and (*R*)-1-phenylethylamine.

Figure 10 presents the electron paramagnetic resonance (EPR) spectra at 14 K and pH 9.0 of the ferric H64D/V68A Mb and its *S*-amine complex.

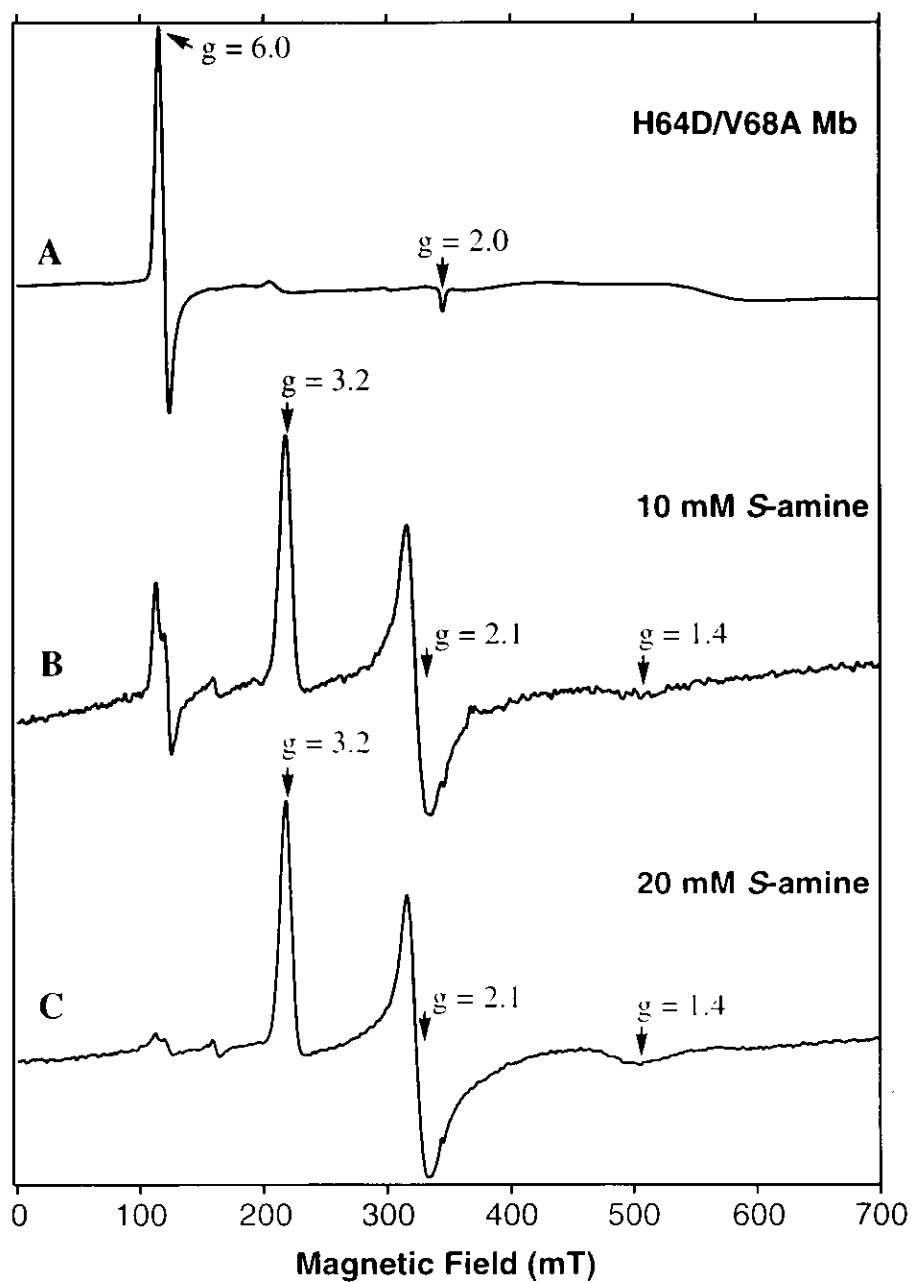


Figure 10. EPR spectra of ferric H64D/V68A Mb and its (*S*)-1-phenylethylamine complex as curve A, B, C, respectively. Measurements were carried out at 14 K in 20 mM of Tris-HCl buffer (pH 9.0).

The spectra of ferric H64D/V68A Mb is analogous to that of the wild type, indicating the high-spin protein with rhombically split signals in the $g = 6.0$ and $g = 2.0$ region. In the presence of *S*-amine (10 mM), the amplitude of the high spin EPR signal of ferric H64D/V68A Mb reduces and three new EPR signals appear at low spin field with $g_1 = 3.2$, $g_2 = 2.1$ and $g_3 = 1.4$. When the concentration of *S*-amine increases to 20 mM, almost all of high spin signal for ferric H64D/V68A Mb turns into the low spin. To examine the heme iron spin state of H64D/V68X Mb-amine-complexes extensively, we have performed EPR measurement with the three typical mutants (H64D/V68A, H64D and H64D/V68I) in 10 mM of *R*- and *S*-amine isomers, except for H64D Mb in 5 mM of *R*-amine (Figure 11).

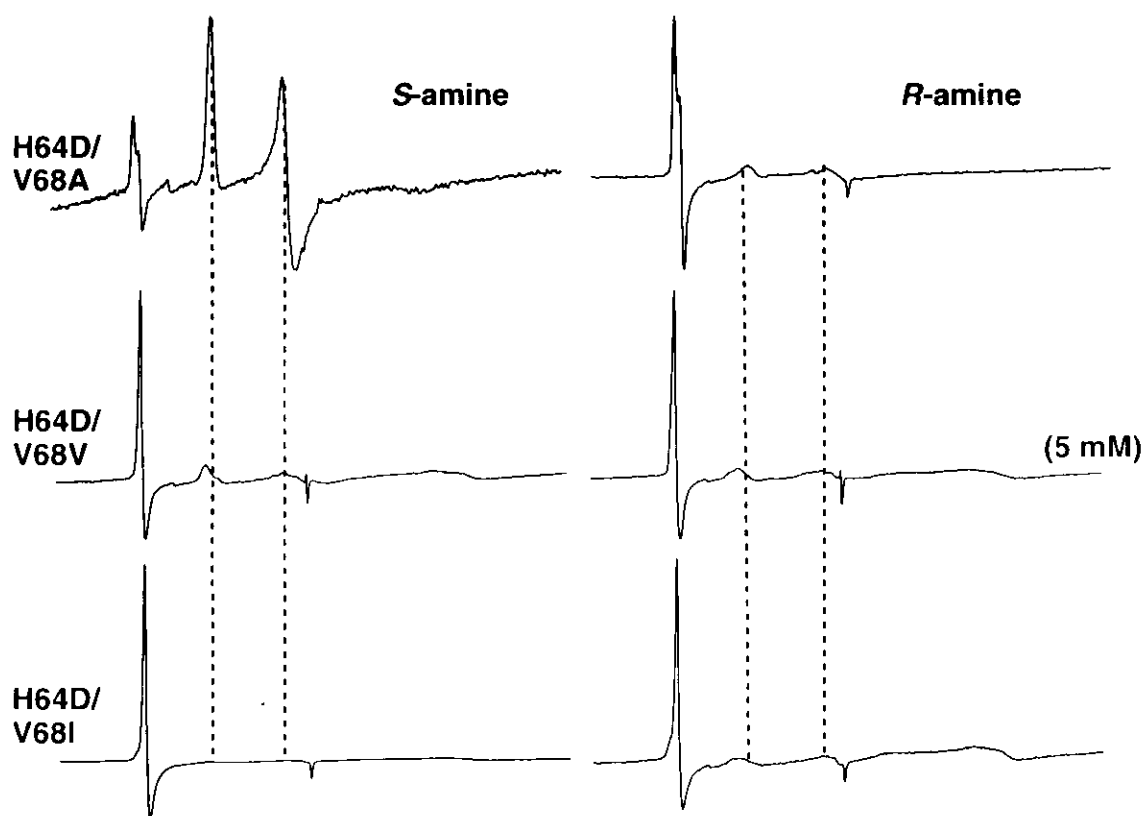


Figure 11. Preferences of (*S* or *R*)-1-phenylethylamine binding on three Mbs in the development of EPR signals, respectively. Amine concentration was 10 mM except where indicated. EPR measurements were carried out at 14 K in 20 mM of Tris-HCl buffer (pH 9.0).

H64D/V68A Mb prefers *S*-amine much to *R*-amine, that is high spin signal of ferric H64D/V68A by *S*-amine reduces greater, giving distinct low spin signals, than by *R*-amine. However in case of H64D/V68I Mb, there is smaller difference between *R* and *S*-amine binding complexes than that in H64D/V68A. Interestingly, H64D can not endure 10 mM of *R*-amine in which the mutant denatures (spectrum not shown), although the mutant prefers *R*-amine to *S*-amine (i.e almost same spectral changes in 10 mM of *S*-amine and 5 mM of *R*-amine). Therefore, the EPR study is in support of the UV-visible results: (1) Amine can coordinate to the heme iron of H64D/V68X Mbs. (2) H64D/V68X Mbs can discriminate between *R*- and *S*-amine isomers.

Crystal Structure of Ferric H64D/V68A Mb. The H64D/V68X mutations (X represents A, S, V, I, L, F residues) to change size and polarity of residue at the 68 position affect the oxidation activity and enantioselectivity in catalytic sulfoxidation of thioanisole. In an attempt to interpret roles of the residue-68 of Mb on the catalytic oxidation, the crystal structures of the H64D/V68X mutants with and without 1-phenylethylamine in the active site are being under determination. Among them, the structure of H64D/V68A Mb has been solved. The mutant exhibits few structural changes upon the double mutations outside the immediate vicinity of the substituted residues. The carboxyl group side chain of Asp-64 in the mutant is directed away from the heme center and towards the adjacent asparagine in a weak hydrogen-bond (3.71 Å, Figure 12). The additional water molecule, compared with the wild type structure, is found in the active site of H64D/V68A Mb.³⁹ The coordination structure of the ferric heme iron (aquo-hexacoordination) of H64D/V68A Mb is consistent with its absorption spectrum (Table 1), in which the coordinated water molecule might be stabilized by a hydrogen-bond with the distal Asp-64 through the additional water molecule in the active site. The distance between O₇ of the distal asparatate and the ferric heme iron is 7.71 Å, which is located farther from the heme center than that of the distal glutamate in CPO (5.06 Å).

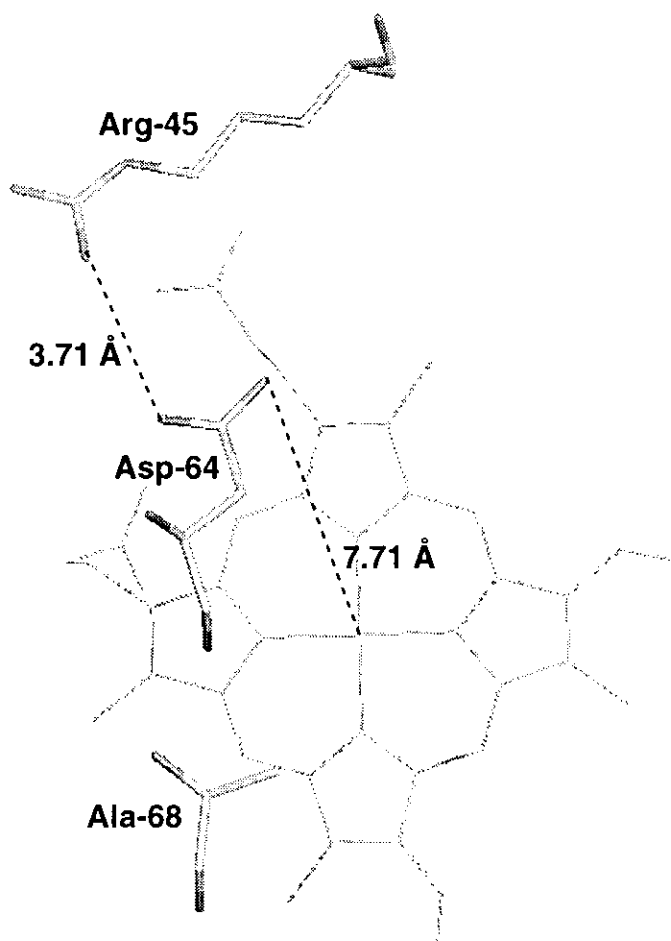


Figure 12. Top view of H64D/V68A Mb crystal structure. Residues 68, 64, 45 are shown.

DISCUSSION

Effects of Residue-68 on Catalytic Activity. The H64D/V68A mutation, by comparison with the H64D mutant, involves the substitution of the isopropyl side chain of valine with a smaller side chain of alanine. Such a replacement seems to alter the stereochemistry of the distal heme pocket in myoglobin. For example, the (*R*)-methyl phenyl sulfoxide is formed by H64D/V68A Mb with 84% ee while the H64D mutant affords only 6% ee.

It is known that polar interactions in the distal pocket are important for a ligand binding process. A good example is that the Val-68 → Thr mutation in pig myoglobin resulted in a 5-fold decrease in CO affinity.^{10,12} The effect has been interpreted in terms of stabilization of the noncovalently bound water molecule in the distal pocket, which inhibits replacement of the water molecule by other ligands through hydrogen bonding either to

His-64 or to Thr-68. In order to examine the effects of polarity of the residue-68 on catalytic activities in sperm whale myoglobin, we have constructed the mutant in which the distal Ala-68 of H64D/V68A Mb is replaced with a serine residue. Since the side chains of serine and alanine are similar, the influence of polarity may be examined without significant alteration of the volume of the distal pocket. The Ala-68 \rightarrow Ser mutation decreases about 2-fold in the sulfoxidation rate and 4-fold in ABTS oxidation activity. In addition, only compound II (spectra not shown) is observed in the reaction with *m*CPBA by spectral changes in stopped-flow experiments. The results suggest that compound I formation is depressed by the mutation. However, the enantiospecificity of the H64D/V68S mutant retains almost same as that of H64D/V68A Mb in the catalytic sulfoxidation (Table 1). These observations demonstrate unambiguously that the Ala-68 \rightarrow Ser substitution in H64D/V68A Mb decreases both one- and two- electron oxidation activity possibly due to the destabilization of compound I as is known that polar residues in the heme pocket remarkably decreased the overall stability of apomyoglobin.⁴⁰ Alternatively, the hydroxy group of Ser-68 might be in a position to form hydrogen-bond with the water molecule either bound or unbound to the iron so that the stabilized water molecule decelerates the rate of H₂O₂ binding to the ferric form of the H64D/V68S mutant. The size instead of polarity of the amino acid residue at position 68 contributes to the enantioselectivity of the catalytic sulfoxidation.

H64D/V68X Mbs, with the exception of the H64D/V68S mutant, afford compound I in the reaction with *m*CPBA. The oxidation of thioanisole by compound I is accelerated in the order of Phe-68 \leq Val-68 < Leu-68 < Ala-68 < Ile-68, which indicates that the residue-68 is a part of the overall kinetic barrier. In Figure 13 is shown the plots of activities for the catalytic sulfoxidation by H₂O₂ and of rates for thioanisole oxidation by compound I *versus* substituted residues at the position 68 in H64D/V68X Mbs. The reactivity of Mb mutants with H₂O₂ is estimated by the catalytic oxidation of ABTS (see the discussion below). The substitution effect at the 68 position on the reactivity of the Mb mutants and H₂O₂ is somewhat different from thioanisole oxidation by compound I. The overall catalytic activity of thioanisole oxidation by Mb mutants / H₂O₂ is, thus, sum of

the formation and reaction of compound I.

It should be noticed that H64D/V68I Mb shows the highest reactivities in thioanisole oxidation by compound I and the catalytic sulfoxidation by H_2O_2 among H64D/V68X Mbs (Table 2, 3). More intriguingly, it is the first Mb mutant which possesses different stereochemistry from others, giving *S*-isomer as a major product in the catalytic sulfoxidation of thioanisole. However, an exact detailed interpretation for the unique enantioselectivity of the H64D/V68I mutant requires the determination of high-resolution structure of the protein.

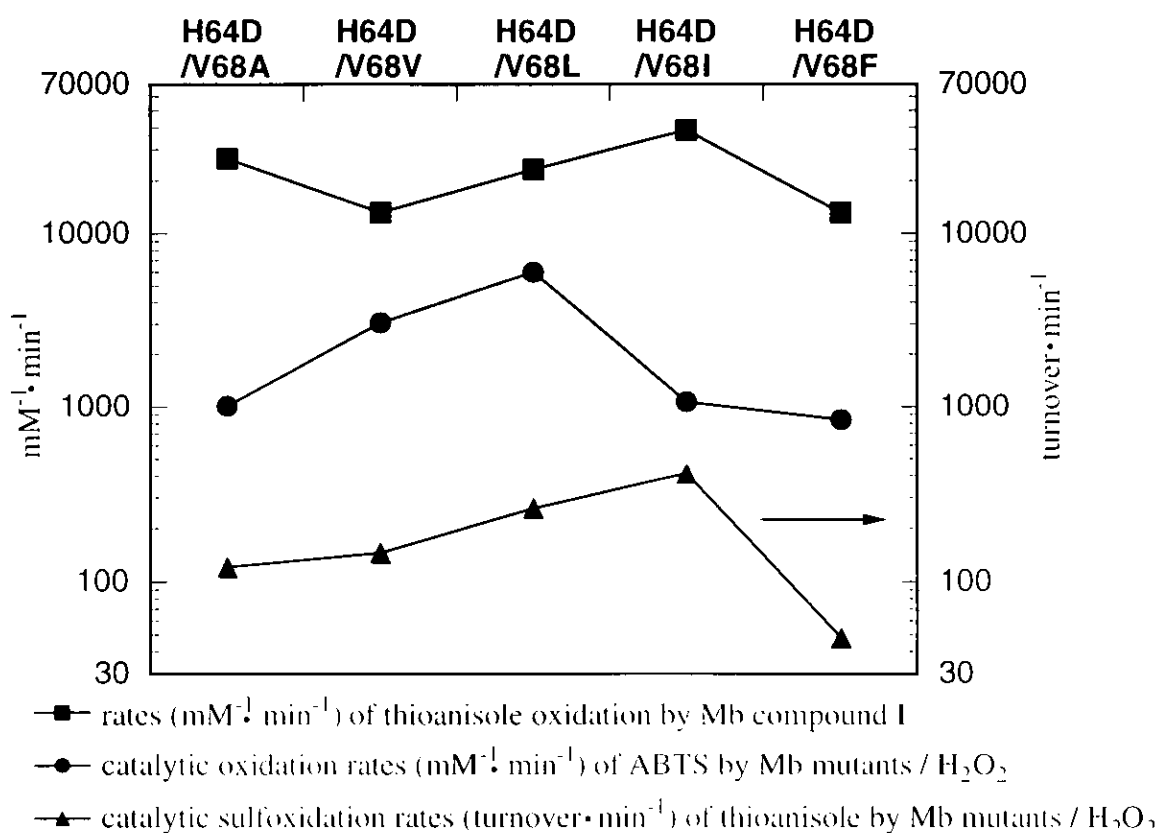


Figure 13. Dependence of catalytic activity and compound I reactivity on the size of the residue 68 (E11).

Apparently, ABTS oxidation was not affected by the residue-68. The results imply that the oxidation could occur either at the protein surface as in cytochrome *c* peroxidase (CcP) or the heme edge as was proposed for horseradish peroxidase (HRP).⁴¹⁻⁴⁴ The observed rate of ferric wild type Mb with H_2O_2 (1 mM) could be determined to be 0.51

s⁻¹, where compound I formation was kinetically negligible.⁴⁵ However, compound I formation rates with 1 mM H₂O₂ in this study are determined to be 55.2 s⁻¹ (standard error 1.4) and 106 s⁻¹ (standard error 2.2) for H64D and H64D/V68L Mb, respectively. As shown in Figure 14, the parallel trends of ABTS oxidation activity and compound I formation rate by H₂O₂ suggest that the factors controlling peroxidation activity of Mb are the formation rate and stability of compound I.

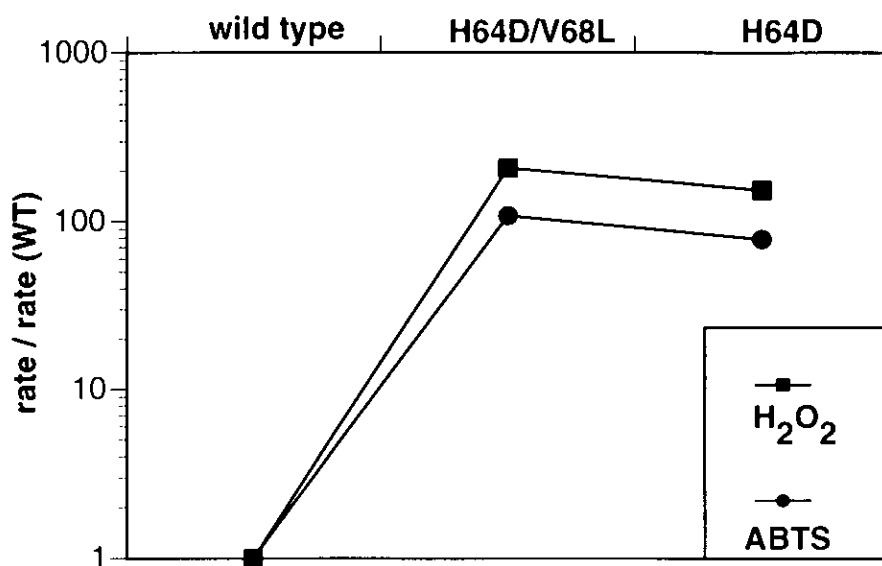


Figure 14. Correlation of ABTS oxidation activity and compound I formation rate with H₂O₂ for H64D and H64D/V68L Mbs, respectively.

Catalytic Mechanism and Enantioselectivity. Although all of H64D/V68X Mb X-ray crystallographic data are not available at this moment, the crystal structure of H64D/V68A Mb has provided the framework in part for interpreting the functional roles of residues at the 64 and 68 positions.

H64D Mb was prepared to mimic the active site of CPO in which Glu-183 residue has been proposed to function as a general acid-base catalyst because the side chain of Glu-183 is positioned directly to the peroxide-binding site.⁴⁶ Through close examination of the crystal structure of H64D/V68A Mb (Figure 12), we find that the carboxyl side chain of Asp-64 is in a distance of 7.71 Å away from the heme iron and lies towards Arg-45, which has a weak hydrogen-bonding interaction (i.e. 3.7 Å) with Asp-64. The carboxyl group of

aspartate is farther away by 2.6 Å from the heme iron than that in Glu-183 of CPO (Glu-183 lies at 5.06 Å from the heme iron.). Thus, it seems that the carboxyl group of Asp-64 in H64D/V68A Mb is not capable of directly working in an acid-base catalytic mechanism required to cleave the peroxide O-O bond in the formation of compound I. This conclusion is in good agreement with the previous report by Matsui, in that Asp-64 in H64D Mb did not appear to function as a general acid-base catalyst in the activation of H₂O₂.¹⁶ Obviously, the polarity of the distal pocket plays a major role in catalytic mechanism through increasing the affinity of H₂O₂ to the pocket or/and fixing H₂O₂ in a preferable position.

In general, when a cavity in a protein is created by a “large-to-small” substitution, the surrounding residues relax somewhat to reduce the volume of the cavity.⁴⁷ In the case of the Val-68 to Ala mutation of H64D Mb, the distal pocket is likely to be open and readily accessible to solvent so that more than one water molecules are present near the heme iron.³⁹ Thus, an extensive hydrogen-bonding network could engage in the catalytic oxidation, leading to about 500-fold higher activity in the catalytic sulfoxidation for the H64D/V68A mutant than the wild type (Table 2).

By the comparison of the crystal structures of the H64D/V68A mutant and the wild type (Figure 15), several factors in the mutant manifest the increased cavity in the active site. 1) The side chain of Asp-64 in the mutant turns round about 100° relative to imidazole ring of the distal histidine which is almost vertical to the heme group in the wild type. 2) Ala-68 of the mutant has smaller volume than Val-68 in the wild type. 3) The rotation of the side chain in residue-64 has forced Arg-45 to swing out of the way in the active site. Such an architecture of the active site in H64D/V68A Mb resembles closely to that occurs in myoglobin with phenylhydrazine bound to the iron atom, in which the side chains of His-64 (E7), Arg-45 (CD3), and Val-68 (E11) have been forced aside to form an open channel to the surface.⁴⁸ Thus, the Val-68 → Ala of H64D mutation opens the distal pocket, and the mutant readily accommodate substrate thioanisole presumably enantiospecifically. On the other hand, the distal space in the wild type is filled with either an aliphatic or imidazole group, both of which direct towards to the heme iron. As

the result, H64D/V68A Mb gives the enhanced rate as well as enantioselectivity (84% ee) with respect to the wild type (25% ee).

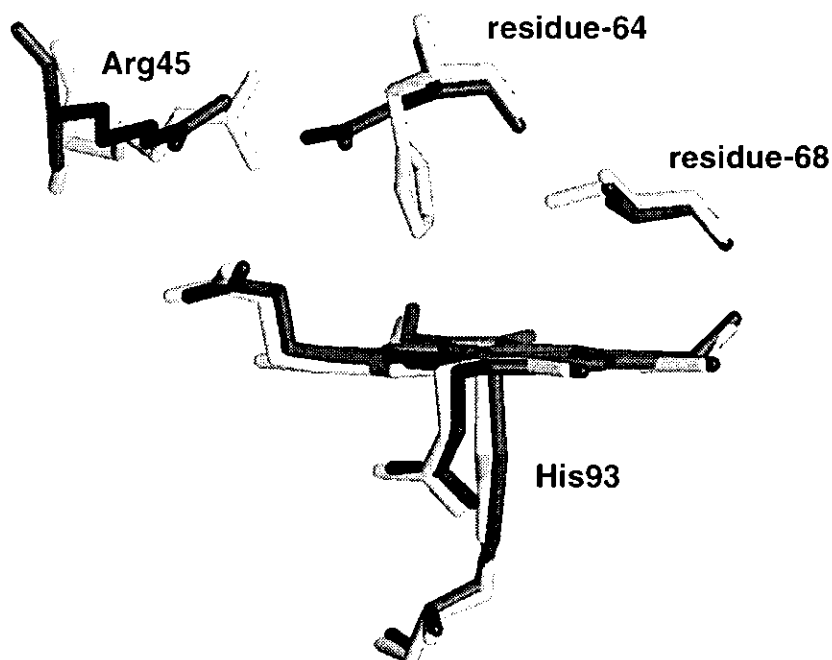


Figure 15. Superposition of the active site structures of wild type myoglobin and the H64D/V68A mutant. Residues 93, 68, 64, 45 are shown.

The substrate-binding site is formed by enlarging the space above the heme. However, crystallographic studies of myoglobin complex with the substrate are seriously limited due to the poor affinity of thioanisole to the protein. Therefore, we decided to simulate the transition state in the sulfoxidation by the replacement of the substrate with 1-phenylethylamine. The reaction between H64D/V68X Mbs and 1-phenylethylamine produces a complex in which amine is coordinated to the heme iron (Figure 8, 10, 11). In Table 4 is summarized the enantio-preferences of H64D/V68X Mbs in amine binding and the dominant enantiomers observed in the catalytic sulfoxidation of thioanisole. If the stability of the transition state in the sulfoxidation is responsible for enantioselectivity of Mb, the heme irons in both the transition state and the amine binding complex should favor the same enantiomer. However, the enantio-preferences in amine binding and the catalytic sulfoxidation are not always same for all of H64D/V68X Mbs as shown in Table 4.

Thus, it would seem that in the thioanisole sulfoxidation the stability of the transition state does not play any specific role in controlling enantioselectivity, high enantioselectivity of the Mb mutants might arise from the way of substrate access to the heme iron.

In order to better understand the origin of high enantioselectivity for the Mb mutants, several approaches for solving amine complex structure, such as crystallographic analysis, molecular dynamics and 2D proton NMR are underway or planned.

Table 4. Enantio-preferences of H64D/V68X Mbs in Thioanisole Sulfoxidation and Amine Binding

	H64D/ V68A	H64D/ V68S	H64D/ V68V	H64D/ V68L	H64D/ V68I	H64D/ V68F
sulfoxide	<i>R</i>	<i>R</i>	<i>R</i>	<i>R</i>	<i>S</i>	<i>R</i>
amine binding	<i>S</i>	<i>S</i>	<i>R</i>	<i>R</i>	<i>R</i>	<i>S</i>

In summary, we have prepared a series of H64D/V68X mutants of sperm whale myoglobin to investigate the function of residues at the position 68 on the oxidation activity. The results presented here demonstrate that the size and polarity of residues 68 in sperm whale myoglobin play absolutely important roles on the oxidation activity and enantioselectivity in peroxidation and peroxygenation. The changes in the oxidation activity would be rationalized by different reactivity of compound I for H64D/V68X Mbs. It has been clearly that polarity of the active site instead of a general acid-base catalyst of residue Asp-64 is involved in catalytic mechanism, but we need to complete analysis of 1-phenylethylamine Mb complex crystal structure in order to elucidate the precise substrate binding mode. This type of information would provide a basis for the development of myoglobin mutants designed to catalyze enantioselective oxidation of interest, an important goal in synthetic organic chemistry.

REFERENCE

- (1) Nagai, K.; Luisi, B.; Shih, D.; Miyazaki, G.; Imai, K.; Poyart, C.; De Young, A.; Kwiatkowski, L.; Noble, R. W.; Lin, S.-H.; Yu, N. T. *Nature* **1987**, *329*, 858-860.
- (2) Mathews, A. J.; Rohlfis, R. J.; Olson, J. S.; Tame, J.; Renaud, J. P.; Nagai, K. *J. Biol. Chem.* **1989**, *264*, 16573-16583.
- (3) Egeberg, K. D.; Springer, B. A.; Sligar, S. G.; Carver, T. E.; Rohlfis, R. J.; Olson, J. S. *J. Biol. Chem.* **1990**, *265*, 11788-11795.
- (4) Springer, B. A.; Sligar, S. G.; Olson, J. S.; Phillips, G. N., Jr. *Chem. Rev.* **1994**, *94*, 699-714.
- (5) Olson, J. S.; Phillips, G. N., Jr.; *J. Bio. Inorg. Chem.* **1997**, *2*, 544-552.
- (6) Olson, J. S.; Mathews, A. J.; Rohlfis, R. J.; Springer, B. A.; Egeberg, K. D.; Sligar, S. G.; Tame, J.; Renaud, J. P.; Nagai, K. *Nature* **1988**, *336*, 265-266.
- (7) Springer, B. A.; Egeberg, K. D.; Sligar, S. G.; Rohlfis, R. J.; Mathews, A. J.; Olson, J. S. *J. Biol. Chem.* **1989**, *264*, 3057-3060.
- (8) Rohlfis, R. J.; Mathews, A. J.; Carver, T. E.; Olson, J. S.; Springer, B. A.; Egeberg, K. D.; Sligar, S. G. *J. Biol. Chem.* **1990**, *265*, 3168-3176.
- (9) Carver, T. E.; Rohlfis, R. J.; Olson, J. S.; Gibson, Q. H.; Blackmore, R. S.; Springer, B. A.; Sligar, S. G. *J. Biol. Chem.* **1990**, *265*, 20007-20020.
- (10) Cameron, A. D.; Smerdon, S. J.; Wilkinson, A. J.; Habash, J.; Helliwell, J. R.; Li, T.; Olson, J. S. *Biochemistry* **1993**, *32*, 13061-13070.
- (11) Egeberg, K. D.; Springer, B. A.; Martinis, S. A.; Sligar, S. G.; Morikis, D.; Champion, P. M. *Biochemistry* **1990**, *29*, 9783-9791.
- (12) Smerdon, S. J.; Dodson, G. G.; Wilkinson, A. J.; Gibson, Q. H.; Blackmore, R. S.; Carver, T. E.; Olson, J. S. *Biochemistry* **1991**, *30*, 6252-6260.
- (13) Brancaccio, A.; Cutruzzolá, F.; Allocatelli, C. T.; Brunori, M.; Smerdon, S. J.; Wilkinson, A. J.; Dou, Y.; Keenan, D.; Ikeda-Saito, M.; Brantley, R. E., Jr.; Olson, J. S. *J. Biol. Chem.* **1994**, *269*, 13843-138453.
- (14) Quillin, M. L.; Li, T.; Olson, J. S.; Phillips, G. N., Jr.; Dou, Y.; Ikeda-Saito, M.; Regan, R.; Carlson, M.; Gibson, Q. H.; Li, H.; Elber, R. *J. Mol. Biol.* **1995**, *245*, 416-436.
- (15) Matsui, T.; Ozaki, S.; Watanabe, Y. *J. Biol. Chem.* **1997**, *272*, 32735-32738.
- (16) Matsui, T.; Ozaki, S.; Watanabe, Y. *J. Am. Chem. Soc.* **1999**, *121*, 9952-9957.
- (17) Takano, T. *J. Mol. Biol.* **1977**, *110*, 537-568.

- (18) Takano, T. *J. Mol. Biol.* **1977**, *110*, 569-584.
- (19) Case, D. A.; Karplus, M. *J. Mol. Biol.* **1979**, *132*, 343-368.
- (20) Kottalam, J.; Case, D. A. *J. Am. Chem. Soc.* **1988**, *110*, 7690-7697.
- (21) Springer, B. A.; Sligar, S. G. *Proc. Natl. Acad. Sci. U.S.A.* **1987**, *84*, 8961-8905.
- (22) Chothia, C. *Nature* **1975**, *254*, 304-308.
- (23) Dunford, H. B.; Stillman, J. S. *Coord. Chem. Rev.* **1976**, *19*, 187-251.
- (24) Schonbaum, G. R.; Chance, B. *The Enzymes*; 3rd ed.; P. D. Boyer, Ed.; Academic Press: New York, **1979**, Vol. 13; pp. 363-408.
- (25) Casella, L.; Gullotti, M.; Ghezzi, R.; Poli, S.; Beringhelli, T.; Colonna, S.; Carrea, G. *Biochemistry* **1992**, *31*, 9451-9459.
- (26) Ozaki, S.; Ortiz de Montellano, P. R. *J. Am. Chem. Soc.* **1995**, *117*, 7056-7064.
- (27) Giacometti, G. M.; Ascenzi, P.; Bolognesi, M.; Brunori, M. *J. Mol. Biol.* **1981**, *146*, 363-374.
- (28) Yonetani, T.; Anni, H. *J. Biol. Chem.* **1987**, *262*, 9547-9554.
- (29) Morikis, D.; Champion, P. M.; Springer, B. A.; Egebey, K. D.; Sligar, S. G. *J. Biol. Chem.* **1990**, *265*, 12143-12145.
- (30) Ikeda-Saito, M.; Hori, H.; Andersson, L. A.; Prince, R. C.; Pickering, I. J.; George, G. N.; Sanders, C. R.; Lutz, R. S.; McKelvey, E. J.; Mattera, R. *J. Biol. Chem.* **1992**, *267*, 22843-22852.
- (31) Phillips, G. N., Jr.; Arduini, R. M.; Springer, B. A.; Sligar, S. G. *Proteins Struct. Funct. Genet.* **1990**, *7*, 358-365.
- (32) Quillin, M. L.; Arduini, R. M.; Olson, J. S.; Phillips, G. N., Jr. *J. Mol. Biol.* **1993**, *234*, 140-155.
- (33) Goto, Y.; Matsui, T.; Ozaki, S.; Watanabe, Y.; Shunichi, F. *J. Am. Chem. Soc.* **1999**, *121*, 9497-9502.
- (34) Ozaki, S.; Yang, H.-J.; Matsui, T.; Goto, Y.; Watanabe, Y. *Tetrahedron: Asymmetry* **1999**, *10*, 183-192.
- (35) Ozaki, S.; Matsui, T.; Mark, P. R.; Watanabe, Y. *Coord. Chem. Rev.* **2000**, *198*, 39-59.
- (36) Ozaki, S.; Matsui, T.; Watanabe, Y. *J. Am. Chem. Soc.* **1996**, *118*, 9784-9785.
- (37) Ozaki, S.; Matsui, T.; Watanabe, Y. *J. Am. Chem. Soc.* **1997**, *119*, 6666-6667.
- (38) Iizuka, T.; Yonetani, T. *Adv. Biophys.* **1970**, *1*, 157-182.
- (39) Personal communication from Phillips, G. N. Jr. at the University of Wisconsin.
- (40) Hargrove, M. S.; Krzywda, S.; Wilkinson, A. J.; Dou, Y.; Ikeda-Saito, M.; Olson, J.

- S. Biochemistry* **1994**, *33*, 11767-11775
- (41) Ator, M. A.; Ortiz de Montellano, P. R. *J. Biol. Chem.* **1987**, *262*, 1542-1551.
- (42) Ator, M. A.; David, S. K.; Ortiz de Montellano, P. R. *J. Biol. Chem.* **1987**, *262*, 14954-14960.
- (43) Ortiz de Montellano, P. R.; David, S. K.; Ator, M. A.; Tew, D. *Biochemistry* **1988**, *27*, 5470-5476.
- (44) Miller, V. P.; DePillis, G. D.; Ferrer, J. C.; Grant Mauk, A.; Ortiz de Montellano, P. R. *J. Biol. Chem.* **1992**, *267*, 8936-8942.
- (45) Matsui, T.; Ozaki, S.; Liong, E.; Phillips, G. N., Jr.; Watanabe, Y. *J. Biol. Chem.* **1999**, *274*, 2838-2844.
- (46) Sundaramoorthy, M.; Turner, J.; Poulos, T. L. *Structure* **1995**, *3*, 1367-1377.
- (47) Quillin, M. L.; Breyer, W. A.; Griswold, Ian J.; Matthews, B. W. *J. Mol. Biol.* **2000**, *302*, 955-977.
- (48) Ringe, D.; Petsko, G. A.; Kerr, D. E.; Ortiz de Montellano, P. R. *Biochemistry* **1984**, *23*, 2-4.

CHAPTER 2

Conversion of Sperm Whale Myoglobin into a Catalase-like Enzyme

ABSTRACT: Comparison of crystal structures of sperm whale Mb and bovine liver catalase (BLC_{ase}) suggests that the Phe-43 → His and His-64 → Asn double mutation could create a heme pocket similar to the active site structure of BLC_{ase}. Thus, we have constructed F43H/H64N Mb as well as the H64N, F43H/H64A, and H64A mutant to investigate the influence of the distal histidine and asparagine on the reactivity. The F43H/H64N mutant exhibits better catalase (i.e. the dismutation of H₂O₂) and peroxidase (i.e. the one-electron oxidation of 2,2'-amino-bis(3-ethylbenzthiazoline-6-sulfonic acid) (ABTS)) activity than the wild type. The primary isotope effects observed in the reaction of Mb with deuterated hydrogen peroxide indicate that the H-O bond cleavage is involved in the rate-determining step for the dismutation of H₂O₂. Although the single replacement of His-64 with an asparagine residue does not enhance the rate of ABTS oxidation, F43H/H64N Mb has 3.4-fold better peroxidase activity than the F43H/H64A Mb. Therefore, the distal histidine in the F43H/H64N mutant appears to work cooperatively with Asn-64 to enhance the reactivity with H₂O₂. Our results presented in this communication infer that the distal asparagine (Asn-147) as well as the histidine (His-74) in BLC_{ase} might also play a role to facilitate compound I formation.

ABBREVIATIONS

Mb, myoglobin;

BLC_{ase}, bovine liver catalase;

compound I, a ferryl porphyrin cation radical;

compound II, a ferryl porphyrin;

Mb-I, myoglobin compound I;

*m*CPBA, *m*-chloroperbenzoic acid;

ABTS, 2,2'-azino-bis(3-ethylbenzothiazoline-6-sulfonic acid).

INTRODUCTION

Myoglobin (Mb), normally functions as a carrier of molecular oxygen,^{1,3} could be converted into a hemoenzyme like peroxidases by either site-directed mutagenesis based on rational design of the active site^{4,7} or random mutagenesis by *in vitro* evolution.⁸ The extensively accumulated biochemical and biophysical data on Mb, including the X-ray crystal structures of native, wild type, and various myoglobin mutants, provide us with a good starting point.⁹⁻¹⁸ We report herein an attempt to convert Mb into a catalase-like enzyme by the Phe-43 and His-64 double substitutions.

Catalase performs the dismutation of hydrogen peroxide (H_2O_2) into molecular oxygen and water.^{19,21} A ferryl porphyrin cation radical, so-called compound I, is believed to be a common reactive species for both peroxidase and catalase activity although the mechanistic details of compound I reduction remains to be clarified (Figure 1).²²⁻²⁴ The active site of catalase bears the distal histidine, functioning as a general acid-

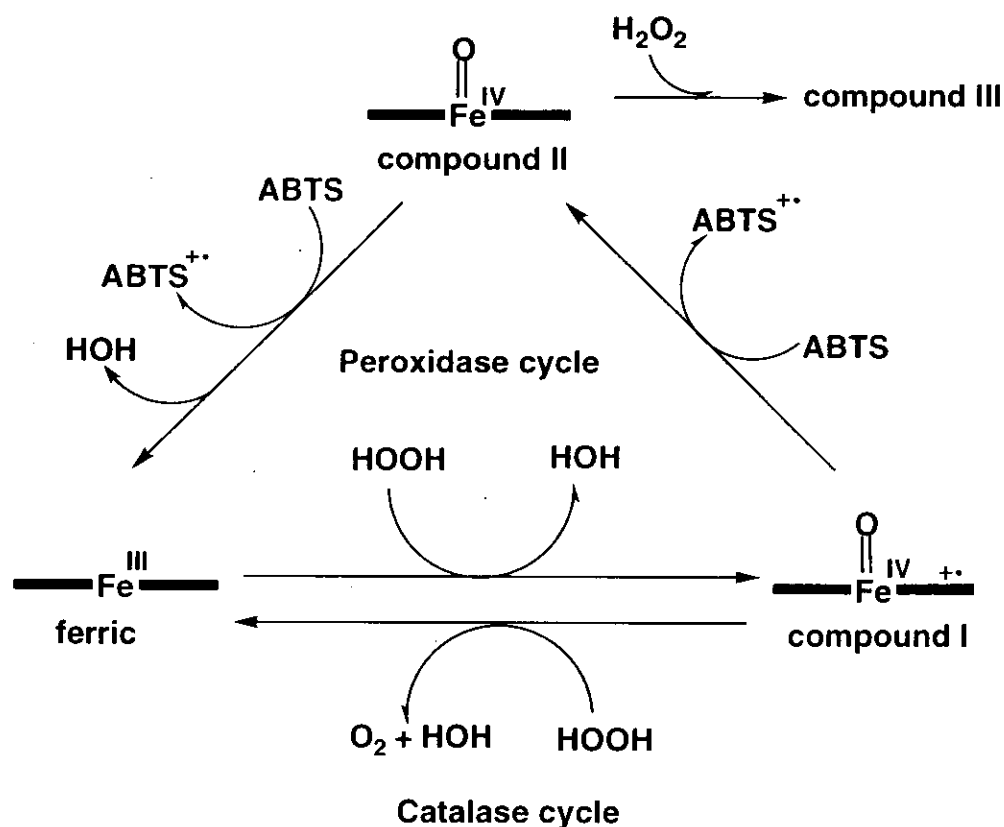


Figure 1. Catalase and Peroxidase Cycle.

base catalyst, as observed in the heme crevice of peroxidase. Furthermore, Asn-147 appears to interact with hydrogen peroxide through hydrogen bonding interaction (Figure 2).²⁵ Such an interaction presumably helps the polarization of the O-O bond of the peroxide to facilitate compound I formation. Comparison of crystal structures of sperm whale Mb and bovine liver catalase (BLCat) suggests that the Phe-43 → His and His-64 → Asn double mutation could create a heme pocket similar to the active site structure of BLCat (Figure 3).^{11,25} Thus, we have constructed F43H/H64N Mb as well as the H64N, F43H/H64A, and H64A mutant to investigate the influence of the distal histidine and asparagine on the reactivity.

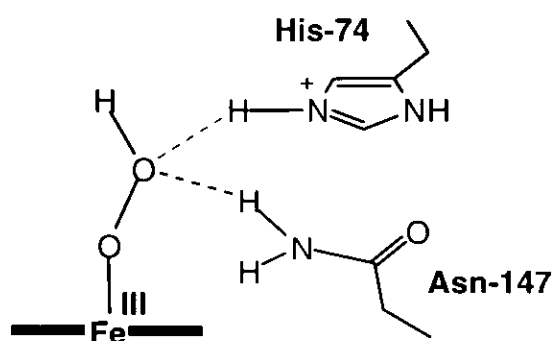


Figure 2. A proposed hydrogen bonding network in a precursor of compound I. The heterolytic cleavage of the O-O bond generates a ferryl porphyrin radical cation.

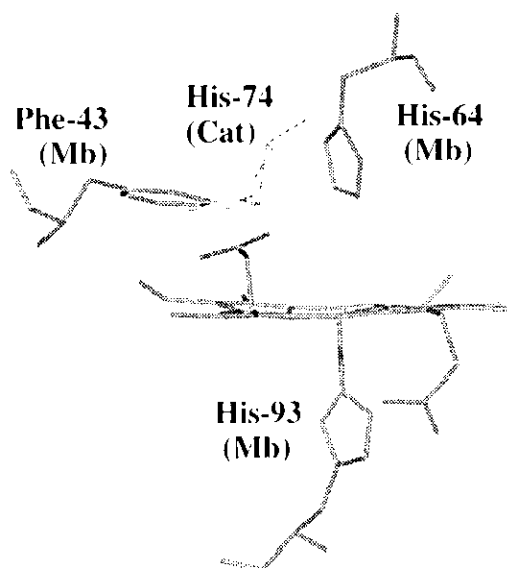


Figure 3. Superimposition of sperm whale myoglobin (Mb) and bovine liver catalase (BLCat). Heme in Mb and some selected residues in the active site are shown.

EXPERIMENTAL PROCEDURES

Preparation of the Myoglobin Mutants. The F43H/H64N, H64N, F43H/H64A and H64A sperm whale myoglobin mutants were constructed by cassette mutagenesis. The expression vector for wild type sperm whale Mb was a gift from J. S. Olson (Rice University, Houston, TX). The cassette including the desired His-64 and Phe-43 substitutions and a new silent *HpaI* restriction site was inserted between the *BglII* and *HpaI* sites. Expression in *Escherichia coli* strain TB-1 and purification of the mutants were described in papers previously reported. To ensure that the proteins used in the experiments were all in the ferric form, the sample was oxidized by the addition of a small excess of potassium ferricyanide. Excess oxidant was subsequently removed by gel filtration on a column packed with Sephadex G-25 equilibrated with the reaction buffer. The final purified protein was stored at -80 °C until used.

ABTS Oxidation (One-electron Oxidation). One-electron oxidation activities were measured at 20 °C in 50 mM sodium phosphate buffer (pH 7.0) on a Shimadzu UV-2400 spectrophotometer. At least two experiments were performed for each experimental data point. Steady-state kinetic constants for the oxidation of ABTS were obtained by measuring the initial rates as varying the H₂O₂ concentration. The formation of ABTS cation radical was monitored at 730 nm where the absorption of Mb was negligible. The absorption coefficient of the ABTS cation at 730 nm ($\epsilon_{730} = 1.44 \times 10^4 \text{ M}^{-1}\text{cm}^{-1}$) was calculated from that at 415 nm ($\epsilon_{415} = 3.6 \times 10^4 \text{ M}^{-1}\text{cm}^{-1}$). The reaction mixture contained 1 mM ABTS and variable amount of H₂O₂ (0.1 – 2 mM). Final concentrations of Mb were 0.5 μM for F43H/H64A and F43H/H64N Mb, 1 μM for wild type, H64A and H64N Mb, respectively.

Compound I Formation and Reduction. All the spectral changes were monitored on a Hi-Tech SF-43 stopped-flow apparatus equipped with a MG6000 diode array spectrophotometer. An optical filter (360 nm) was used for avoiding possible photoreduction of compound I by UV light. The reactions with *m*CPBA were carried out at pH 5.0 to observe complete accumulation for compound I. The reactivity of compound I with hydrogen peroxide was determined by means of a double-mixing rapid

scan technique at 5.0 °C and pH 5.0. The first mixing of the ferric Mb with a slight excess of *m*CPBA (1.3 – 2.0 mol equivalents) resulted in more than 80% accumulation of compound I, which was subsequently mixed with at least 10-fold excess of substrate hydrogen peroxide. The bimolecular rate constants were calculated from observed rates at the least four different concentrations of hydrogen peroxide.

Measurement of Catalase Activity. Catalase activity of Mb was measured at 25 °C from amount of molecular oxygen formed with a Hansatech DW1 oxygen electrode. The reaction mixture contained 10 μ M and 1 mM H₂O₂.

RESULTS AND DISCUSSION

The Phe-43 \rightarrow His mutation in H64N and H64A Mb accelerates the evolution of molecular oxygen by 12- and 6-fold, respectively (Table 1). Since the introduction of His-43 in H64N Mb enhances the catalase activity greater than in H64A Mb, the distal histidine appears to work cooperatively with Asn-64 as we hypothesized.

The one-electron oxidation of 2,2'-aminobis(3-ethylbenzthiazoline-6-sulfonic acid) (ABTS) (i. e. peroxidase activity) is a good probe to examine if the mutations facilitate compound I formation.^{6,26} With increasing concentrations of H₂O₂, the mutants exhibit a linear increase in ABTS oxidation (Figure 4); therefore, the rate-determining step for the one-electron process appears to be the reaction of ferric Mb with H₂O₂. The rate of ABTS oxidation would reflect the efficiency of compound I formation. The 360-fold enhancement is observed for F43H/H64N Mb with respect to the H64N mutant, but F43H/H64A Mb oxidizes ABTS 20-fold faster than H64A Mb (Table 1). In addition, the H64N mutant has only one twenty thirds of one-electron oxidation activity by the wild type; therefore, the distal asparagine alone does not facilitate compound I formation. The results clearly indicate that Asn-64 improves the reactivity of ferric Mb with H₂O₂ when His-43 is present in the active site.

However, the turnover numbers for molecular oxygen evolution by F43H/H64N and F43H/H64A Mb are less than the values of ABTS oxidation by more than 10-fold. Thus, compound I formation does not seem to be the only step controlling the catalase

activity. We have next attempted to examine the reaction of compound I with H₂O₂.

Table 1. Catalase and ABTS Oxidation Activity by Myoglobin Mutants.

Mba	catalase activity (turnover/min)	ABTS oxidation activity (turnover/min)
Wild type	1.7	20
H64N	0.72	1.7
F43H/H64N	8.7	510
H64A	2.0	7.4
F43H/H64A	13	150

It is known that compound I of the distal histidine deletion mutants can be generated with a stoichiometric amount of *m*-chloroperbenzoic acid (*m*CPBA), and the addition of H₂O₂ to compound I enables us to measure the reduction rate.²⁷ The kinetic constants for the H64N and H64A mutants are determined to be 1.0×10^4 and 5.9×10^3 M⁻¹s⁻¹, respectively. The relatively fast reduction compared with the rate of molecular oxygen evolution suggests that the low catalase activity of the His-64 deletion mutants is due to the slow compound I formation. On the contrary, F43H/H64N and F43H/H64A Mb require more than 25 equivalents of *m*CPBA with respect to the protein to form compound I. In addition, the instability of compound I of those double mutants does not allow us to determine the exact rate of compound I reduction with H₂O₂. Although the values similar to the rate constants for H64N and H64A Mb ($\cong 10^4$ M⁻¹s⁻¹) are expected, such a fast reduction of compound I with H₂O₂ does not explain the relatively slow evolution of oxygen molecule. Since compound I of F43H/H64N and F43H/H64A Mb is easily decay to compound II, which could further react with H₂O₂ to form compound III,^{22,23} the balance between the reduction and decay of compound I would control the catalase activity.

In order to study the reaction mechanism further, we have used deuterium labeled hydrogen peroxide (D₂O₂) and measured the catalase activity in the buffer prepared from deuterium oxide (D₂O). The rate of O₂ evolution by F43H/H64N and F43H/H64A Mb decreases to 1.7 and 3.0 turnover/min, respectively. The approximately

4-fold decrease in the rate in the deuterated reaction system suggests that the H-O bond cleavage is involved in the rate-determining step. However, at this time, we have not clarified if the bond breakage occurs via either the hydride (H⁻) transfer or the proton (H⁺) abstraction by compound I. Further studies are under way to solve the problem.

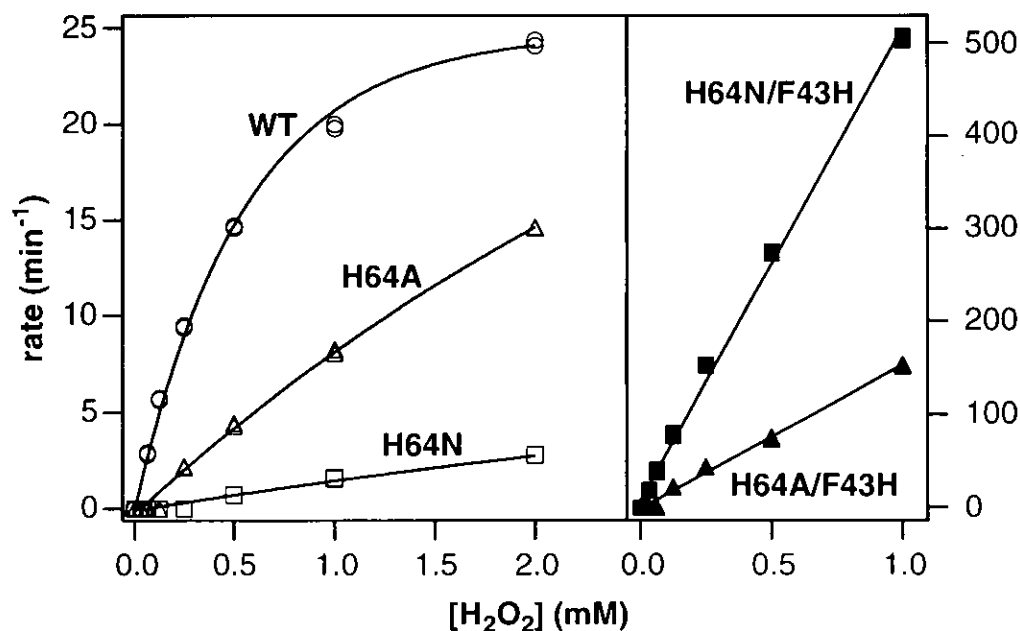


Figure 4. The plots of ABTS oxidation rates versus concentrations of H₂O₂ at 20 °C in 50 mM sodium phosphate buffer (pH 7.0).

In summary, F43H/H64N Mb constructed to mimic the active site of catalase exhibits better catalase and peroxidase activity. The primary isotope effects observed in the reaction of Mb with deuterated hydrogen peroxide indicate that the H-O bond cleavage is involved in the rate-determining step for the dismutation of H₂O₂. Although the single replacement of His-64 with an asparagine residue does not enhance the rate of ABTS oxidation, F43H/H64N Mb has 3.4-fold better peroxidase activity than the F43H/H64A Mb. Therefore, the distal histidine in the F43H/H64N mutant appears to work cooperatively with Asn-64 to enhance the reactivity with H₂O₂. Our results presented in this communication infer that the distal asparagine (Asn-147) as well as histidine (His-74) in BLCase might also play a role to facilitate compound I formation.

REFERENCE

- (1) Antonini, E.; Brunori, M. *Hemoglobin and Myoglobin in Their Reactions with Ligands*; North-Holland Publishing Co.: Amsterdam, 1971.
- (2) Perutz, M. *Trends Biochem. Sci.* **1989**, *14*, 42-44.
- (3) Wittenberg, J.; Wittenberg, B. *Annu. Rev. Biophys. Biophys. Chem.* **1990**, *19*, 217-241.
- (4) Ozaki, S.; Matsui, T.; Watanabe, Y. *J. Am. Chem. Soc.* **1996**, *118*, 9784-9785.
- (5) Ozaki, S.; Matsui, T.; Watanabe, Y. *J. Am. Chem. Soc.* **1997**, *119*, 6666-6667.
- (6) Matsui, T.; Ozaki, S.; Watanabe, Y. *J. Am. Chem. Soc.* **1999**, *121*, 9952-9957.
- (7) Ozaki, S.; Matsui, T.; Roach, P. M.; Watanabe, Y. *Coord. Chem. Rev.* **2000**, *198*, 39-59.
- (8) Wan, L.; Twitchett, M. B.; Eltis, L. D.; Mauk, A. G.; Smith, M. *Proc. Natl. Acad. Sci. U.S.A.* **1998**, *95*, 12825-12831.
- (9) Phillips, S. E. *J. Mol. Biol.* **1980**, *142*, 531-554.
- (10) Springer, B. A.; Sligar, S. G. *Proc. Natl. Acad. Sci. U.S.A.* **1987**, *84*, 8961-8965.
- (11) Phillips, G. N. Jr.; Arduini, R. M.; Springer, B. A.; Sligar, S. G. *Proteins: Struct. Funct. Genet.* **1990**, *7*, 358-365.
- (12) Wilks, A.; Ortiz de Montellano, P. R. *J. Biol. Chem.* **1992**, *267*, 8827-8833.
- (13) Quillin, M. L.; Li, T.; Olson, J. S.; Phillips, G. N.; Dou, Y.; Ikeda-Saito, M.; Regan, R.; Carlson, M.; Gibson, Q. H.; Li, H.; Elber, R. *J. Mol. Biol.* **1995**, *245*, 416-436.
- (14) Decatur, S. M.; DePillis, G. D.; Boxer, S. G. *Biochemistry* **1996**, *35*, 3925-3932.
- (15) Brittain, T.; Baker, A. R.; Butler, C. S.; Little, R. H.; Lowe, D. J.; Greenwood, C.; Watmough, N. J. *Biochem. J.* **1997**, *326*, 109-115.
- (16) Alayash, A. I.; Ryan, B. A.; Eich, R. F.; Olson, J. S.; Cashion, R. E. *J. Biol. Chem.* **1999**, *271*, 2029-2037.
- (17) Kolczak, U.; Hauksson, J. B.; Davis, N. L.; Pande, U.; de Ropp, J. S.; Langry, K. C.; Smith, K. M.; La Mar, G. N. *J. Am. Chem. Soc.* **1999**, *121*, 835-843.

- (18) Tomita, T.; Hirota, S.; Ogura, T.; Olson, J. S.; Kitagawa, T. *The Journal of Physical Chemistry B* **1999**, *103*, 7044-7054.
- (19) Deisseroth, A.; Dounce, A. L. *Physiol. Rev.* **1970**, *50*, 319-375.
- (20) Schonbaum, G. R.; Chance, B. In *The Enzymes*; 3rd ed.; P. D. Boyer, Ed.; Academic Press: New York, 1976; Vol. 13; pp 363-408.
- (21) Beyer, W. F. Jr.; Fridovich, I. *Basic Life Sci.* **1988**, *49*, 651-661.
- (22) Dunford, H. B.; Stillman, J. S. *Coord. Chem. Rev.* **1987**, *19*, 187-251.
- (23) *Peroxidases in Chemistry and Biology*; Everse, J.; Everse, K. E.; Grisham, M. B., Ed.; CRC: Boca Raton, 1991.
- (24) Dunford, H. B. *Heme Peroxidases*; Academic Press: New York, 1999.
- (25) Fita, I.; Silva, A. M.; Murthy, M. R. N.; Rossmann, M. G. *Acta Crystallogr.* **1986**, *B42*, 497-515.
- (26) Matsui, T.; Ozaki, S.; Liong, E.; Phillips, G. N. Jr.; Watanabe, Y. *J. Biol. Chem.* **1999**, *274*, 2838-2844.
- (27) Matsui, T.; Ozaki, S.; Watanabe, Y. *J. Biol. Chem.* **1997**, *272*, 32735-32738.

PART III

CATALYTIC OXIDATION BY DISTAL HISTIDINE RELOCATION MYOGLOBIN MUTANTS

Chapter 1.

Asymmetric Oxidation Catalyzed by Sperm Whale Myoglobin Mutants

Chapter 2.

Characterization of I107H/H64L Myoglobin Mutant

CHAPTER 1

Asymmetric Oxidation Catalyzed by Sperm Whale Myoglobin Mutants*

*published in *Tetrahedron: Asymmetry* **1999**, *10*, 183-192

Asymmetric Oxidation Catalyzed by Myoglobin Mutants.

Shin-ichi Ozaki, Hui-Jun Yang, Toshitaka Matsui, Yoshio Goto,

and Yoshihito Watanabe

ABSTRACT: The sperm whale myoglobin active site mutants (L29H/H64L and F43H/H64L Mb) have been shown to catalyze the asymmetric oxidation of sulfides and olefins. Thioanisole, ethyl phenyl sulfide, and *cis*- β -methylstyrene are oxidized by L29H/H64L Mb with more than 95% enantiomeric excess (% ee). On the other hand, the F43H/H64L mutant transforms *trans*- β -methylstyrene into *trans*-epoxide with 96% ee. The dominant sulfoxide product in the incubation of alkyl phenyl thioethers is the *R* isomer; however, the mutants afford dominantly the *S* isomer of aromatic bicyclic sulfoxides. The results help us for the rationalization of the difference in the preferred stereochemistry of the Mb mutants-catalyzed reactions. Furthermore, the Mb mutants exhibit the improvement of the oxidation rate up to 300-fold with respect to wild type.

ABBREVIATIONS

Mb, myoglobin;

CPO, chloroperoxidase from the marine fungus *Caldariomyces fumagus*;

compound I, a ferryl porphyrin cation radical;

compound II, a ferryl porphyrin;

ee, enantiomeric excess.

INTRODUCTION

Asymmetric biotransformations have been applied to organic synthesis as excellent alternatives to chemical procedures.¹ Chloroperoxidase from *Caldariomyces fumago* (CPO),² a heme enzyme, is one of the well studied enzymes for enantioselective oxidation of sulfides and olefins.³ Recently, a vanadium-containing non-heme bromoperoxidase from the alga *C. officinalis* (VBrPO)⁴ has been shown to perform sulfoxidation of aromatic bicyclic sulfides in high enantiomeric excess (% ee).⁵ The structural feature of active site of native enzyme is successfully utilized to achieve high optical and chemical yields. In order to extend the biocatalytic methodology, we have examined the oxygenation by sperm whale myoglobin (Mb) mutants.

Mb has protoporphyrin IX as a prosthetic group, and its major physiological role is the storage and transfer of molecular oxygen.⁶ However, Mb can support the peroxide dependent one and two electron oxidation of a variety of substrates at the very slow rate.⁷ Recently, we reported as communications that L29H/H64L and F43H/H64L Mb exhibit high catalytic turnover with high stereospecificity for the sulfoxidation of thioanisole and the epoxidation of styrene.⁸ More importantly, a ferryl porphyrin radical cation species ($\text{O}=\text{Fe}^{\text{IV}}\text{Por}^{+\bullet}$), equivalent to compound I of peroxidase, has recently been confirmed as the catalytic species of two electron oxidation process by F43H/H64L, H64S, H64A, and H64L Mb.⁸ The mutants were designed to increase the life time of catalytic intermediate as well as the accessibility of substrates. In this report, we have explored the scope of asymmetric oxygenation by the use of aromatic bicyclic sulfides and methyl styrene. The results help us understanding the substrate binding orientation on the basis of the preferred stereochemistry for L29H/H64L and F43H/H64L Mb. Furthermore, we have confirmed that compound I of L29H/H64L Mb is also a catalytic species for the oxidation of sulfides and styrene.

EXPERIMENTAL PROCEDURES

Materials. All substrates except for sulfide **4**, **5**, and **6** are commercially available. **4**, **5**, and $\text{H}_2^{18}\text{O}_2$ were chemically synthesized as previously reported.^{3g,7a} Sulfoxides and epoxides were synthesized from the corresponding starting substrates by the oxidation with *m*-chloroperbenzoic acid (*m*CPBA) or H_2O_2 and used to make standard curves. The L29H/H64L and F43H/H64L Mb were constructed utilizing polymerase chain reaction based method.⁹ The Mbs were expressed and purified as previously reported.¹⁰ The protein concentration was determined by spectrometrically at 408 nm ($\epsilon = 1.8 \times 10^5 \text{ M}^{-1} \text{ cm}^{-1}$).

Synthesis of Sulfide **6 and Its Sulfoxide.** A mixture of thiosalicylic acid (4.0 g), methyl iodide (36 mL), and 28% ammonium hydroxide (24 mL) were stirred at 25 °C for 48 hours. The products (a mixture of **6** and its free acid) were extracted with dichloromethane, and purified by Silica Gel 60 (2.1 cm × 8 cm). The column was washed with dichloromethane to elute **6** and then with 20% isopropanol containing hexane to recover the free acid. NMR: δ (CDCl_3) = 2.49 (3H, s), 3.95 (3H, s), 7.18 (1H, t), 7.30 (1H, d), 7.50 (1H, t) 8.02 (1H,d). GC-MS: Calculated for $\text{C}_9\text{H}_{10}\text{O}_2\text{S}$ 182.23 Found 182.05. The sulfoxide of **6** was synthesized in a water/methanol mixture (2.0 mL) containing **6** (10 mg) and H_2O_2 (0.01 mol) at 25 °C for 4.5 hours. The sulfoxide product was purified by Silica Gel 60 (2.1cm × 8 cm) with the eluent system of 20% isopropanol: 80% hexane. NMR: δ (CDCl_3) = 2.85 (3H, s), 3.96 (3H, s), 7.47 (1H, t), 7.72 (1H, t), 8.09 (1H, d) 8.32 (1H, d). GC-MS: Calculated for $\text{C}_9\text{H}_{10}\text{O}_3\text{S}$ 198.24 Found 198.10. The *S* and *R* isomers were separated and collected by isocratic HPLC on Dical chiral column OD (0.46 cm × 25 cm) at a flow rate of 0.5 mL/min (isopropanol/hexane = 20/80). The CD spectra were obtained by JASCO J-40 spectropolarimeter, and the absolute configuration was assigned by comparison of CD spectra of (*R*)-methyl phenyl sulfoxide and synthetic sulfoxide of **6** (Figure 1).

Enzymatic Sulfoxidation. 1 mM H_2O_2 was added to a solution of either Mb or the Mb mutants (5 μM) and 1 mM sulfide in 0.5 mL of 50 mM sodium phosphate buffer

(pH 7.0) at 25 °C. A selected internal standard was added, the mixture was extracted with dichloromethane, and analyzed by isocratic HPLC on Dical chiral column OD (0.46 cm × 25 cm) at a flow rate of 0.5 mL/min.¹¹ The reaction time varies from 1 to 30 minutes, and the rates were determined from the linear portion of the product vs time plot. Since the enzymes were inactivated during the reaction, we normally observed up to 2500 turnovers. Standard curves prepared using synthetic sulfoxides were used for quantitative analysis, and the values of % enantiomeric excess were determined on a basis of peak area of HPLC traces. It was previously reported that the *S* sulfoxides of **1** and **2** eluted from the column.¹¹ The absolute configuration for sulfoxides of **3** and **6** were confirmed by the comparison of CD spectrum of (*R*)-methyl phenyl sulfoxide and those of sulfoxide isomers for **3** and **6** collected from the chiral column. To determine the stereochemistry for sulfoxides of **4** and **5**, authentic *R* sulfoxides were synthesized by CPO as described previously,³⁸ and the retention times were determined 21 (**4**) and 36 min (**5**), respectively. The sulfoxide formed in control incubations without enzyme was subtracted when necessary.

Reactions of Compound I with Sulfides or Styrene. Rapid scan spectra were collected on a Hi-Tech SF-43 stopped-flow apparatus equipped with a MG 6000 diode array spectrometer. Single mixing experiments (i.e. mixing of ferric Mb and *m*CPBA) were performed to determine the rate of compound I formation. *m*CPBA was used as an oxidant because it was better than H₂O₂ to generate compound I in a time scale of stopped-flow experiments. The reaction of L29H/H64L Mb (10 μM) with *m*CPBA (250 μM) was performed in 50 mM sodium acetate buffer (pH 5.3) at 5 °C. Since the F43H/H64L mutant (10 μM) does not require a large excess of *m*CPBA to generate compound I, the *m*CPBA concentration was reduced to 100 μM. Based on the results of single mixing experiments, the delay times, defined as the interval between the first and the second mixing, were set as 10 and 0.3 sec, for L29H/H64L and F43H/H64L Mb, respectively. Sulfides (100 μM) or styrene (100 μM) were added to compound I by the second mixing after the appropriate delay time to collect spectral changes.

The rates of compound **1** reduction for L29H/H64L Mb by thioanisole, 2,3-dihydrobenzothiophene, and styrene were $5.9 \pm 0.1 \text{ s}^{-1}$, $4.5 \pm 0.1 \text{ s}^{-1}$, and $0.92 \pm 0.02 \text{ s}^{-1}$, respectively. The values for the F43H/H64L mutant were $66 \pm 3 \text{ s}^{-1}$, $44 \pm 1 \text{ s}^{-1}$, and $44 \pm 2 \text{ s}^{-1}$, respectively.

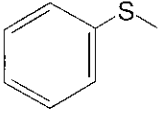
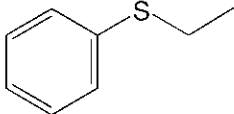
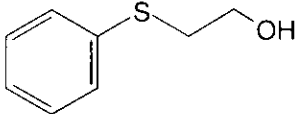
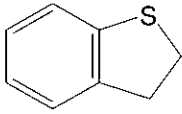
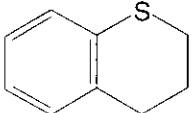
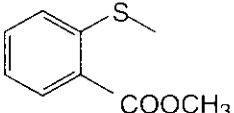
Enzymatic Epoxidation. The wild type or mutants (10 μM) in 0.5 mL of 50 mM sodium phosphate buffer (pH 7.0) was incubated with 0.5 μL of neat styrene, *cis*-, or *trans*- β -methylstyrene and 1 mM H_2O_2 at 25 $^\circ\text{C}$. A selected internal standard was added, and the dichloromethane extracts were analyzed by GC equipped with Chiraldex G-TA capillary column at 80 $^\circ\text{C}$. The reaction time varies from 2 to 20 minutes, and the rates were determined from the linear portion of the product *vs* time plot. Since the enzymes were inactivated during the reaction, we normally observed up to 100 turnovers. The standard curve was prepared for quantitative analysis, and the absolute stereochemistry was determined based on a retention time of the authentic epoxide.

RESULTS AND DISCUSSION

Asymmetric Sulfoxidation of Cyclic and Acyclic Sulfides. Among the Mbs studied here, L29H/H64L Mb is the best chiral catalyst (Table 1). The values of % ee for the L29H/H64L mutant are greater than those of wild type and F43H/H64L Mb for the oxidation of sulfides examined here. The largest improvement from 7.6% to 95% in enantioselectivity is observed for the sulfoxidation of ethyl phenyl sulfide (**2**) by the L29H/H64L mutant. On the other hand, the F43H/H64L mutant is the best catalyst in terms of the sulfoxidation rate. The Phe-43 \rightarrow His and His-64 \rightarrow Leu mutation increases the rate of thioanisole (**1**) oxidation by 190-fold with respect to the wild type, which is the largest enhancement achieved herein.

In order to elucidate the substrate recognition by the Mb mutants, we have determined the enantioselectivity for 2-hydroxyethyl phenyl sulfide (**3**) oxidation. The absolute configuration for the sulfoxide isomers of **3** was determined by comparison of their CD spectra with that of *R*-methyl phenyl sulfoxide (Figure 1). In the reaction with

Table 1. Enantiospecific sulfoxidation of cyclic and acyclic thioether^a

		wild type		L29H/H64L		F43H/H64L	
		rate ^b	%ee	rate ^b	%ee	rate ^b	%ee
1		0.25 ^c	25 ^c (<i>R</i>)	5.5 ^c	97 ^c (<i>R</i>)	47 ^c	85 ^c (<i>R</i>)
2		0.46 ^c	7.6 ^c (<i>R</i>)	6.5 ^c	95 ^c (<i>R</i>)	26	54 (<i>R</i>)
3		0.65	27 (<i>R</i>)	1.6	71 (<i>R</i>)	3.2	27 (<i>R</i>) ^c
4		2.2	0.2 (<i>R</i>)	24	67 (<i>S</i>)	95	17 (<i>S</i>)
5		0.8	5.4 (<i>R</i>)	3.2	66 (<i>S</i>)	50	34 (<i>S</i>)
6		0.4	4.3 (<i>S</i>)	2.4	82 (<i>R</i>)	7.5	8.5 (<i>R</i>)

(a) HPLC conditions: 20 % isopropanol : 80 % hexane for **1**, 10 % isopropanol : 90 % hexane for **2** and **6**, 15 % isopropanol : 85 % hexane for **3**, and, 5 % isopropanol : 95 % hexane for **4** and **5**. Retention times of the sulfoxide products: **1** 17 and 20 min, **2** 17 and 21 min, **3** 17 and 20 min, **4** 36 and 38 min, **5** 64 and 68 min, and **6** 19 and 21 min. Except for the sulfoxide of **6**, the *S* isomers always elute from the column first.

(b) The unit for rate is turnover/min.

(c) The results are taken from reference 8a and 8b.

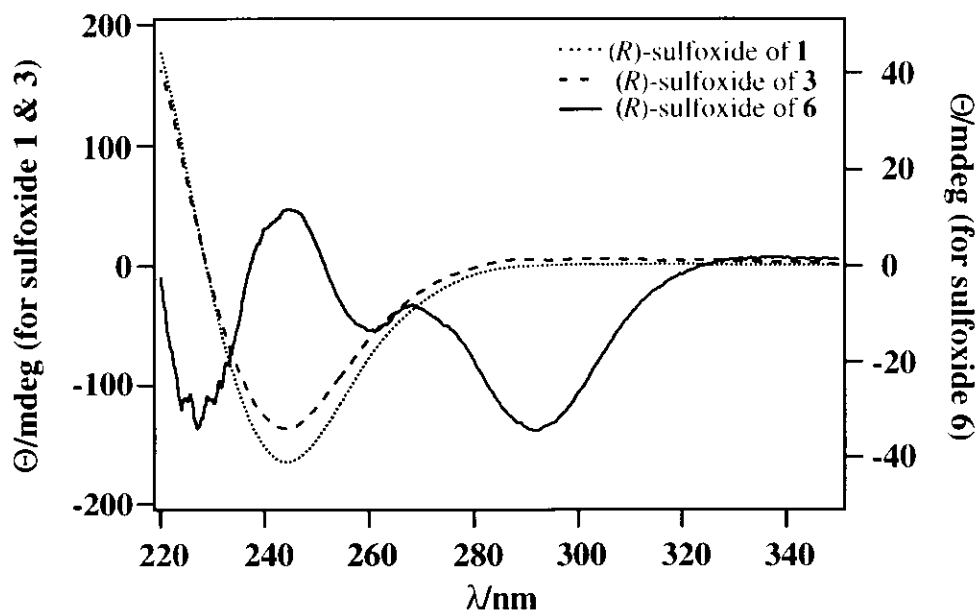


Figure 1. CD spectra of *R*-methyl phenyl sulfoxide, *R*-sulfoxide of **3** (eluted at 20 min), and **6** (eluted at 19 min).

L29H/H64L and F43H/H64L Mb, the hydroxy group of **3** decreases the value of % ee by approximately 25% with respect to ethyl phenyl sulfide (**2**), but the *R* enantiomers are still the major sulfoxide products for **2** and **3** (Table 1). Thus, the orientation of substrate binding does not appear to be controlled by hydrophilic properties of alkyl group in the case of sulfoxidation catalyzed by L29H/H64L and F43H/H64L Mb. Interestingly, cyclic sulfides give different stereospecificity from acyclic thioethers for the L29H/H64L mutant. The values of % ee in the oxidation of 2,3-dihydrobenzothiophene (**4**) and 1-thiochroman (**5**) by L29H/H64L Mb are 67 and 66% ee, respectively, and the dominant isomers are *S* sulfoxides (Table 1). On the contrary, *R* is the major enantiomer with 97% ee for thioanisole (**1**) oxidation by the L29H/H64L mutant. Since sulfide **6** bearing an *ortho* substituent is oxidized to the corresponding *R* sulfoxide with 82% ee by L29H/H64L Mb, the cyclic moiety but not *ortho* substituent of benzene ring appears to be important for the formation of *S* isomer. The similar changes in dominant isomers are also observed for F43H/H64L Mb.

In this study, hydrogen peroxide was added in one portion at the beginning of the reaction to obtain the initial rate, and the values can not be directly compared with the results from the continuous addition of oxidants to the reaction mixture with CPO^{3z} or VBrPO⁵ as previously reported. However, the sulfoxidation system with F43H/H64L appear to be comparable to that of CPO in terms of the rate.¹²

Catalytic Species for the Sulfoxidation Reaction. In order to confirm that compound I is the catalytic species for the oxidation of sulfides by the L29H/H64L and F43H/H64L mutant, we have performed double mixing stopped-flow experiments. Compound I was generated in the first mixing, and sulfides were added to compound I in the second mixing. UV-visible spectra began to be collected just after the second mixing to monitor the spectral changes.

The decrease in the absorbance of the Soret and the increase in the absorbance around 650 nm are characteristic for the formation of ferryl porphyrin radical cation from the ferric state (Figure 2). Compound I (O=Fe^{IV} Por^{+•}) of L29H/H64L Mb is reduced back to the ferric state in the presence of an excess of thioanisole (**1**). Since compound II (O=Fe^{IV} Por), bearing one oxidation equivalent with respect to the ferric state, is not observed, the sulfoxidation appears to proceed with a direct two-electron process. Essentially the same spectral changes are observed in the presence of 2,3-dihydrobenzothiophene (**4**) with L29H/H64L Mb. Therefore, the bicyclic sulfide does not change the oxidation mechanism. Thioanisole and dihydrobenzothiophene also reduce compound I of the F43H/H64L mutant directly to the ferric state.

The similar UV-visible spectral changes were observed in the reaction of compound I of both mutants with styrene (**7**). Thus, the results indicate that the ferryl porphyrin radical cation (O=Fe^{IV} Por^{+•}) is the reactive species for the peroxide dependent monooxygenation by the mutants.

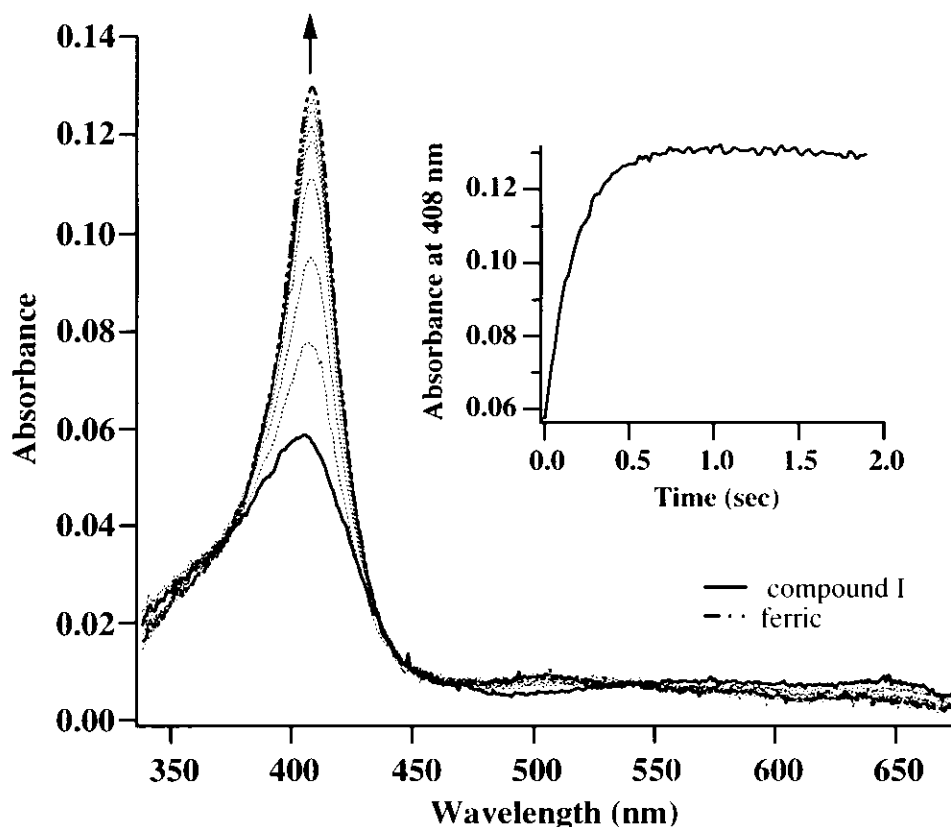
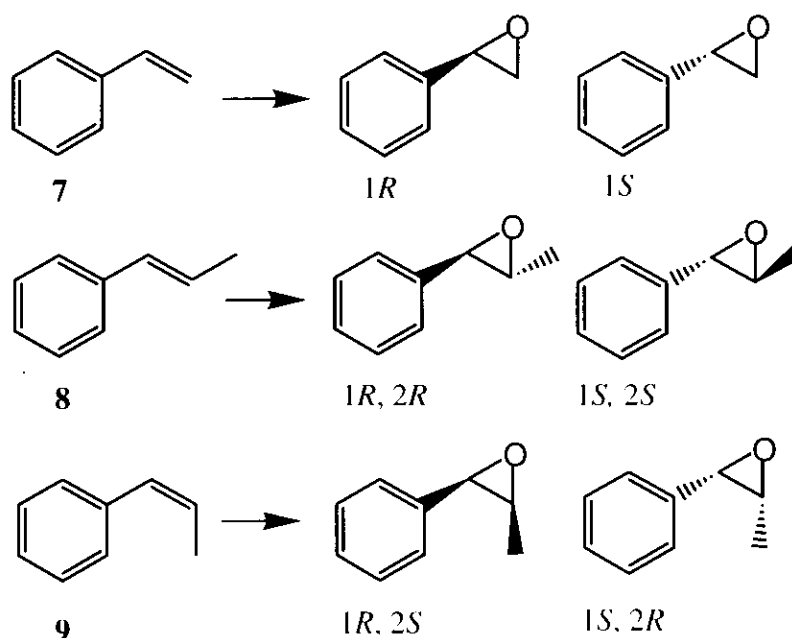


Figure 2. The UV-visible spectral changes from compound I of L29H/H64L Mb to the ferric state in the presence of thioanisole in 50 mM NaOAc buffer (pH 5.3) at 5 °C.

Asymmetric Epoxidation of Styrene and β -Methylstyrene. In order to gain an insight into the highly enantiospecific oxidation by the L29H/H64L and F43H/H64L mutant, we have next studied epoxidation reactions. The epoxidation rate for styrene (**7**), *trans*- (**8**), and *cis*- β -methylstyrene (**9**) catalyzed by the L29H/H64L mutant is increased by 9-fold, 4-fold, and 46-fold, respectively, comparing with the rate of wild type Mb (Table 2). The highest value of enantiomeric excess is 99% ee for *cis*- β -methylstyrene epoxidation catalyzed by L29H/H64L Mb. On the other hand, F43H/H64L Mb oxidized *trans*- β -methylstyrene to (*1R, 2S*)-*trans*-epoxide with 96% ee. The F43H/H64L mutant is the best enzyme in terms of epoxidation rate, and styrene, *trans*- and *cis*- β -methylstyrene are found to be oxidized 300-, 210-, and 57-times faster by F43H/H64L than wild type Mb, respectively. Synthetic iron porphyrins, hemoprotein model compounds, oxidize the *cis*-

much faster than the *trans*-isomer,¹³ but *cis*- β -methylstyrene is less reactive to Mbs than the *trans* isomer (Table 2), presumably due to the limited accessibility for the *cis* isomer to the active site.

Table 2. Enantioselective Epoxidation of Olefins.



		wild type Mb		L29H/H64L Mb		F43H/H64L Mb	
		rate ^b	ee(%)	rate ^b	ee(%)	rate ^b	ee(%)
7 ^c	styrene	0.015	9 (1 <i>R</i>)	0.14	80 (1 <i>R</i>)	4.5	68 (1 <i>R</i>)
8	<i>trans</i> - β -methylstyrene	0.076	39 (1 <i>R</i> , 2 <i>R</i>)	0.29	83 (1 <i>R</i> , 2 <i>R</i>)	16	96 (1 <i>R</i> , 2 <i>R</i>)
9	<i>cis</i> - β -methylstyrene	0.0026	3 (1 <i>R</i> , 2 <i>S</i>)	0.12	99 (1 <i>R</i> , 2 <i>S</i>)	0.15 ^d	45 (1 <i>R</i> , 2 <i>S</i>)

(a) Retention times: styrene oxide 8.5 min (1*S*) and 10.6 min (1*R*), *trans*-methylstyrene oxide 13.5 min (1*S*, 2*S*) and 15.4 min (1*R*, 2*R*), *cis*-methylstyrene oxide 12.1 min (1*S*, 2*R*) and 17.1 min (1*R*, 2*S*).

(b) The unit for rate is turnover/min.

(c) The results are taken from reference 8a and 8b.

(d) Phenylacetone was also formed in the reaction. The ratio of *cis*-epoxide : phenylacetone was 1 : 3.

No more than a trace of *trans*- β -methylstyrene oxide is detected as a side product in *cis*- β -methylstyrene oxidation. Thus, the epoxidation proceeds with the retention of olefin stereochemistry. Since *trans*-epoxide was generated in the oxidation of *cis*- β -methylstyrene by sterically unhindered Mn porphyrin, the active site of the mutants might prevent the rotation of the two vinyl carbons of *cis*- β -methylstyrene by the steric reasons (Figure 3).¹³

Only a trace of side product is observed in the oxidation of styrene and *trans*- β -methylstyrene; however, a significant amount of phenylacetone is generated in the incubation of *cis*- β -methylstyrene with F43H/H64L Mb. Compound I, an oxo-ferryl porphyrin π -cation radical species ($O=Fe^{IV} \text{Por}^{\bullet+}$), is responsible for the epoxide production, but phenylacetone seems to be generated by the 1,2-hydrogen rearrangement of the cationic species as previously proposed for the cytochrome *c* peroxidase-catalyzed oxidation of olefin (Figure 3).¹⁴ Since β -methylstyrene oxide is not transformed into phenylacetone in the presence of F43H/H64L Mb and hydrogen peroxide, the carbocation at the benzylic position would be formed from the reaction of compound I with β -methylstyrene.

Substrate Binding Orientation. The dominant isomers observed in the oxidation of thioanisole, dihydrobenzo-thiophene, and styrene by L29H/H64L Mb are summarized in Figure 4. We previously found that *para* substituents of thioanisole (**1**) did not change the Mbs' preference in enantioselectivity.^{8a} In addition, a bulky substituent at the *ortho*-position of **1** did not change the enantioselectivity (Table 1). Thus, the origin of enantioselectivity could be rationalized by the conformational difference of sulfur or benzylic carbon in the putative reaction intermediates. If we assume the aromatic group is bound in a fixed position, dihydrobenzothiophene (**4**) and styrene seem to share a common binding orientation (Figure 4, 5). The vinyl group of styrene could be on the same plane of benzene ring to form a flat molecule like dihydrobenzothiophene (Figure 5). On the contrary, methyl phenyl sulfide approaches to the ferryl oxygen with S-CH₃ bond

approximately perpendicular to the plane of benzene ring. The similar substrate binding mode can be proposed for the F43H/H64L mutant (Figure 5).

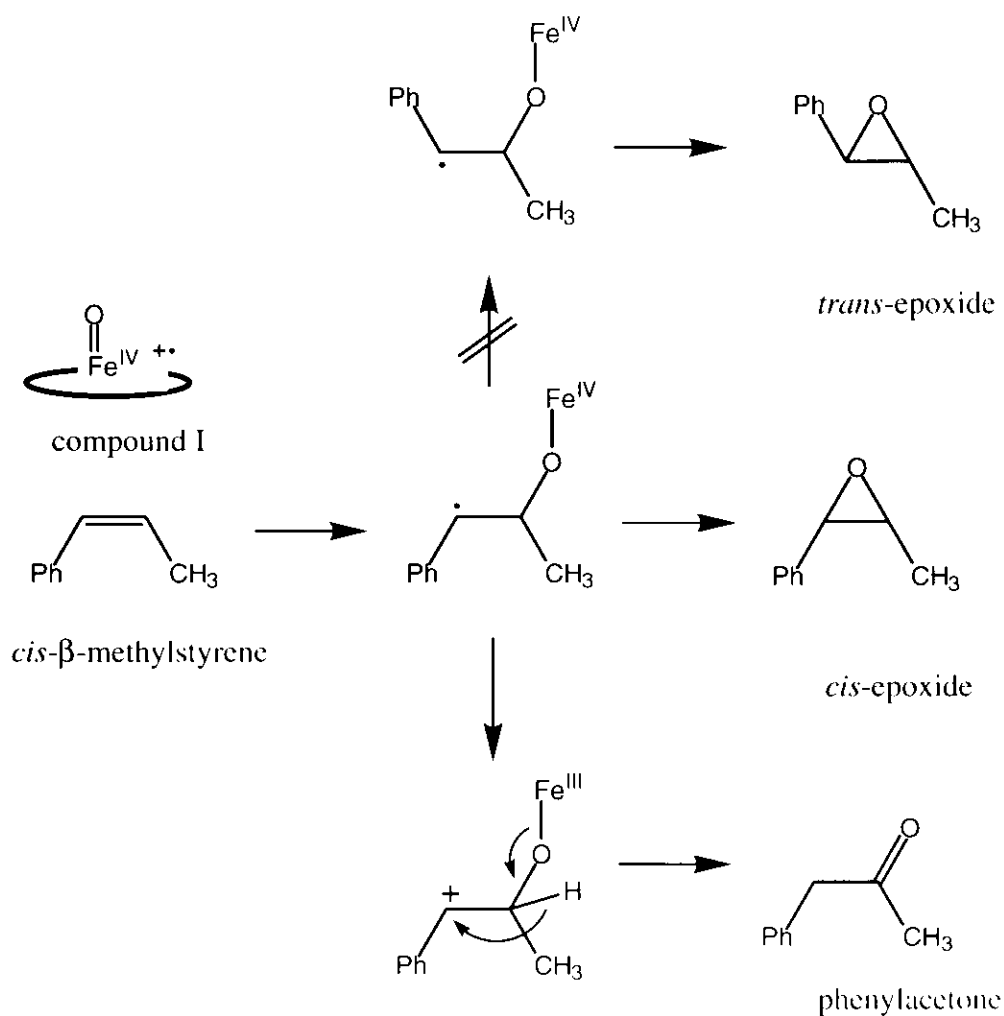


Figure 3. Proposed mechanism for the oxidation of *cis*- β -methylstyrene by Mbs.¹⁴

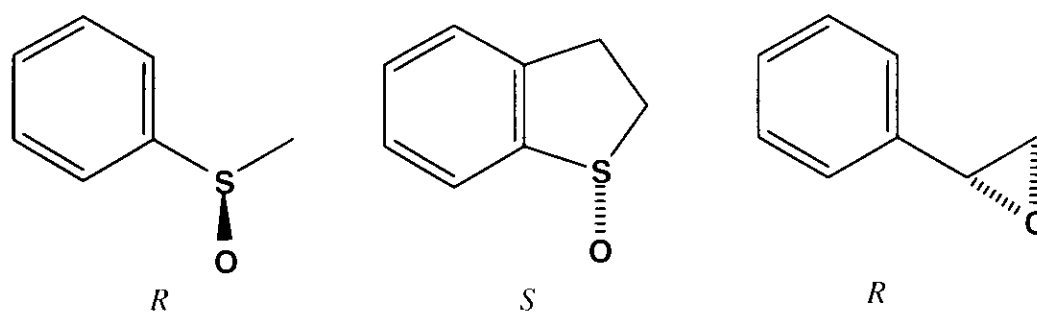


Figure 4. The dominant isomers observed for sulfoxidation and epoxidation.

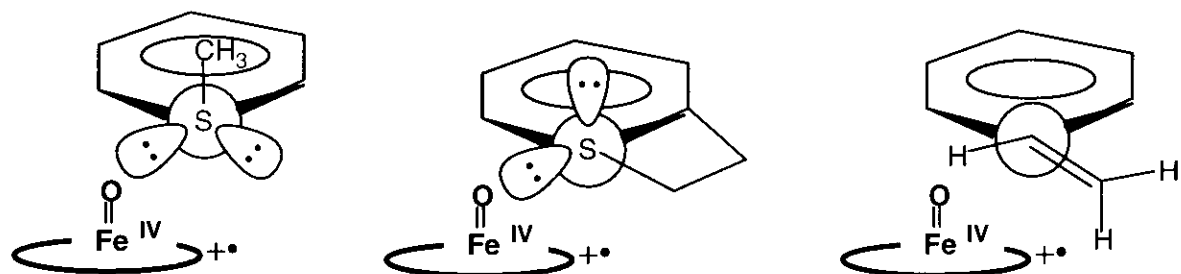


Figure 5. Proposed conformational rationalization for the asymmetric oxidation by the Mb mutants.

In order to elucidate the origin of enantioselectivity for L29H/H64L Mb, we have crystallized the mutant and performed the X-ray crystal structure analysis.¹⁵ Energy minimization followed by docking either the substrates or products in the active site of L29H/H64L Mb did not immediately provide an obvious rationale for the difference in enantiospecificity.¹⁶ The effort to soak the substrate into the crystals are underway to elucidate the reason for high stereospecificity of the Mb mutants.

REFERENCE AND NOTES

- (1) (a) Anderson, B. A.; Hansen, M. M.; Harkness, A. R.; Henry, C. L.; Vicenzi, J. T.; Zmijewski, M. J. *J. Am. Chem. Soc.* **1995**, *117*, 12358-12359
- (b) Brunel, J. -M.; Diter, P.; Duetsch, M.; Kagan, H. B. *J. Org. Chem.* **1995**, *60*, 8086-8088.
- (c) Stein, K. A.; Toogood, P. L. *J. Org. Chem.* **1995**, *60*, 8110-8112.
- (d) Parmar, V. S.; Singh, A.; Bisht, K. S.; Kumar, N.; Belokon, Y. N.; Kochetkov, K. A.; Ikonnikov, N. S.; Orlova, S. A.; Tararov, V. I.; Saveleva, T. F. *J. Org. Chem.*

- 1996**, *61*, 1223-1227.
- (e) Itoh, T.; Takagi, Y.; Murakami, T.; Hiyama, Y.; Tsukube, H. *J. Org. Chem.* **1996**, *61*, 2158-2163.
- (f) Hudlicky, T.; Endoma, M. A. A.; Butora, G. *Tetrahedron: Asymmetry* **1996**, *7*, 61-68.
- (g) Huber, P.; Bratovanov, S.; Bienz, S.; Syldatk, C.; Pietzsch, M. *Tetrahedron: Asymmetry* **1996**, *7*, 69-78.
- (2) Morris, D. R.; Hager, L. P. *J. Biol. Chem.* **1966**, *241*, 1763-1768.
- (3) (a) Pasta, P. *Biochemistry* **1990**, *29*, 10465-10468.
- (b) Colonna, S.; Gaggero, N.; Casella, L.; Carrea, G.; Pasta, P. *Tetrahedron: Asymmetry* **1992**, *3*, 95-106.
- (c) Colonna, S.; Gaggero, N.; Casella, L.; Carrea, G.; Pasta, P. *Tetrahedron: Asymmetry* **1993**, *4*, 1325-1330.
- (d) Allain, E. J.; Hager, L. P.; Deng, L.; Jacobsen, E. N. *J. Am. Chem. Soc.* **1993**, *115*, 4415-4416.
- (e) Dexter, A. F.; Lakner, F. J.; Campbell, R. A.; Hager, L. P. *J. Am. Chem. Soc.* **1995**, *117*, 6412-6413.
- (f) Zaks, A.; Dodds, D.R. *J. Am. Chem. Soc.* **1995**, *117*, 10419-10424.
- (g) Allenmark, S. G.; Andersson, M. *Tetrahedron: Asymmetry* **1996**, *7*, 1089-1094.
- (h) Lakner, F. J.; Cain, K. P.; Hager, L. P. *J. Am. Chem. Soc.* **1997**, *119*, 443-444.
- (4) Butler, A.; Walker, J. V.; *Chem. Rev.* **1993**, *93*, 1937-1944.
- (5) Andersson, M.; Willetts, A.; Allenmark, S. *J. Org. Chem.* **1997**, *62*, 8455-8458.
- (6) Antonini, E. B., M. *Hemoglobin and Myoglobin in Their Reactions with Ligands* North-Holland, Amsterdam, 1971.
- (7) (a) Catalano, C. E.; Ortiz de Montellano, P. R. *Biochemistry* **1987**, *26*, 9265-9271.
- (b) Adachi, S.; Nagano, S.; Ishimori, K.; Watanabe, Y.; Morishima, I.; Egawa, T.; Kitagawa, T.; Makino, R. *Biochemistry* **1993**, *32*, 241-252.
- (c) Rao, S. I.; Wilka, A.; Ortiz de Montellano, P. R. *J. Biol. Chem.* **1993**, *268*, 803-809.

- (d) Matsui, T.; Nagano, S.; Ishimori, K.; Watanabe, Y.; Morishima, I. *Biochemistry* **1996**, *35*, 13118-13124.
- (e) Tschirret-Guth, R. A.; Ortiz de Montellano, P. R. *Arch. Biochem. Biophys.* **1996**, *335*, 93-101.
- (8) (a) Ozaki, S.; Matsui, T.; Watanabe, Y. *J. Am. Chem. Soc.* **1996**, *118*, 9784-9785.
(b) Ozaki, S.; Matsui, T.; Watanabe, Y. *J. Am. Chem. Soc.* **1997**, *119*, 6666-6667.
(c) Matsui, T.; Ozaki, S.; Watanabe, Y. *J. Biol. Chem.* **1997**, *272*, 32735-32738.
- (9) For general procedures, see Ausubel, F. M.; Brent, R.; Kingston, R. E.; Moore, D. D.; Seidman, J. G.; Smith, J. A.; Struhl, K. *Current Protocols in Molecular Biology*, John Wiley & Sons, Inc. New York, 1996.
- (10) (a) Springer, B.A.; Sligar, S. G. *Proc. Natl. Acad. Sci. U.S.A.* **1987**, *84*, 8961-8965.
(b) Wilks, A., Ortiz de Montellano, P. R. *J. Biol. Chem.* **1992**, *267*, 8827-8833.
- (11) Ozaki, S.; Ortiz de Montellano, P. R. *J. Am. Chem. Soc.* **1995**, *117*, 7056-7064.
- (12) The oxidation of 25 μmol of dihydrobenzothiophene (**4**) by the CPO^{3c} and VBrPO⁵ incubation system requires 1 hr and 10 hrs, respectively. Our F43H/H64L Mb system produces 7 μmol of the oxidation product of **4** in 30 min, and the linearity of the relationship between time and product formation has been observed for at least 30 min under the reaction condition.
- (13) (a) Groves, J. T.; Stern, M. K. *J. Am. Chem. Soc.* **1988**, *110*, 8628-8638.
(b) Groves, J.T.; Viski, P. *J. Org. Chem.* **1990**, *55*, 3528-3634.
- (14) Miller, V. P.; DePhillis, G. D.; Ferrer, J. C.; Mauk, A. G.; Ortiz de Montellano, P. R. *J. Biol. Chem.* **1992**, *267*, 8936-8942.
- (15) Matsui, T.; Ozaki, S.; Liong, E.; Phillips, G. N., Jr.; Watanabe, Y. manuscript in preparation. The coordinate (PDB ID, 1OFJ) is deposited with the Protein Data Bank.
- (16) Discover and Dock Modules from Molecular Simulation Inc. are used for the studies.

CHAPTER 2

Characterization of I107H/H64L Myoglobin Mutant*

*part published in *J. Am. Chem. Soc.* **1999**, *121*, 2007-2011

Tasuya Murakami, Isao Morishima, Toshitaka Matsui, Shin-ichi Ozaki, Isao Hara,
Hui-Jun Yang, and Yoshihito Watanabe

ABSTRACT: Since the alignment of the distal histidine is important for the reactivity with hydrogen peroxide as well as the prolonged life time of Mb-I [Ozaki *et. al. J. Am. Chem. Soc.* **1997**, *119*, 6666], I107H/H64L Mb was constructed with an objective of obtaining highly active Mb in the reaction with H₂O₂. However, the increased activities in peroxidation and peroxygenation are not observed for the I107H/H64L mutant in comparison with H64L and WT Mbs. The finding indicates that not only the distance of distal histidine to the heme iron but also its conformation might be crucial in the activation of H₂O₂ for Mb. In addition, attempts are made to define the mechanism of influence of the distal histidine on regioselectivity in the coupled oxidation of several distal histidine relocation Mbs including I107H/H64L. HPLC analysis of biliverdin isomers shows that relocation of the distal histidine at the 107 position (I107H/H64L Mb) affords the amount of γ -isomer to 22%, while L29H/H64L Mb almost exclusively gives γ -isomer compared with H64L and WT Mb which mainly afford α -isomer.

ABBREVIATIONS

Mb, myoglobin;

HRP, horseradish peroxidase;

compound I, a ferryl porphyrin cation radical;

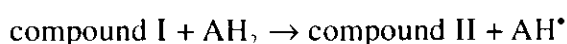
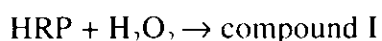
compound II, a ferryl porphyrin;

*m*CPBA, *m*-chloroperbenzoic acid;

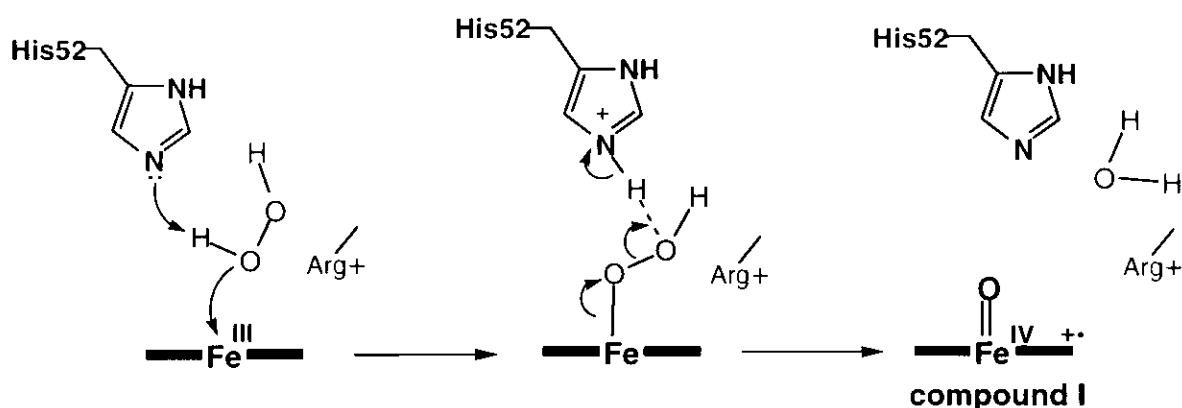
ABTS, 2,2'-azino-bis(3-ethylbenzothiazoline-6-sulfonic acid).

INTRODUCTION

Catalytic turnover of classical peroxidases with a histidine as the ligand to the heme iron involves the reaction with H_2O_2 to give a ferryl porphyrin radical cation known as compound I.^{1,2} HRP is the prototype for peroxidases as depicted in the reaction scheme below, in which compound I contains two oxidizing equivalents comparing to the native enzyme and compound II one equivalent. The two sequential single-electron transfers from substrate molecules reduce compound I, first to compound II and then to the resting state.



Many reports, including the high resolution crystal structure of HRP,³ indicate that the histidine (His-52) in the distal pocket is a critical residue in the activation of H_2O_2 , and its replacement by aliphatic residues retards compound I formation by 5~6 orders of magnitude.⁴ As shown in Scheme 1, the distal histidine is believed to function as (i) a general base to accelerate binding of H_2O_2 to the ferric heme iron by deprotonating the peroxide and (ii) a general acid to facilitate the heterolytic cleavage of the O-O bond of a plausible $\text{Fe}^{\text{III}} \text{OOH}$ complex by protonating the terminal oxygen atom.⁵



Scheme 1. Proposed roles of the distal histidine and arginine in the compound I formation for peroxidases.

Myoglobin (Mb), a carrier of molecular oxygen, similarly possesses a distal histidine (His-64) in the heme pocket (Figure 1) and can catalyze various oxidation reactions using H_2O_2 .⁶⁻¹⁰ However, Mb reacts with H_2O_2 much slower ($\sim 10^2 \text{ M}^{-1}\text{s}^{-1}$) than HRP ($\sim 10^7 \text{ M}^{-1}\text{s}^{-1}$) to afford ferryl myoglobin (Mb-II) but not a ferryl porphyrin radical cation (Mb-I) which is considered to decay to Mb-II immediately (Scheme 2).

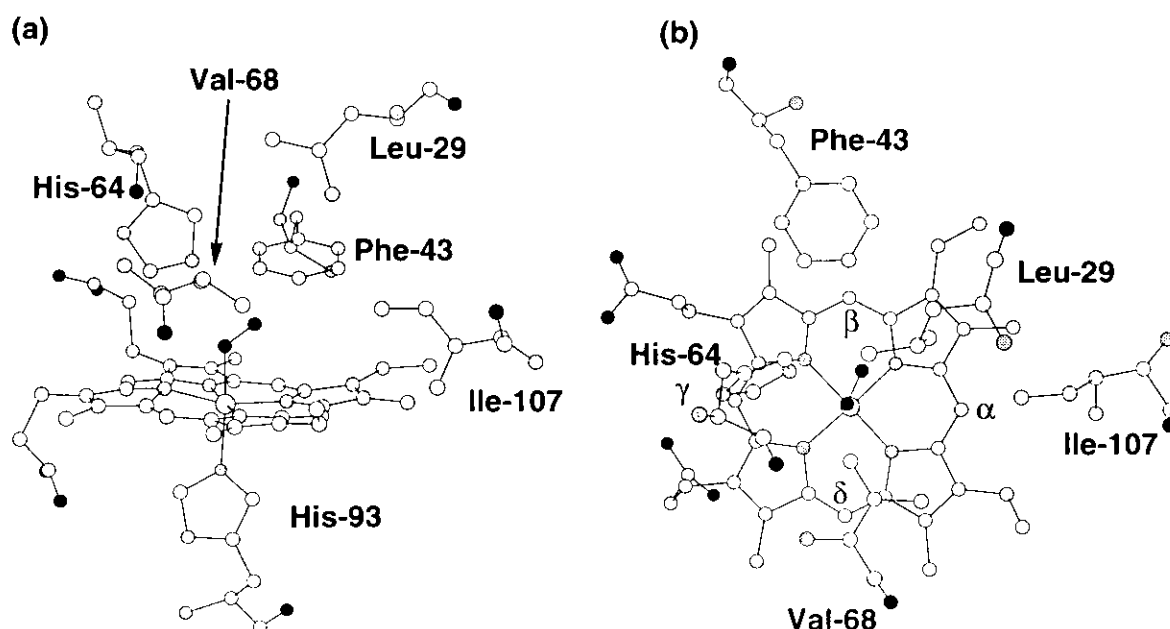
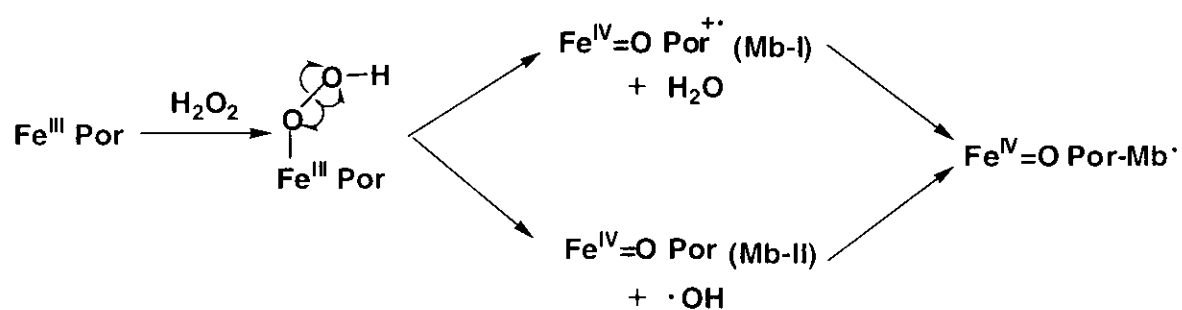


Figure 1. Heme environmental structure of myoglobin. Heme and some selected residues are shown: (a) side view; (b) top view.



Scheme 2. Reactions of ferric Mb with hydrogen peroxide.

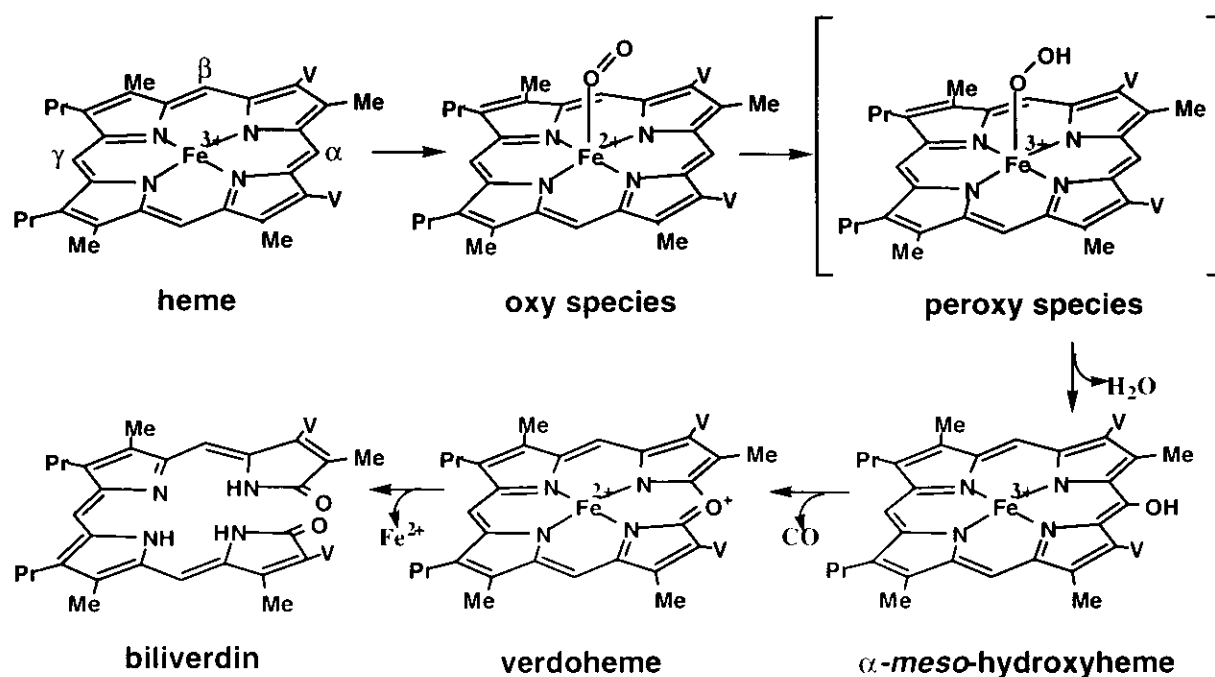
By comparing crystal structures of sperm whale myoglobin and horseradish peroxidase, Ozaki *et al.* have hypothesized that the distal histidine in Mb is too close to the heme iron to facilitate compound I formation, and Mb's reactivity with H_2O_2 is

consequently lower than that of the peroxidase.¹¹⁻¹³ The distances between N_ε of the distal histidine and the heme iron are normally 4.1~4.6 Å for globin (4.3 Å for sperm whale Mb) and 5.5~6.0 Å for peroxidases (6.0 Å and 5.6 Å for horseradish peroxidase and cytochrome *c* peroxidase, respectively). In order to examine the above hypothesis, distal histidine relocation mutants (F43H/H64L and L29H/H64L) were prepared in our research group previously and the crystal structures solved at 1.8 Å show the iron-distal histidine distances are 5.7 Å and 6.6 Å for F43H/H64L and L29H/H64L Mb,¹⁴ respectively. The F43H/H64L mutation caused 11-fold increase in the activation of H₂O₂ *versus* WT Mb presumably because the distance between distal histidine and the heme iron is similar to that of peroxidases. With a similar strategy, we, in this study, have prepared a I107H/H64L Mb mutant because the estimated iron-histidine distance in the I107H/H64L mutant is 5.6 Å similar to that in peroxidase.³

In the coupled oxidation, heme is degraded into biliverdin IX_α and CO as normally performed by heme oxygenase (Scheme 3).¹⁵ The initial step is the formation of an oxy complex,¹⁶ followed by the hydroxylation of the α -*meso*-carbon presumably via a ferric hydroperoxide intermediate.^{17,18} The release of carbon monoxide from hydroxyheme and subsequent ring opening affords biliverdin.¹⁵ Therefore, α -*meso*-hydroxyheme formation from the oxy complex is a key step for the regiospecific opening of the tetrapyrrole macrocycle. Recently, Torpey and co-workers reported that the regiochemistry of the reaction is primarily controlled by the electronic effect of the heme.^{19,20} However, resonance Raman studies suggested that an oxygen molecule of the O₂-bound heme oxygenase complex had a bent structure and that the terminal oxygen atom was in van der Waals contact with the α -*meso*-carbon of the porphyrin ring.²¹ These results might imply that orientation of the bound oxygen also affects the regioselective heme degradation by heme oxygenase.

In the presence of ascorbate under the aerobic condition, heme in myoglobin is transformed into biliverdin IX_α.^{22,23} Although the coupled oxidation of Mb is much slower than the heme degradation catalyzed by heme oxygenase, Mb and heme oxygenase both have a histidine residue as a ligand of the heme iron.^{23,24} Furthermore,

the crystal structure of oxy-Mb indicates that the molecular oxygen bound to the heme is restricted by the distal histidine (His-64) toward the α -*meso*-position, and the oxy complex is stabilized by a hydrogen bond with His-64 (Figure 1a, b). In order to examine if the reorientation of the bound oxygen molecule caused by the removal or relocation of the distal histidine affects the regiospecific degradation of heme in Mb, the coupled oxidation of wild type, H64L, L29H/H64L, F43H/H64L Mbs were examined,²⁵ previously. To extend the examination, we studied the coupled oxidation by I107H/H64L Mb in this study.



Scheme 3. Probable reaction sequence of intermediates in the heme oxygenase-catalyzed conversion of heme to biliverdin.

EXPERIMENTAL PROCEDURES

Materials. All the chemicals were obtained from Wako and Nakalai Tesque and used without further purification. The buffers used for the reactions were 50 mM sodium phosphate (pH 6.0–9.0), 50 mM sodium acetate (pH 5.0) and 50 mM borate buffer (pH 10).

Site-Directed Mutagenesis, Expression and Purification of Mb. The express-

ion vector for wild type and H64L mutant of sperm whale myoglobin are gifts from Olson (Springer, 1987).²⁶ Site-directed mutagenesis of Ile-107 in recombinant sperm whale myoglobin was carried out by using the polymerase chain reaction (PCR) according to a method previously reported by Springer *et al.*, 1989,²⁷ and then confirmed by DNA sequence analysis on a ABI Prim 373 DNA Sequencer (Applied Biosystems). The expression and purification of the mutant were performed according to methods previously described.²⁷

Assay of One-electron Oxidation Activity. All UV-Visible measurements were done on a Shimadzu UV-24000 spectrophotometer. One-electron oxidation activities of guaiacol and ABTS were measured at 20 °C in 50 mM sodium phosphate buffer (pH 7.0). The formation rate of the guaiacol oxidation product was determined from the increase in the absorbance at 470 nm ($\epsilon_{470} = 2.6 \times 10^4 \text{ M}^{-1}\text{cm}^{-1}$).²⁸ The 1 ml final assay volume contained 2 mM guaiacol, variable amounts of H₂O₂ (0.2 - 5 mM), and the concentrations were 1.0 μM for wild type and 10 μM for I107H/H64L Mb. The formation of ABTS cation radical was monitored at 730 nm ($\epsilon_{730} = 1.44 \times 10^4 \text{ M}^{-1}\text{cm}^{-1}$) as noted in Chapter 1 of part II. The reaction mixture contained 1 mM ABTS and variable amounts of H₂O₂ (0.1 - 2 mM), and the concentrations were 1.0 μM for the wild type and 10 μM for the mutant.

Assay of Two-electron Oxidation Activity. Enzymatic sulfoxidation and epoxidation were performed with the same procedures as described in Chapter 1 of part III except for 10 μM of the mutant.

Reaction of I107H/H64L Mb with *m*-Chloroperbenzoic Acid. The reactions between ferric Mb and *m*CPBA were performed at 5.0 °C in different pH value buffers (50 mM). All the spectral changes was monitored on a Hi-Tech SF-43 stopped-flow apparatus equipped with a MG6000 diode array spectrophotometer. An optical filter (360 nm) was used to avoid possible photoreduction of compound I by UV light.

Biliverdin Extraction and HPLC Analysis. To a 250 μL solution of the ferric complexes of wild-type and mutant Mb in 50 mM sodium phosphate buffer (pH 7.0) was added sodium ascorbate (2 mg), and the resulting solution was incubated at 37 °C for 3

hours. Extraction of biliverdin regioisomers was performed as previously reported.²⁹ The products dissolved in methanol were loaded on a high-pressure liquid chromatograph (Waters 600) equipped with Waters 741 data module and TOSOH CO-8020 column oven. A reverse phase HPLC column (Whatman Partisil 5 ODS-3) was employed at 40 °C at a flow rate of 0.7 ml/min with 75:25 (v/v) methanol-25 mM ammonium phosphate buffer (pH 3.5) and detected at 380 nm. A mixture of four biliverdin regioisomers was prepared from protoheme IX according to the method reported.¹⁹

RESULTS AND DISCUSSION

Spectroscopic Features of I107H/H64L Mb. The ferric state of wild type Mb exhibits the absorption spectrum with the Soret band at 408 nm, which is typical of hexacoordinated ferric high-spin heme.³⁰ The sixth ligand in the wild type is a water molecule stabilized by His-64 through hydrogen bonding.³¹ On the other hand, ferric I107H/H64L Mb exhibits absorption spectrum similar to that of the ferric H64L mutant, which loses the water ligation to cause a blue-shift of the Soret to 395 nm (Figure 2).

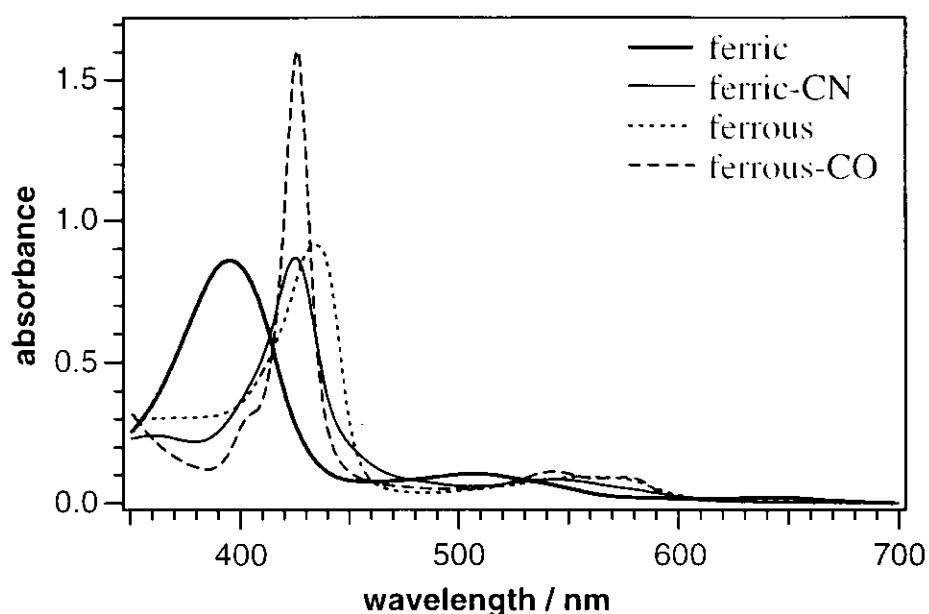


Figure 2. Absorption spectra of ferric and ferrous of I107H/H64L Mb in 50 mM sodium phosphate buffer (pH 7.0).

Although the crystal structure of I107H/H64L Mb is not available at present, it is likely that N_ε of His-107 is too far from the heme iron to stabilize the water molecule bound to the heme iron through direct or indirect hydrogen bonding interaction. The λ_{max} for the ferric, ferric-CN, ferrous, and ferrous-CO forms of the I107H/H64L mutant are summarized in Table 1, essentially identical to those of the corresponding forms of the wild type and H64L Mb.

Table 1. Wavelength of the absorption maximum of I107H/H64L Mb in 50 mM sodium phosphate buffer (pH 7.0).

		Soret / nm	visible / nm
I107H/H64L	ferric	395	508 / 645
	ferric-CN	425	543
	ferrous	435	560
	ferrous-CO	426	545 / 578

One- and Two-electron Oxidation Activities. In order to estimate the reaction rate between the ferric Mb and H₂O₂, the oxidation of guaiacol and ABTS are examined at pH 7.0 and 20 °C by using H₂O₂ as an oxidant. The I107H/H64L mutant exhibits much less reactivity than the wild type in both guaiacol and ABTS oxidation, and the values for I107H/H64L Mb are similar to those of the H64L mutant.¹¹ That is to say, any considerable activities are not found for both H64L and I107H/H64L Mbs compared to the wild type (Figure 3).

In the measurement of peroxygenase activity of the I107H/H64L mutant, the increase in the rate and the value of % ee are not observed in thioanisole sulfoxidation and styrene epoxidation with respect to the wild type Mb (Table 2).

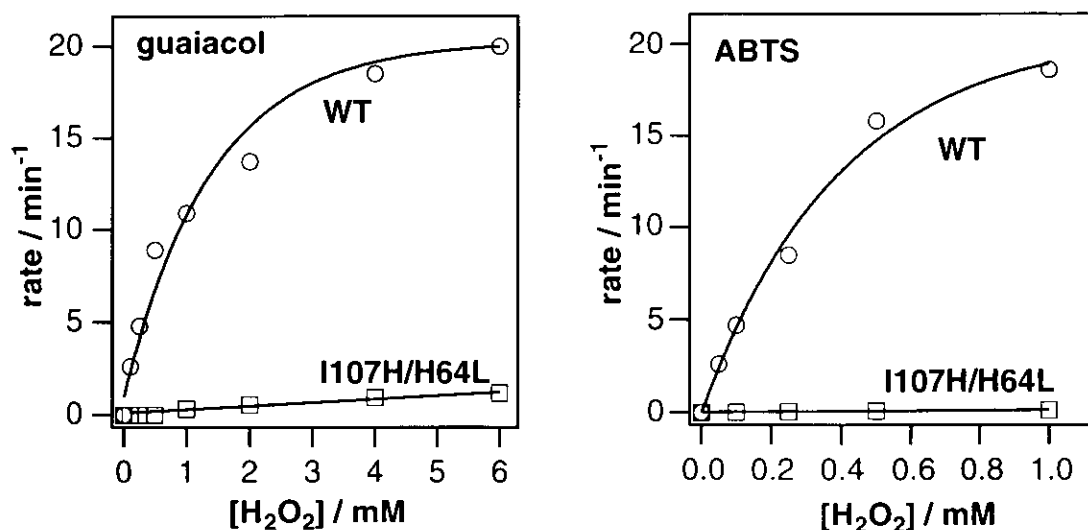


Figure 3. The dependence of initial oxidation rates in one-electron oxidation on the concentration of H_2O_2 at 20 °C in 50 mM sodium phosphate buffer (pH 7.0).

Table 2. H_2O_2 -dependent peroxygenations catalyzed by Mb mutants at 20 °C in 50 mM sodium phosphate (pH 7.0).

	thioanisole sulfoxidation		styrene epoxidation	
	rate / min ⁻¹	ee %	rate / min ⁻¹	ee %
wild type	0.25	25	0.015	9
H64L	0.072	27	0.020	34
I107H/H64L	0.063	19	ND*	ND*

R is the dominant isomer and ND means not determinable

Compound I and II Formation for the I107H/H64L Mutant. Along with increasing pH, the rates in the reaction of I107H/H64L Mb with *m*CPBA decrease linearly (Figure 4). The results imply the presence of ionizable groups affecting the reactivities with *m*CPBA. At pH 8 or higher, the I107H/H64L mutant is oxidized directly to compound II (Mb-II) without the accumulation of Mb-I because the decay rate of Mb-I to II appears to be greater at higher pHs.

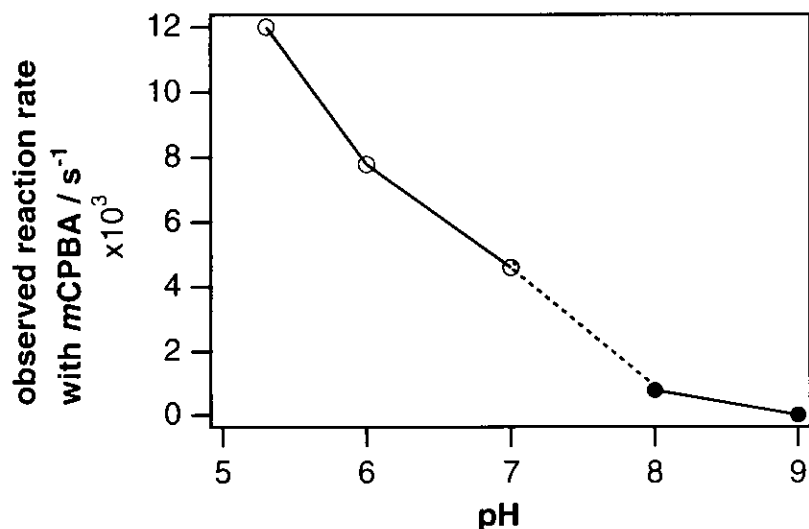


Figure 4. pH profiles of the reaction rates of I107H/H64L Mb with *m*CPBA at 5.0 °C in 50 mM buffers. The open and close circles correspond to the formation rates of Mb-I and Mb-II, respectively.

Figure 5 shows yields of Mb-I in the reactions of I107H/H64L Mb with a varied amount of *m*CPBA at pH 5.3. At least 20 equivalents of *m*CPBA are required to observe compound I in which only 67% of I107H/H64L Mb could be converted into Mb-I. The double mutant does not show accumulation of Mb-I with less than 20 equivalents of *m*CPBA due to lower formation rate of compound I ($k = 2.4 \times 10^2 \text{ M}^{-1}\text{s}^{-1}$). Figure 6 shows the spectral changes in the compound I formation of I107H/H64L Mb with 50 equivalents of *m*CPBA. The decrease in the absorbance of the Soret and the increase in the absorbance around 650 nm are characteristic for the formation of compound I from the ferric state. The following Soret shift is due to the decay of compound I (Por^{••} Fe^{IV}=O) to II (Por Fe^{IV}=O) as observed for other heme containing peroxidase. While 50 equivalents of *m*CPBA was used to generate enough compound I (> 80%), thioanisole is able to reduce in part of compound I of the mutant back to the ferric state. Therefore, the exact value of Cpd I reduction rate is difficult to be determined under the condition.

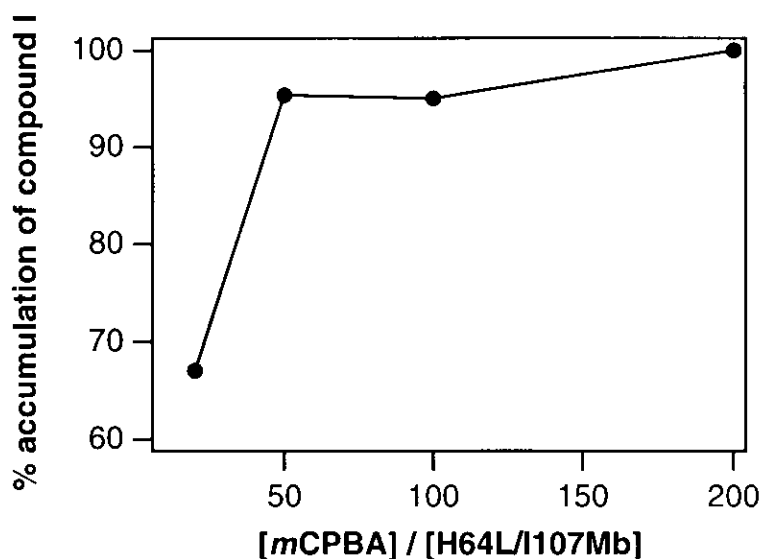


Figure 5. Yields of Mb-I in the reactions of I107H/H64L Mb with varied amount of *m*CPBA at 5.0 °C in 50 mM sodium acetate buffer (pH 5.3).

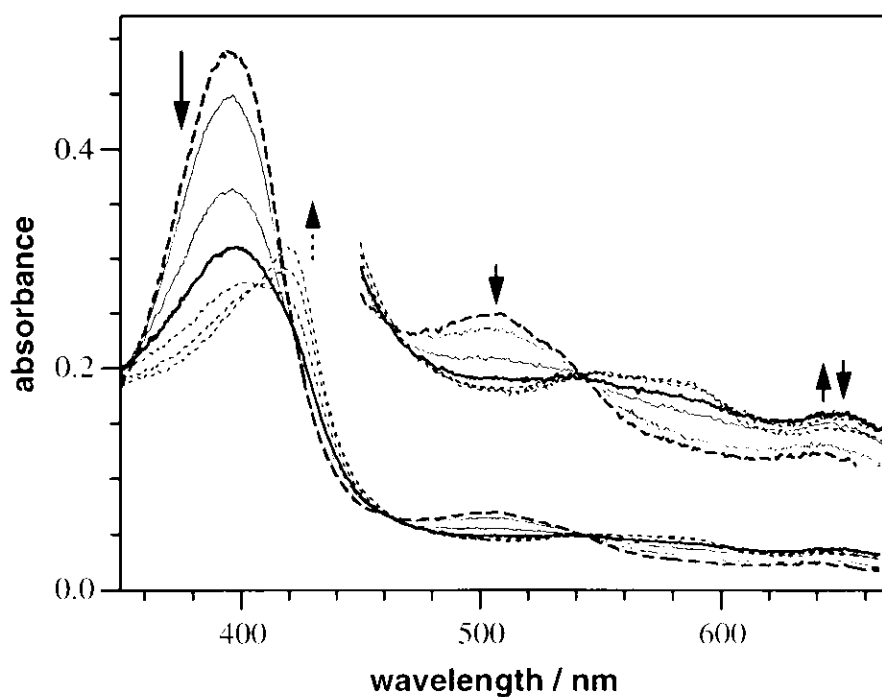


Figure 6. Absorption spectral changes of I107H/H64L Mb in the reaction with *m*CPBA at 5.0 °C in 50 mM sodium acetate buffer, pH 5.3. Final concentrations: 5.0 μ M I107H/H64L Mb, 250 μ M *m*CPBA. The spectra were recorded before mixing (broken line) and at 20, 80, 160 ms (solid line) and 320-800 ms (dotted line).

Effects of the Distal Histidine on Regioselectivity in the Coupled Oxidation.

The regiospecificity of the coupled oxidation of I107H/H64L mutant has been examined with the same procedure in reference.²⁵ Since Fe³⁺-biliverdin is known to be formed instead of a free form of biliverdin³² in the coupled oxidation with ascorbate, we have converted Fe³⁺-biliverdin·Mb complex to biliverdin by the treatment with acetic acid and HCl. The HPLC system separates the four biliverdin regioisomers derived from heme.

Figure 7 shows a HPLC trace for the products of the coupled oxidation of hemin and the distal histidine relocation myoglobin mutants.³³ Peaks at the retention times of 8.4, 9.8, 10.4, and 13.6 min correspond to the four biliverdin isomers (Figure 7a, c). The major product in coupled oxidation for I107H/H64L is determined in the same method as described for H64L and L29H/H64L as well as F43H/H64L Mbs.²⁵

We have observed the difference in the regioselectivity of the coupled oxidation for the I107H/H64L mutant from other distal histidine relocation Mbs (Table 3). H64L Mb might be a good starting point, giving only 6% γ -isomer product, to elucidate effects of the distal histidine on the coupled oxidation. The introduction of a histidine residue at the 29, 43, 107 positions of H64L Mb increases the ratio of γ -biliverdin to 97, 44, and 22%, respectively. The polarized water molecule in L29H/H64L Mb might be the reason for the unexpectedly high γ -specificity for the mutant.²⁵ However, I107H/H64L Mb which shows the lack of water-coordination heme iron in UV-spectrum, yields only 22% biliverdin IX $_{\gamma}$ in the coupled oxidation. The results suggest that polar or charged residues in the heme pocket, except for the distal histidine of the wild type (His-64), somehow facilitate the formation of γ -biliverdin, but His-64 in wild type Mb sterically blocks the γ -meso position giving only a trace amount of γ -isomer product (Figure 1, table 3).

In summary, the distal His-107 in the active site of I107H/H64L Mb does not function efficiently as a general acid-base catalyst to facilitate the formation of compound I. We suppose that His-107 is too far from the heme iron or the imidazole ring has adapted the conformation in which it is directed away from the heme center. In addition, our observation in regiospecificity for the coupled oxidation of I107H/H64L

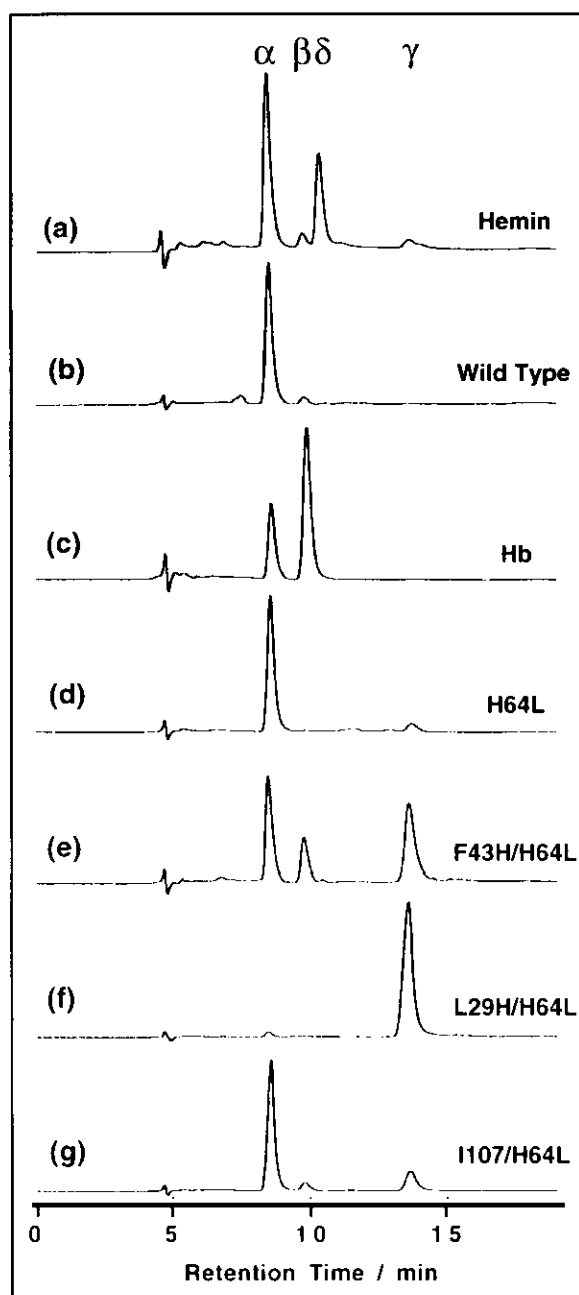
Mb, combining with previous results,²⁵ would be summarized as follows: (1) The introduction of a charged residue such as histidine in the heme pocket of H64L Mb increases the γ -specificity due to the polar effect. (2) Amino acid residues like histidine could also regulate the regiospecificity by hydrogen bond interaction.

Table 3. Ratio of four biliverdin isomers produced by the coupled oxidation of Mbs^a

	α	β	γ	δ
WT	95	5	trace	trace
H64L	94	trace	6	trace
F43H /H64L	40	16	43	trace
L29H /H64L	3	trace	97	trace
I107H /H64L	72	6	22	trace

^aRatio of the peak area.

Figure.7 HPLC analysis of product isolated from the coupled oxidation of Mbs.



REFERENCE AND NOTES

- (1) Dunford, H. B. *Peroxidase in Chemistry and Biology* Everse, J.; Everse, K. E.; Grisham, M. B. Ed.; Vol. II, P1-24, CRC Press, Boca Raton, 1991.
- (2) Ortiz de Montellano, P. R. *Annu. Rev. Pharmacol. Toxicol.* **1991**, *32*, 89-107.
- (3) Gajhede, M.; Schuller, D. J.; Henriksen, A.; Smith, A. T.; Poulos, T. L. *Nat. Struct. Biol.* **1997**, *4* 1032-1038
- (4) Newmyer, S. L.; Ortiz de Montellano, P. R. *J. Biol. Chem.* **1995**, *270*, 19430-19438.
- (5) Poulos, T. L.; Kraut, J. *J. Biol. Chem.* **1980**, *255*, 8199-8205.
- (6) Phillips, G. N., Jr.; Arduini, R. M.; Springer, B. A.; Sligar, S. G. *Proteins Struct. Funct. Genet.* **1990**, *7*, 358-365.
- (7) Ortiz de Montellano, P. R.; Catalano, C. E. *J. Biol. Chem.* **1985**, *260*, 9265-9271.
- (8) Rao, S. I.; Wilks, A.; Ortiz de Montellano, P. R. *J. Biol. Chem.* **1993**, *268*, 803-809.
- (9) Matsui, T.; Nagano, S.; Ishimori, K.; Watanabe, Y.; Morishima, I. *Biochemistry* **1996**, *35*, 13118-13124.
- (10) Evers, J.; Johnson, M. C.; Marini, M. A. *Methods Enzymol.* **1994**, Vol. 231; pp 547-561.
- (11) Ozaki, S.; Matsui, T.; Watanabe, Y. *J. Am. Chem. Soc.* **1996**, *118*, 9784-9785.
- (12) Ozaki, S.; Matsui, T.; Watanabe, Y. *J. Am. Chem. Soc.* **1997**, *119*, 6666-6667.
- (13) Ozaki, S.; Matsui, T.; Mark, P. R.; Watanabe, Y. *Coord. Chem. Rev.* **2000**, *198*, 39-59.
- (14) Matsui, T.; Ozaki, S.; Liang, E.; Phillips, G. N., Jr.; Watanabe, Y. *J. Biol. Chem.* **1999**, *274*, 2838-2844.
- (15) Tenhunen, R.; Marver, H. S.; Schmid, R. *J. Biol. Chem.* **1969**, *244*, 6388-6394.
- (16) Yoshida, T.; Noguchi, M.; Kikuchi, G. *J. Biol. Chem.* **1980**, *255*, 4418-4420.
- (17) Noguchi, M.; Yoshida, T.; Kikuchi, G. *J. Biochem. (Tokyo)* **1983**, *93*, 1027-1036.
- (18) Wilks, A.; Torpey, J.; Ortiz de Montellano, P. R. *J. Biol. Chem.* **1994**, *269*, 29553-

29556.

- (19) Torpey, J.; Ortiz de Montellano, P. R. *J. Biol. Chem.* **1996**, *271*, 26067-26073.
- (20) Torpey, J.; Ortiz de Montellano, P. R. *J. Biol. Chem.* **1997**, *272*, 22008-22014.
- (21) Takahashi, S.; Ishikawa, K.; Takeuchi, N.; Ikeda-Saito, M.; Yoshida, T.; Rousseau, D. L. *J. Am. Chem. Soc.* **1995**, *117*, 6002-6006.
- (22) Lemberg, R. *Rev. Pure. Appl. Chem.* **1956**, *6*, 1.
- (23) Takahashi, S.; Wang, J.; Rousseau, D. L.; Ishikawa, K.; Yoshida, T.; Host, J. R.; Ikeda-Saito, M. *J. Biol. Chem.* **1994**, *269*, 1010-1014.
- (24) Sun, J.; Loehr, T. M.; Wilks, A.; Ortiz de Montellano, P. R. *Biochemistry* **1994**, *33*, 13734-13740.
- (25) Murakami, T.; Morishima, I.; Matsui, T.; Ozaki, S.; Hara, I.; Yang, H.-J.; Watanabe, Y. *J. Am. Chem. Soc.* **1999**, *121*, 2007-2011.
- (26) Springer, B. A.; Sligar, S. G. *Proc. Natl. Acad. Sci. U.S.A.* **1987**, *84*, 8961-8965.
- (27) Springer, B. A.; Egeberg, K. D.; Sligar, S. G.; Rohlf, R. J.; Mathews, A. J.; Olson, J. S. *J. Biol. Chem.* **1989**, *264*, 3057-3060.
- (28) Ozaki, S.; Ortiz de Montellano, P. R. *J. Am. Chem. Soc.* **1995**, *117*, 7056-7064.
- (29) Brown, S. B.; Docherty, J. C. *Biochem. J.* **1978**, *173*, 985-987.
- (30) Takano, T. *J. Mol. Biol.* **1977**, *110*, 537-568.
- (31) Antonini, E.; Brunori, M. *Hemoglobin and Myoglobin in Their Reactions with Ligands*; North-Holland Publishing Co.: Amsterdam **1971**, pp 10-11.
- (32) Yoshida, T.; Ishikawa, K.; Sato, M. *Eur. J. Biochem.* **1991**, *199*, 729-733.
- (33) Except for I107H/H64L Mb, HPLC analysis on other Mbs took from *J. Chem. Soc. Chem. Commun.* **1998**, 773-774.

Part IV

SUMMARY AND CONCLUSION

In the present thesis, the author aimed to clarify enantioselectivity of oxidation reactions catalyzed by heme proteins. Sperm whale myoglobin (Mb) is employed as a model hemoprotein for the purpose, and some Mb mutants have been prepared by site-directed mutagenesis.

Heme as a common prosthetic group performs surprisingly diverse tasks such as oxygen transport and storage, electron transfer, monooxygenation, dismutation of hydrogen peroxide, *etc.* by virtue of surrounding protein matrix. However, molecular mechanisms of the enantiospecific regulation by hemoprotein are complicated, and the elucidation of them has been the subject of extensive studies.

In this thesis, following General Introduction, the author commences the study on construction of high enantioselective and active enzymes using myoglobin as a model. In chapter 1 of part II, a series of Mb mutants (H64D/V68X Mb) have been prepared by replacing Val-68 with Gly, Ala, Ser, Leu, Ile, and Phe in H64D Mb, which showed the highest oxidation activity but lower enantioselectivity among Mbs in previous studies. As the results, substituted amino acid residues at position 68 give rise to higher enantioselective and active Mb mutants. The rates of thioanisole oxidation by compound I of H64D/V68X Mbs were found to exhibit a nearly parallel trend to the catalytic sulfoxidation activity by the mutants with H₂O₂. Such a relationship suggests that the sulfoxidation rate might partly be controlled by the compound I reactivity of H64D/V68X Mbs. The varied reactivity of the mutants with H₂O₂ were estimated by the one-electron oxidation activity of ABTS, because the rate determining step at the ABTS oxidation was revealed to be the formation of compound I by H₂O₂. Interestingly, apolar residues in the H64D/V68X mutants appeared to regulate the enantioselectivity of thioanisole oxidation, *i.e.*, enhancement of the the enantioselectivity from 25% ee (*S*) for H64D/V68S to 84% ee (*R*) for H64D/V68A Mb. In an effort to shed light on the origin of high enantioselectivity for the H64D/V68X mutants, the investigation of UV-visible spectroscopy, EPR and X-ray crystallography on phenylethylamine complexes for H64D/V68X Mbs have been performed.

In chapter 2 of part II, F43H/H64N Mb constructed to mimic the active site of

catalase exhibits better catalase and peroxidase activity. Although the single replacement of His-64 with an asparagine residue does not enhance the rate of ABTS oxidation, F43H/H64N Mb has 3.4-fold better peroxidase activity than the F43H/H64A Mb. Therefore, the distal histidine in the F43H/H64N mutant appears to work cooperatively with Asn-64 to enhance the reactivity with H₂O₂. The results presented in this study infer that the distal asparagine (Asn-147) as well as histidine (His-74) in BLCase might also play a role to facilitate compound I formation.

In addition, substrate specificity is also important in controlling enantioselectivity of enzymatic oxidation. Previously, L29H/H64L and F43H/H64L Mb were reported to exhibit catalytic turnover with high enantiospecificity for the sulfoxidation of thioanisole and the epoxidation of styrene. To determine how substrate structures influence on the enantioselective oxidations by Mb, in chapter 1 of part III, the scope of asymmetric oxygenation by the use of various sulfides and styrene were explored for L29H/H64L and F43H/H64L Mb. On the basis of changes in enantioselectivity, the substrate binding mode for Mb mutant-catalyzed reactions was rationalized. Furthermore, compound I of L29H/H64L Mb was confirmed to be a catalytic species for the oxidation of sulfides and styrene.

The location of distal histidine in Mb is not only critical for catalytic oxidation as studied in previous work, but also affects regiospecificity in heme degradation. The results on H107H/H64L Mb were described in Chapter 2 of part III.

Significant progress has been made in the elucidation of catalytic mechanism for the enantioselective oxidation by sperm whale myoglobin mutants. The Mb mutants the author prepared in this thesis works would be useful as asymmetric synthetic tools.

ACKNOWLEDGMENT

In January of 1998, I had an honor to become a Monbusho fellow as a graduate student of the Graduate University for Advanced Studies. I am very grateful to the Japanese Government Fellowship which made it possible for me to accomplish the fruitful outcome of the present thesis. The present thesis is a summary on my studies from 1998 to 2000 at Department of Structural Molecular Science under the supervision of Prof. Yoshihito Watanabe.

I wish to express my cordial gratitude to Prof. Yoshihito Watanabe for his enthusiasm, stimulating discussion and hearty encouragement. I also gratefully acknowledge Dr. Shin-ichi Ozaki for the discerning advice in my accomplishment of the studies and constructive comments on the thesis.

It is really grateful to Prof. John S. Olson and Prof. George N. Phillips, Jr. (Rice university) for providing a kind gift, cDNA of sperm whale myoglobin, and X-ray structural analysis.

Special thanks also go to all members and co-workers in Prof. Watanabe's group. I am deeply indebted to Drs. Seiji Ogo, Takahumi Ueno, Toshitaka Matsui, Kwang-Hyun Ahn, Cheal Kim, W. J. Puspita, Hidetaka Nakai, Kazuharu Suzuki, Manabu Yanase, Isao Hara, Nobuyuki Makihara, Ryo Yamahara, Masataka Ohashi, Shigeru Kato, Tsutomu Abura for valuable suggestion and unfailing encouragement. Acknowledgments are also due to Mrs. Misako Tanizawa and Mrs. Akiyo Ota for their office work and heartfelt kindness.

Finally, I would express my sincere gratitude to my family for their generous understanding and affectionate encouragement.

Okazaki, January 2001

Hui-Jun YANG

LIST OF PUBLICATIONS

- 1 Asymmetric Oxidation Catalyzed by Myoglobin Mutants
Shin-ichi Ozaki, Hui-Jun Yang, Toshitaka Matsui, Yoshio Goto, and Yoshihito Watanabe
Tetrahedron: Asymmetry **1999**, *10*, 183-192
- 2 Effects of the Arrangement of a Distal Catalytic Residue on Regioselectivity and Reactivity in the Coupled Oxidation of Sperm Whale Myoglobin Mutants
Tasuya Murakami, Isao Morishima, Toshitaka Matsui, Shin-ichi Ozaki, Isao Hara, Hui-Jun Yang, and Yoshihito Watanabe
J. Am. Chem. Soc. **1999**, *121*, 2007-2011
- 3 The Role of Val68 (E11) on Oxidation Activity and Enantioselectivity of Sperm Whale Myoglobin
In preparation
- 4 Conversion of Sperm Whale Myoglobin into a Catalase-like Enzyme
In preparation